



Contents lists available at [ScienceDirect](http://www.sciencedirect.com)

Journal of Sound and Vibration

journal homepage: www.elsevier.com/locate/jsvi



Time modes and nonlinear systems

Hayrani Öz^a, John K. Ramsey^{b,*}

^a The Ohio State University, Department of Aerospace Engineering, 328 Bolz Hall, 2036 Neil Avenue, Columbus, OH 43210-1276, United States

^b NASA Glenn Research Center, 21000 Brookpark Road, M.S. 86-10, Cleveland, OH 44135, United States

ARTICLE INFO

Article history:

Received 18 March 2009

Received in revised form

18 November 2009

Accepted 16 December 2009

Handling Editor: M.P. Cartmell

Available online 4 February 2010

ABSTRACT

A vector-space implementation of the equation that has been known as Hamilton's Law of Varying Action is used with a non-virtual perspective to generate direct solutions to nonlinear initial value response problems in the time domain. This novel vector-space perspective unleashes the power of linear algebra to provide new capabilities with Hamilton's Law of Varying Action and new insights into nonlinear dynamics. In particular, this perspective permits the use of unconstrained temporal-basis-functions without the need to augment Hamilton's Law of Varying Action with Lagrange multipliers, and provides a linearly independent set of spatiotemporal functions spanning the solution space of the response. These spatiotemporal functions are descriptively denoted as fundamental-time-modes. By providing this basis of fundamental-time-modes, the concepts of linear algebra can be taken advantage of to accomplish model reduction and superposition for nonlinear systems. In particular, classical model reduction techniques are used to eliminate non-dominant fundamental-time-modes from the solution process, resulting in model reduction in the time domain. In addition, using the novel concept of eigen-direction iteration, linearly independent fundamental-time-mode response trajectories along eigen-directions are superposed to yield new response trajectories for nonlinear systems. These capabilities of the vector-space approach are demonstrated for nonlinear systems exhibiting nonlinear normal mode response. The article concludes with an Appendix A entitled "The Law of Evolutionary Energy, Hamilton's Law of Varying Action and the Principle of Virtual Work", providing essential insight to the non-virtual working equation of the authors' previous articles and the current article, referred to as Hamilton's Law of Varying Action, to distinguish it from virtual concepts and virtual variational principles of classical dynamics. It is shown that this particular equation referred to as Hamilton's Law of Varying Action is a special case of the Law of Evolutionary Energy which inherently encompasses the First Law of Thermodynamics involving quantifiable real changes (alterations) along the real dynamic path, the application of which to mechanical systems yields both the current non-virtual working form of Hamilton's Law of Varying Action and the original form of the only enunciated (non-virtual) "law of varying action" by Hamilton which are not the same expressions.

Published by Elsevier Ltd.

* Corresponding author. Tel.: +1 216 433 6032.

E-mail addresses: oz.1@osu.edu (H. Öz), john.k.ramsey@nasa.gov (J.K. Ramsey).

Nomenclature			
a_i	i th expansion coefficient for the temporal-basis-function in real time	\mathbf{q}^R	column vector (N -tuple) of coordinates q_r^R , for the range-space solution, $\in \mathcal{F}^{HLVA}$
\mathbf{A}	column vector of temporal-basis-function expansion coefficients, $\{A_i\}$	q_r	coordinate of r th degree-of-freedom, $\in \mathcal{F}^{HLVA}$, $1 \leq r \leq N$
\mathbf{A}_{conv}	column vector of converged temporal-basis-function expansion coefficients, $\{A_i\}_{\text{conv}}$	q_r^R	coordinate of r th degree-of-freedom for range-space solution, $\in \mathcal{F}^{HLVA}$, $1 \leq r \leq N$
A_i	i th expansion coefficient for the temporal-basis-function in nondimensional time	$q_{ri}^*(\tau)$	r th component function for the i th fundamental-time-mode, $\in \mathcal{F}^{HLVA}$, $1 \leq i \leq 2N$ ($\leq Nn$ for forced systems)
\mathbf{A}_R	$[\mathbf{E}]_R \mathbf{\beta}_R$	r	index of degrees-of-freedom, $1 \leq r \leq N$
\mathbf{b}	right-hand column vector of external forcing functions and/or initial conditions	s	index of eigenvalue, λ
c	damping coefficient	$[\mathbf{S}]$	diagonal matrix of singular values
\mathcal{DE}	evolutionary energy, see Appendix A, Eq. (A.1a)	t	time
\mathcal{E}	time-integral of all of the running energy expenditures in a dynamic process; evolving energy, see Appendix A, Eq. (A.1b)	t_f	upper temporal limit of Hamilton's Law of Varying Action
\mathbf{E}	modal vector $\in \mathbf{F}^n$	t_i	lower temporal limit of Hamilton's Law of Varying Action
$[\mathbf{E}]_N$	matrix of null-space basis vectors, $[\mathbf{E}_1, \dots, \mathbf{E}_{2N}]$	t_k	initial time of transition interval
$[\mathbf{E}]_R$	matrix of range-space basis vectors, $[\mathbf{E}_{2N+1}, \dots, \mathbf{E}_{Nn}]$	t_{k+1}	final time of transition interval
f	external forcing function	T	kinetic energy
\mathcal{F}^{HLVA}	vector-space of functions that satisfy Hamilton's Law of Varying Action, $\in \mathbf{P}$	$[\mathbf{U}]$	column orthonormal matrix containing basis vectors that span the range-space, $\in \mathbf{F}^n$
\mathbf{F}^n	vector-space of coordinates	$[\mathbf{V}]$	orthonormal matrix containing basis vectors that span the null-space, $\in \mathbf{F}^n$
$HLVA$	Hamilton's Law of Varying Action	δW	evolutional work expression
i	summation, matrix, and vector indice	β	modal coordinate, $\in \mathbf{F}^n$
j	summation, matrix, and vector indice	$\mathbf{\beta}_N$	null-space modal coordinates $[\beta_1, \dots, \beta_{2N}]^T \in \mathbf{F}^n$
k	summation, matrix, vector, and transition interval indice	$\mathbf{\beta}_R$	range-space modal coordinates $[\beta_{2N+1}, \dots, \beta_{Nn}]^T \in \mathbf{F}^n$
k_i	linear stiffness coefficient	δ	evolutional operator set equivalent to \mathcal{D} for compatibility with Öz [24]
k_{nl_i}	nonlinear stiffness coefficient	δ_t	see Eq. (31)
K_i	exponent governing spread of Gaussian temporal-basis-function with center at τ_i	\mathcal{D}	evolutionary operator defined in Öz [24], see Appendix A
l	summation, matrix, vector, and transition interval indice	σ	singular value
m_i	mass associated with the i th degree-of-freedom	λ	eigenvalue of $[\mathbf{P}]$
n	total number of temporal-basis-functions	τ	nondimensional time
N	total number of degrees-of-freedom	τ_{ij}	temporal center of Gaussian temporal-basis-function
$[\mathbf{P}]$	matrix representation of Hamilton's Law of Varying Action	ψ	row vector of temporal-basis-functions, $\in \mathcal{F}^{HLVA}$
\mathbf{P}	vector space of polynomials	$(\dots)'$	derivative with respect to nondimensional time
\mathbf{q}	column vector (N -tuple) of coordinates q_r , $\in \mathcal{F}^{HLVA}$	(\dots)	derivative with respect to real time
q_0	initial displacement	(\dots)	trial entities
\dot{q}_0	initial velocity in real time	(\dots)	entities associated with reduced modal matrices
\mathbf{q}_i^*	i th vector-valued fundamental-time-mode being an N -tuple of component functions $q_{ri}^*(\tau)$, $1 \leq i \leq 2N$ ($\leq Nn$ for forced systems)	$(\dots)_N$	entities in null-space, $\in \mathbf{F}^n$
		$(\dots)_R$	entities in range-space, $\in \mathbf{F}^n$
		Δt	$= t_{k+1} - t_k$, time span of transition interval when time-marching.
			$= t_f - t_i$, without time-marching

1. Introduction

Over the past three decades, an equation referred to as Hamilton's Law of Varying Action has been applied to linear, nonlinear, time invariant and time varying dynamic systems to solve the response problem directly, without the use of differential equations of motion [1–14]. Direct control methodologies have also been implemented using Hamilton's Law of

Varying Action [15–19]. In other endeavors, Hamilton's Law of Varying Action has been used to develop perturbation techniques [20] and sensitivity analysis [21], and to model stochastic systems [22].

The equation referred to as Hamilton's Law of Varying Action may be expressed as

$$\int_{t_0}^{t_f} (\delta T + \delta W) dt - \sum_r \left. \frac{\partial T}{\partial \dot{q}_r} \delta q_r \right|_{t_0}^{t_f} = 0, \quad (1)$$

where $q_r(t)$ is the dependent variable representing the displacement (which may or may not be a generalized coordinate) of the r th degree-of-freedom for an N -degree-of-freedom system. However, in the use of Eq. (1) in this paper (and in all of the previous works of the authors') the variations of energy and work quantities are not virtual variations but real path alterations which we refer to as evolutionary changes along the dynamically real path of motion and must not be misconstrued as virtual variations associated with the variational principles of classical dynamics (see Appendix A). T is the kinetic energy of the system and $\delta W = \sum Q_r \delta q_r$ is the (real) evolutionary work expression, which includes the work of the conservative, non-conservative, and damping forces, where Q_r are the associated (generalized) forces. The concepts associated with the operator symbol δ signify real changes or alterations in a particular direction (defined as evolutions) in the real system processes and are associated with the recently enunciated Law of Evolutionary Energy and its methodology referred to as the Evolutionary Energy Method [23,24]. The physical and mathematical nature of the evolutionary symbol δ within the context of the Law of Evolutionary Energy is illustrated in Appendix A, and more details are included in Ref. [24]. The Law of Evolutionary Energy is an ultimate statement of energy conservation in the form of a time-integral of energy-work interactions for real physical processes of a dynamic system, and inherently encompasses the First Law of Thermodynamics. Appendix A provides insight to the background of Eq. (1) as we use it, which is the working equation of this article and has been the working equation of the authors' previous articles, to distinguish it from virtual concepts and virtual variational principles of classical dynamics. It is shown in Appendix A that Eq. (1), as we use and have been using it in our works, falls under the umbrella of the broader concept of the Law of Evolutionary Energy involving quantifiable real path changes which must also satisfy the underlying energy conservation law along (or attached to) the real dynamic path. Thus, the symbol δ corresponds to the real physical and mathematical nature of these (energy-conservation compliant) evolutionary path changes, and therefore is recognized and defined as an evolutionary symbol or operator. It is not the variational symbol or operator, which is often associated with virtual principles and variations in classical dynamics.

In applying Eq. (1), it is comforting to note that the mathematical use of the symbol δ remains the same as in variational and differential calculus. With this understanding and distinction from virtual variations emphasized, in this article for the last time, we will use the symbol δ to denote the real variation (evolution) and real variational (evolutional) operator for compatibility with the previous companion paper [25]. Subsequent articles will use the new evolutionary operator symbol \mathcal{D} [24] instead of δ , and Eq. (1) will be referred to as the Mechanical Law of Evolutionary Energy. As shown in Appendix A, the application of the Law of Evolutionary Energy to a mechanical system leads to the appearance in the same equation of both the current working form of Hamilton's Law of Varying Action, Eq. (1), and the authentic form of the only enunciated "law of varying action" by Hamilton [26] which are not the same expressions. The latter expression does not appear in the classical dynamics texts and literature. Eq. (1) has never been explicitly stated by Hamilton, but can only be inferred (perhaps subjectively) from Hamilton's second essay [27] following and with proper use of his authentic "law of varying action" [26]. Recently, Hamilton's Law of Varying Action has been viewed from a vector-space perspective, which resulted in the implementation of Hamilton's Law of Varying Action using a vector-space algorithm denoted as the "Universal Procedure". This procedure was first applied to linear systems in Ref. [25], and is extended to nonlinear systems herein. Prior to the vector-space perspective, researchers had been bound to the idea that the dependent variables must be represented by a basis function expansion constrained in form to include the initial conditions explicitly [6], or that the use of basis functions unconstrained in form to include the initial conditions explicitly required the augmentation of Hamilton's Law of Varying Action with Lagrange multipliers [28]. However, neither of these notions is a requirement for implementing Hamilton's Law of Varying Action as demonstrated in Ref. [25].

The "universal procedure" represents the dependent variables by an expansion of *any* admissible set of *temporal-basis-functions* unconstrained in form, while preserving Hamilton's Law of Varying Action in its original form (without Lagrange multipliers). This vector-space implementation generates a basis of spatiotemporal functions over the time interval (t_i, t_f) . These spatiotemporal functions are denoted as *fundamental-time-modes* that constitute a basis for the response of linear and nonlinear systems. For linear systems, the vector-space perspective provides the capability to generate the general response solution, in addition to the unique response also provided by other methods [25]. Perhaps most importantly, the vector-space perspective provides the framework necessary to overcome the line of thought that the upper temporal limit of Hamilton's Law of Varying Action must conceptually have a finite value, which would infer that Hamilton's Law of Varying Action could only be successfully applied over small time intervals. However, the upper temporal limit of Hamilton's Law of Varying Action is in concept unbounded. The only limitation on the value of the upper limit with regard to the direct implementation of Hamilton's Law of Varying Action, is the availability of suitable temporal-basis-functions.

Since Hamilton's Law of Varying Action is valid over any time interval, there exist fundamental-time-modes that span the solution space of Hamilton's Law of Varying Action for infinite-time, providing a basis for the infinite-time response. Fundamental-time-modes spanning the solution space for infinite-time are denoted as *genuine* fundamental-time-modes, which may not be known explicitly, but may be approximated in a *local* or *global* sense using the vector-space approach

presented in this work. The only impediments to accurately approximating the genuine fundamental-time-modes are the availability of suitable temporal-basis-functions. These concepts will be presented in more detail in Section 1.1.

When eigenfunctions span the solution space of Hamilton's Law of Varying Action for all time, they will likewise be denoted as genuine eigenfunctions. For linear systems, the fundamental-time-modes characterizing free-motion, are the vector-valued eigenfunctions of temporal dependency, which satisfy Hamilton's Law of Varying Action excluding the generalized forcing vector.

Even though the fundamental-time-modes are the eigenfunctions of Hamilton's Law of Varying Action for linear systems exhibiting free-motion, they are not always equivalent to the natural modes of the system. Also, the fundamental-time-modes are not always the eigenfunctions of Hamilton's Law of Varying Action for nonlinear systems. Therefore, fundamental-time-modes cannot be characterized in general as natural modes or eigenfunctions, and thus their distinctive name is warranted.

The main intent of this work is aimed at presenting the vector-space implementation of Hamilton's Law of Varying Action for nonlinear systems. Key features and capabilities resulting from this vector-space perspective will be illustrated. Classical model reduction techniques will be used to eliminate non-dominant fundamental-time-modes from the solution process, demonstrating model reduction in the time domain. In addition, linear independent fundamental-time-mode response trajectories along eigen-directions can be superposed to yield new response trajectories for the nonlinear system. This capability of the vector-space approach will be demonstrated for systems exhibiting nonlinear normal mode response.

Although it is not commonly taught, superposition is possible for nonlinear systems. Two examples of other efforts in this area are presented in Refs. [29,30]. Nonetheless, even though superposition for nonlinear systems is not new, it is remarkably demonstrated in this work. In addition, the search for superposable trajectories is made possible by introduction of the novel concept of eigen-direction iteration.

1.1. Preliminaries

From the vector-space viewpoint, Hamilton's Law of Varying Action is an operator that maps to zero the time-integral of the work done by all of the forces (including inertia forces), acting on or within the system. Hamilton's Law of Varying Action operates in the vector-space of functions \mathcal{F}^{HLVA} , spanning the displacements and their derivatives, which satisfy the operator over the time interval ($t_i \leq t \leq t_f$). The basis functions of \mathcal{F}^{HLVA} are the fundamental-time-modes of Hamilton's Law of Varying Action.

The temporal limits t_i and t_f are completely arbitrary and unbounded. Finite values are usually assigned to the temporal limits t_i and t_f in time-domain initial value problems, either because the response solution is only sought over a finite time, or due to limitations imposed by the particular method used to implement Hamilton's Law of Varying Action. For frequency domain problems where synchronous or harmonic motion is assumed, the temporal limits are usually chosen such that time may be easily integrated out of the problem. Assigning temporal limits to t_i and t_f does not mean that Hamilton's Law of Varying Action has some limit of applicability, but merely indicates a limitation imposed by the analyst for whatever reason.

In the most general sense, \mathcal{F}^{HLVA} spans the displacements and their derivatives that are valid for infinite-time ($0 \leq t \leq \infty$). In this case, the basis functions of \mathcal{F}^{HLVA} are denoted as the genuine fundamental-time-modes. For single-degree-of-freedom and multi-degree-of-freedom systems, these fundamental-time-modes are scalar and vector-valued, respectively. The time-space path is continuous with continuous first derivatives over some time interval (t_i, t_f) and therefore is a continuous function over (t_i, t_f) [1]. Consequently, it may be represented by a power series expansion according to the Weierstrass theorem. Since the power series are a natural basis for the vector-space of polynomials \mathbf{P} , it can be concluded that \mathcal{F}^{HLVA} (spanning the time-space path) is a subspace of the vector-space \mathbf{P} .

Any response may be represented by an admissible expansion of temporal-basis-functions. An admissible set of basis functions are those exhibiting continuous derivatives over the time interval (t_i, t_f). For distributed-parameter systems, spatial-basis-functions are included, which typically satisfy the spatial boundary conditions. In situations where abrupt changes in forces occur, the interval ($t_i \leq t \leq t_f$) may need to be chosen such that the expansion of temporal-basis-functions can adequately approximate the time-space path. However, this is merely a limitation imposed by the particular set of basis functions.

Consider Hamilton's Law of Varying Action from the view-point of infinite-time

$$\int_{t_i=0}^{t_f=\infty} (\delta T + \delta W) dt - \sum_r \left. \frac{\partial T}{\partial \dot{q}_r} \delta q_r \right|_{t_i=0}^{t_f=\infty} = 0. \quad (2)$$

In this situation, $\cos(\omega t)$, $\sin(\omega t)$ and $e^{i\omega t}$ are examples of genuine fundamental-time-modes of Hamilton's Law of Varying Action for many single degree-of-freedom discrete linear systems undergoing simple harmonic free-motion. For multi-degree-of-freedom linear systems exhibiting simple harmonic free-motion, the genuine fundamental-time-modes are vector-valued with temporal components $\cos(\omega t)$, $\sin(\omega t)$ or $e^{i\omega t}$ common to each degree-of-freedom. In fact, in these cases the genuine fundamental-time-modes are equivalent to the genuine eigenfunctions of Hamilton's Law of Varying Action. Clearly, these genuine fundamental-time-modes are equally valid for finite temporal limits as well. Since in most practical applications, the temporal-basis-functions chosen (e.g., $\{\tau, \tau^2, \tau^3, \dots\}$) are not the temporal part of the genuine fundamental-time-modes (e.g., $\{\cos(\omega t), \sin(\omega t)\}$) of Hamilton's Law of Varying Action, the response can only be accurately approximated over a finite interval of time (t_l, t_u). Outside of this interval, the ability of the temporal-basis-functions to

approximate the genuine fundamental-time-modes is reduced. Therefore, in order to generate response solutions for times exceeding the span of the temporal-basis-functions $(t_i \leq t \leq t_f) > (t_l, t_u)$, the total time of interest $(t_i \leq t \leq t_f)$ is divided into sequential transition intervals $(t_k, t_{k+1}) \leq (t_l, t_u)$.

Hamilton’s Law of Varying Action is expressed in terms of sequential transition intervals as

$$\int_{t_i}^{t_f} (\delta T + \delta W) dt - \sum_r \frac{\partial T}{\partial \dot{q}_r} \delta q_r \Big|_{t_i}^{t_f} = \sum_{k=0}^K \left\{ \int_{t_k}^{t_{k+1}} (\delta T + \delta W) dt - \sum_r \frac{\partial T}{\partial \dot{q}_r} \delta q_r \Big|_{t_k}^{t_{k+1}} \right\} = 0, \quad k = 0, 1, 2, \dots, K \quad (3)$$

where k is the transition interval index, $t_i = t_0$, $t_f = t_{k+1}$, and K is the number of intervals. Continuity of displacement and velocity are satisfied at the temporal boundaries of the transition intervals as shown in terms of nondimensional time τ

$$q_r^{k+1}(\tau = 0) = q_r^k(\tau = 1), \quad \Delta t q_r^{k+1}(\tau = 0) = \Delta t q_r^k(\tau = 1), \quad (4)$$

where $\Delta t = t_{k+1} - t_k$, $t = \Delta t \tau$ and $(\cdot)' = d(\cdot)/d\tau$. The transition intervals do not need to be equispaced in time. It is possible, and will be demonstrated herein, that (t_l, t_u) can span one period of oscillation for nonlinear systems. In situations where the temporal-basis-functions are chosen as the temporal part of the genuine fundamental-time-modes [25], $(t_k, t_{k+1}) = (t_l, t_u) = (0, \infty)$.

In general, the genuine fundamental-time-modes are not known a-priori and are approximated over the transition intervals (t_k, t_{k+1}) in due course of implementing the vector-space approach via the choice of temporal-basis-functions. An approximation, spanning the minimum time required to fully characterize a genuine fundamental-time-mode, is denoted as a “global” approximation. An example of a global approximation would be that which spans one period of a synchronous linear or nonlinear system. If the approximations are not “global”, they are “local”, i.e., over a transition interval smaller than a characteristic time. Global fundamental-time-modes approximate the response over a complete period and thus each time-mode repeats itself over each period.

The vector-space perspective is a view of Hamilton’s Law of Varying Action in terms of vector-spaces (including functions spaces), which are defined by the principles of linear algebra. The “universal procedure” is an algorithm that generates the response by taking advantage of this vector-space perspective. In this work, “universal procedure” will be used synonymously with “vector-space implementation” or “vector-space approach”.

2. Vector-space perspective

A concise overview of the vector-space and temporal viewpoints of Hamilton’s Law of Varying Action has been presented in Section 1. This section, presents an in-depth look at the process of implementing Hamilton’s Law of Varying Action for nonlinear systems from a vector-space perspective. By combining the method of iteration with the linear algebraic principles and vector-space concepts, the vector-space implementation of Hamilton’s Law of Varying Action is made possible for nonlinear systems.

2.1. Traditional approach

The traditional method of implementing Hamilton’s Law of Varying Action for nonlinear systems will not be presented here in detail, but a brief statement is made to provide a comparison to the vector-space approach. This method utilizes an iteration scheme that depends on the use of temporal-basis-functions $[\Psi(t)]$ constrained in form to explicitly include the initial conditions $\mathbf{A}_0 = [q_0 \ q_0']^T$ as shown for the single degree-of-freedom system.

$$q(\tau) = [\Psi_0(\tau)]\mathbf{A}_0 + [\Psi(\tau)]\bar{\mathbf{A}} \quad (5)$$

The reader is referred to Bailey [1,2] for further details.

While the procedure of Bailey [1,2] works fine for temporal-basis-functions that inherently contain the initial conditions explicitly, it requires the modification of other temporal-basis-functions that are not inherently constrained in form to explicitly include the initial conditions to meet the form of Eq. (5). This may, depending on the temporal-basis-functions chosen, alter their approximation characteristics initially desired by the analyst. The vector-space implementation through the universal procedure, removes the constraints in form imposed on the basis function expansions by the traditional approach. This permits the use of *any* set of admissible unconstrained basis functions, preserving their unique characteristics, which may have been compromised by altering them to include the initial conditions as required by the traditional approach.

2.2. Vector-space approach

The vector-space approach is implemented using unconstrained temporal-basis-functions as shown,

$$q(\tau) = [\Psi(\tau)]\mathbf{A}, \quad t = \Delta t \tau \quad (6)$$

and as a result, the expansion coefficients are not segregated into those that represent the initial conditions and those that are unknown, as in Eq. (5) for the traditional approach. Instead, all of the expansion coefficients are treated as unknowns.

Substituting the unconstrained temporal-basis-function expansions into Hamilton’s Law of Varying Action for a nonlinear system results in a set of nonlinear algebraic equations of motion in the following homogeneous or nonhomogeneous forms:

$$[\mathbf{P}(\mathbf{A})]\mathbf{A} = 0 \tag{7}$$

and

$$[\mathbf{P}(\mathbf{A}_R)]\mathbf{A}_R = \mathbf{b}. \tag{8}$$

Unforced nonlinear systems result in homogeneous equations. The nonlinear system is generally nonhomogeneous ($\mathbf{b} \neq 0$) when external forces are present. External forces that are functions of the displacement and/or its derivatives (e.g., follower forces) may be incorporated into $[\mathbf{P}(\mathbf{A})]$ so that for systems subjected solely to follower forces, a system of homogeneous equations also results just as for an unforced system. $[\mathbf{P}(\mathbf{A})]$ is in general not unique for a given nonlinear system.

For the sake of understanding the generality of the exposition, one may consider that $\{\psi(t)\}$ in Eq. (6) are the temporal components of the genuine fundamental-time-modes of the system and \mathbf{A} are the participation factors characterizing the motion in the overall response for the global transition interval. The vector-space approach for linear systems as described in Ref. [25] is a special case of the approach presented herein.

2.2.1. Free-motion (null-space solution)

With all of the expansion coefficients \mathbf{A} treated as unknowns, the resulting algebraic equations of motion as shown in Eq. (7) for the free-motion of any N -degree-of-freedom dynamic system, requires that a nontrivial solution vector \mathbf{A} reside in the null-space of $[\mathbf{P}(\mathbf{A})] \in \mathbf{F}^n$. Moreover, \mathbf{A} will be comprised of a linear combination of the null-space basis vectors, determined from the following eigenvalue problem

$$[\mathbf{P}(\mathbf{A}(\mathbf{E}_N))]\mathbf{E}_i = \lambda_i \mathbf{E}_i \quad (\lambda_i = 0, i = 1, 2, \dots, 2N) \tag{9}$$

where $2N$ zero eigenvalues are sought by iteration, their corresponding eigenvectors forming a basis for the null-space of $[\mathbf{P}(\mathbf{A}(\mathbf{E}_N))]$. For each eigenvalue λ_i there corresponds an eigenvector \mathbf{E}_i consisting of n components for each degree-of-freedom $[e_1^1 e_2^1 \dots e_n^1 e_2^2 e_3^2 \dots e_n^2 \dots e_1^N e_2^N \dots e_n^N]^T$, where each degree-of-freedom is represented by n temporal-basis-functions. $[\mathbf{P}(\mathbf{A}(\mathbf{E}_N))]$ is of size $nN \times nN$, where N is the total number of degrees-of-freedom. $\mathbf{A}(\mathbf{E}_N)$ represents an expansion of \mathbf{A} in terms of the null-space basis vectors \mathbf{E}_N , and modal coordinates β_N

$$\mathbf{A}(\mathbf{E}_N) \begin{Bmatrix} \mathbf{A}^1 \\ \mathbf{A}^2 \\ \vdots \\ \mathbf{A}^N \end{Bmatrix} = \{\mathbf{E}_1 \beta_1 + \mathbf{E}_2 \beta_2 + \dots + \mathbf{E}_{2N} \beta_{2N}\} = \{[\mathbf{E}]_N \beta_N\} \tag{10}$$

From here on, the functional dependency of \mathbf{A} on \mathbf{E} will not be explicitly indicated.

Two initial conditions, $q(0)$ and $\dot{q}(0)$, in the free-motion solution space (null-space) in \mathcal{F}^{HLVA} are necessary to uniquely characterize the trajectory for each degree-of-freedom. Since these initial conditions must be spanned by the null-space, the dimension of the null-space of \mathcal{F}^{HLVA} for an N -degree-of-freedom system, must be $2N$, which is twice the number of degrees-of-freedom.

Now, consider the vector-space \mathbf{F}^n . From linear algebra, the solutions of $[\mathbf{P}(\mathbf{A})]\mathbf{A} = 0$ reside in the null-space of $[\mathbf{P}(\mathbf{A})] \in \mathbf{F}^n$. Since $[\mathbf{P}(\mathbf{A})] \in \mathbf{F}^n$ is the matrix representation of Hamilton’s Law of Varying Action $\in \mathcal{F}^{HLVA}$ per the representation theorem [31, pp. 364–365], the null-space of $[\mathbf{P}(\mathbf{A})] \in \mathbf{F}^n$ must be of the same dimension as the null-space of Hamilton’s Law of Varying Action $\in \mathcal{F}^{HLVA}$. In other words, the $2N$ initial conditions spanned by the null-space in \mathcal{F}^{HLVA} must be accommodated by $2N$ null-space basis vectors in \mathbf{F}^n , since $[\mathbf{P}(\mathbf{A})]$ is the matrix representation of Hamilton’s Law of Varying Action. Therefore, there must be $2N$ null-space basis vectors $\{\mathbf{E}_i : \lambda_i = 0, i = 1, 2, \dots, 2N\} \in \mathbf{F}^n$ that compose \mathbf{A} . At the same time, the set of eigenvectors $\mathbf{E}_R = \{\mathbf{E}_i : \lambda_i \neq 0, i = 2N + 1, \dots, nN\}$ form a basis for the range-space of $[\mathbf{P}(\mathbf{A})] \in \mathbf{F}^n$. The $N(n-2)$ number of range-space basis vectors follows from the rank and nullity theorem of linear algebra.

The displacement and velocity response for the N -degree-of-freedom dynamic system may be expressed more succinctly in terms of fundamental-time-modes \mathbf{q}_i^* as

$$\mathbf{q}(\tau) = \begin{Bmatrix} q_1(\tau) \\ q_2(\tau) \\ \vdots \\ q_N(\tau) \end{Bmatrix} = \begin{bmatrix} \backslash & & & \\ & \Psi(\tau) & & \\ & & \backslash & \\ & & & \end{bmatrix} \begin{Bmatrix} \mathbf{A}^1 \\ \mathbf{A}^2 \\ \vdots \\ \mathbf{A}^N \end{Bmatrix} = \begin{bmatrix} \backslash & & & \\ & \Psi(\tau) & & \\ & & \backslash & \\ & & & \end{bmatrix} [\mathbf{E}]_N \beta_N = \sum_{i=1}^{2N} q_i^*(\tau) \beta_i = [\mathbf{q}_i^*(\tau)]_N \beta_N \tag{11}$$

$$\mathbf{q}'(\tau) = \begin{Bmatrix} q'_1(\tau) \\ q'_2(\tau) \\ \vdots \\ q'_N(\tau) \end{Bmatrix} = \begin{bmatrix} \backslash & & & \\ & \Psi'(\tau) & & \\ & & \backslash & \\ & & & \end{bmatrix} \begin{Bmatrix} \mathbf{A}^1 \\ \mathbf{A}^2 \\ \vdots \\ \mathbf{A}^N \end{Bmatrix} = \begin{bmatrix} \backslash & & & \\ & \Psi'(\tau) & & \\ & & \backslash & \\ & & & \end{bmatrix} [\mathbf{E}]_N \beta_N = \sum_{i=1}^{2N} q_i'^*(\tau) \beta_i = [\mathbf{q}_i'^*(\tau)]_N \beta_N, \tag{12}$$

where the fundamental-time-modes are defined as

$$\mathbf{q}_i^*(\tau) = \begin{Bmatrix} q_1^*(\tau) \\ q_2^*(\tau) \\ \vdots \\ q_N^*(\tau) \end{Bmatrix}_i = \begin{bmatrix} \backslash & & \\ & \Psi(\tau) & \\ & & \backslash \end{bmatrix} \mathbf{E}_i \quad (i = 1, 2, \dots, 2N), \tag{13}$$

and consist of an N -tuple of scalar functions $q_n^*(\tau)$ designated as the r th component function of the i th fundamental-time-mode.

Arranging Eqs. (11) and (12) in matrix form, results in

$$[\Psi(\tau)][\mathbf{E}]_N \boldsymbol{\beta}_N = \begin{Bmatrix} \mathbf{q}(\tau) \\ \mathbf{q}'(\tau) \end{Bmatrix}, \tag{14}$$

where

$$[\Psi(\tau)] = \begin{bmatrix} \backslash & & \\ & \Psi(\tau) & \\ & & \backslash \\ & & & \Psi'(\tau) \\ & & & & \backslash \end{bmatrix}, \tag{15}$$

From Eq. (14), the null-space modal coordinates may be expressed in terms of the known initial conditions as shown

$$\boldsymbol{\beta}_N = ([\Psi(0)][\mathbf{E}]_N)^{-1} \begin{Bmatrix} \mathbf{q}(0) \\ \mathbf{q}'(0) \end{Bmatrix}. \tag{16}$$

Hamilton's Law of Varying Action in the form of Eqs. (1) or (7) is exactly satisfied and provides the exact response, when the temporal part of the genuine fundamental-time-modes of Hamilton's Law of Varying Action are used as the temporal-basis-functions. However, the genuine fundamental-time-modes for nonlinear systems are not generally known. Many problems will not have known closed-form genuine fundamental-time-modes, so constructing their approximation using an expansion of temporal-basis-functions spanning \mathcal{F}^{HLVA} is the only alternative. Consequently, trial temporal-basis-functions will be used which will serve to span the vector-space \mathcal{F}^{HLVA} , and thus approximate the response of the system. The degree to which the unique response of a dynamic system will be approximated is dependent on how completely these trial temporal-basis-functions span this vector-space. These trial temporal-basis-functions may be varied in quantity and character, until a satisfactory approximation to the response is achieved. The eigenvalue problem resulting from the use of these trial temporal-basis-functions is solved by iteration and will be expressed as

$$[\hat{\mathbf{P}}(\hat{\mathbf{A}})]\hat{\mathbf{E}} = \hat{\lambda}\hat{\mathbf{E}}, \tag{17}$$

where $(\hat{\cdot})$ denotes trial or non-converged entities. An initial value of the expansion coefficients $\hat{\mathbf{A}}_h$ (see Section 2.2.6 for details) are selected, fixing $[\hat{\mathbf{P}}(\hat{\mathbf{A}})]$ for the current iterate, whereby $2N$ trial eigenvalues $\hat{\lambda}$ closest to nullity and their corresponding trial basis vectors $\hat{\mathbf{E}}_N$ are selected. Using these basis vectors, updated trial expansion coefficients $\hat{\mathbf{A}}_{h+1}$ are generated as shown

$$\hat{\mathbf{A}}_{h+1} = \begin{Bmatrix} \mathbf{A}^1 \\ \mathbf{A}^2 \\ \vdots \\ \mathbf{A}^N \end{Bmatrix}_{h+1} = \{\hat{\mathbf{E}}_1\hat{\beta}_1 + \hat{\mathbf{E}}_2\hat{\beta}_2 + \dots + \hat{\mathbf{E}}_{2N}\hat{\beta}_{2N}\}_h = \{[\hat{\mathbf{E}}]_N\hat{\boldsymbol{\beta}}_N\}_h, \tag{18}$$

using the trial modal coordinates

$$\hat{\boldsymbol{\beta}}_N = ([\Psi(0)][\hat{\mathbf{E}}]_N)^{-1} \begin{Bmatrix} \mathbf{q}(0) \\ \mathbf{q}'(0) \end{Bmatrix}. \tag{19}$$

The trial expansion coefficients $\hat{\mathbf{A}}_{h+1}$ may be compared to $\hat{\mathbf{A}}_h$ to determine convergence. If the expansion coefficients $\hat{\mathbf{A}}_{h+1}$ have not converged, they are substituted back into $[\hat{\mathbf{P}}(\hat{\mathbf{A}})]$ seeking yet another set of trial eigenvalues closest to nullity along with their corresponding trial basis vectors. This is repeated until convergence of $\hat{\mathbf{A}}_{h+1}$ is achieved.

When the trial expansion coefficients converge, the set of trial eigenvalues are checked for $2N$ null values. If $2N$ zero eigenvalues exist, Eq. (9) is satisfied and the trial system matrix $[\hat{\mathbf{P}}(\hat{\mathbf{A}})]$ has converged to the correct matrix representation of Hamilton's Law of Varying Action denoted as $[\mathbf{P}(\mathbf{A})]$. At this point, the correct converged expansion coefficients will have been obtained, and are denoted as \mathbf{A}_{conv} . If $2N$ zero eigenvalues do not result, then the converged expansion coefficients are not correct. In this case, the set of temporal-basis-functions is modified in quantity or character or the temporal limits on Hamilton's Law of Varying Action adjusted, before solving the trial eigenvalue problem again.

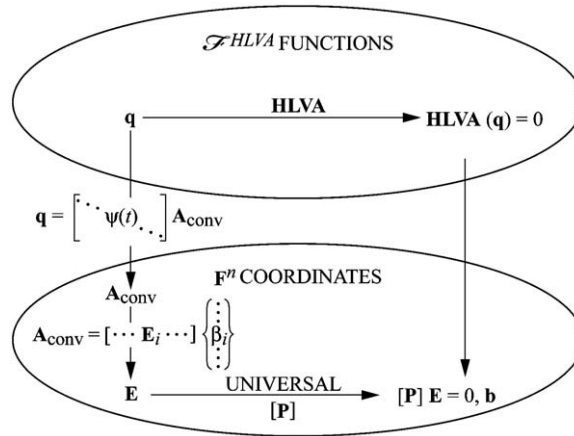


Fig. 1. Representation theorem as applied to Hamilton's Law of Varying Action for nonlinear systems. $HLVA(\mathbf{q}) = \int_{t_i}^{t_f} (\delta T + \delta W) dt - \sum_r \frac{\delta T}{\delta \dot{q}_r} \delta \dot{q}_r |_{t_i}^{t_f} = 0$.

A satisfactory selection of temporal-basis-functions is indicated by the degree to which $2N$ eigenvalues of $[\mathbf{P}]$ approach zero, the expansion coefficients having also converged to their respective values. Ultimately, a satisfactory approximation to the response is determined as put forth in Section 2.2.5. It is possible to obtain convergence of the expansion coefficients without $2N$ eigenvalues converging to zero, but this would not constitute a solution of Hamilton's Law of Varying Action. The expansion coefficients \mathbf{A} , satisfying Hamilton's Law of Varying Action, are those that have converged, and at the same time have provided a set of $2N$ zero eigenvalues.

At this point, the trial entities are now converged quantities; $[\hat{\mathbf{P}}(\hat{\mathbf{A}})] = [\mathbf{P}(\mathbf{A}_{conv})]$, $\hat{\mathbf{E}} = \mathbf{E}$, $\hat{\lambda} = \lambda$, $\hat{\beta}_N = \beta_N$, the null-space basis vectors $\mathbf{E}_N = \{\mathbf{E}_i : \lambda_i = 0, i = 1, \dots, 2N\}$ and the range-space basis vectors $\mathbf{E}_R = \{\mathbf{E}_i : \lambda_i \neq 0, i = 2N + 1, \dots, nN\}$ of $[\mathbf{P}(\mathbf{A})] \in F^n$ having been determined simultaneously. Since \mathbf{A}_{conv} has been determined at this point, $[\mathbf{P}(\mathbf{A}_{conv})]$ is now an invariant matrix of known scalars for the time interval at hand

$$[\mathbf{P}]\mathbf{A} = 0. \tag{20}$$

The expansion coefficients \mathbf{A}_{conv} , are not explicitly shown in Eq. (20) indicating that the iteration is complete, the expansion coefficients being "absorbed" into $[\mathbf{P}]$. At this point, $[\mathbf{P}]$ is the true matrix representation of the Hamilton's Law of Varying Action transformation or mapping for the transition interval (t_k, t_{k+1}) considered, according to the representation theorem of linear algebra [31, pp. 364–366].

Fig. 1 shows pictorially, the representation theorem as applied to the universal procedure associated with Hamilton's Law of Varying Action. Here, in the vector-space of coordinates F^n , the coordinates \mathbf{A}_{conv} are related to the null-space modal coordinates β_N through the null-space modal matrix \mathbf{E}_N . The representation theorem is being used only at the point where the coefficients \mathbf{A} have converged, and where $2N$ eigenvalues are zero.

The unique free response for the N -degree-of-freedom nonlinear system in \mathcal{F}^{HLVA} , may be expressed by re-attaching the converged set of expansion coefficients $\mathbf{A}_{conv} \in F^n$ to the temporal-basis-functions $[\Psi\tau] \in \mathcal{F}^{HLVA}$, resulting in the $2N$ null-space fundamental-time-mode composition of the unique free response

$$\begin{Bmatrix} \mathbf{q}(\tau) \\ \mathbf{q}'(\tau) \end{Bmatrix} = \begin{bmatrix} \Psi(\tau) \\ \Psi'(\tau) \end{bmatrix} \mathbf{A}_{conv} = \begin{bmatrix} \Psi(\tau) \\ \Psi'(\tau) \end{bmatrix} \begin{Bmatrix} \mathbf{A}^1 \\ \mathbf{A}^2 \\ \vdots \\ \mathbf{A}^N \end{Bmatrix}_{conv} = [\Psi(\tau)][\mathbf{E}]_N \beta_N = \begin{bmatrix} \mathbf{q}^*(\tau) \\ \mathbf{q}'^*(\tau) \end{bmatrix}_N \beta_N, \tag{21}$$

where the superscript on \mathbf{A} is the degrees-of-freedom index.

The unique response satisfying the initial conditions is provided by the null-space modal coordinates β_N , which are simultaneously generated by the iteration process along with the null-space basis vectors \mathbf{E}_N . In contrast, the process for linear systems [25] determines the null-space modal coordinates after the basis vectors are generated. The modal coordinates β_N serve to scale the basis vectors \mathbf{E}_N such that the initial conditions are satisfied.

2.2.2. Forced-motion (range-space solution)

For the following discussion, it is assumed that \mathbf{A}_{conv} , have been obtained via iteration, resulting in a $[\mathbf{P}]$ matrix having $2N$ zero eigenvalues for the transition interval (t_k, t_{k+1}) .

By virtue of the fact that $[\mathbf{P}]$ has zero eigenvalues, it is singular and therefore cannot be inverted to solve for \mathbf{A}_R per Eq. (8). From linear algebra, the solutions of Eq. (8) reside in the range-space of $[\mathbf{P}] \in F^n$ and therefore the range-space

expansion coefficients \mathbf{A}_R are composed of the $N(n-2)$ range-space basis vectors $\mathbf{E}_R = \{\mathbf{E}_i : \lambda_i \neq 0, i = 2N+1, \dots, nN\}$ obtained simultaneously with the null-space basis vectors.

$$\mathbf{A}_R = [\mathbf{E}]_R \boldsymbol{\beta}_R \tag{22}$$

As with the null-space solution, the range-space solution $\mathbf{q}^R(\tau) \in \mathcal{X}^{HLVA}$ may be composed of the $N(n-2)$ fundamental-time-modes \mathbf{q}_i^* for the range-space

$$\begin{Bmatrix} \mathbf{q}^R(\tau) \\ \mathbf{q}^R(\tau) \end{Bmatrix} = \boldsymbol{\Psi}(\tau)[\mathbf{E}]_R \boldsymbol{\beta}_R = \boldsymbol{\Psi}(\tau)\mathbf{A}_R = \begin{Bmatrix} \backslash \\ \mathbf{q}_i^*(\tau) \\ \backslash \\ \mathbf{q}_i^{*'}(\tau) \\ \backslash \\ \end{Bmatrix}_R \boldsymbol{\beta}_R, \tag{23}$$

where the fundamental-time-modes for the range-space solution are defined the same as for the null-space, as shown in Eq. (13). The range-space modal coordinates $\boldsymbol{\beta}_R$ may be obtained by re-writing Eq. (8) as shown

$$[\mathbf{P}]\mathbf{A}_R = [\mathbf{P}][\mathbf{E}]_R \boldsymbol{\beta}_R = [\mathbf{E}]_R \begin{Bmatrix} \backslash \\ \lambda \\ \backslash \\ \end{Bmatrix}_R \boldsymbol{\beta}_R = \mathbf{b}, \tag{24}$$

where the identity $[\mathbf{P}]\mathbf{E}_i = \lambda_i \mathbf{E}_i$ has been employed, and by left multiplying Eq. (24) by $[\mathbf{E}]_R^T$ and rearranging to obtain

$$\boldsymbol{\beta}_R = ([\mathbf{E}]_R^T [\mathbf{P}] [\mathbf{E}]_R)^{-1} [\mathbf{E}]_R^T \mathbf{b} = \begin{Bmatrix} \backslash \\ \lambda^{-1} \\ \backslash \\ \end{Bmatrix}_R ([\mathbf{E}]_R^T [\mathbf{E}]_R)^{-1} [\mathbf{E}]_R^T \mathbf{b}. \tag{25}$$

If the eigenvectors are orthonormal $[\mathbf{E}]_R^T [\mathbf{E}]_R = [\mathbf{I}]$, Eq. (25) simplifies accordingly and no matrix inversion will be needed. The range-space solution as shown in Eq. (23) may then be obtained by using the range-space basis vectors and their modal coordinates from Eq. (25). Alternatively, \mathbf{A}_R may be calculated directly by left multiplying Eq. (25) by $[\mathbf{E}]_R$, thus providing the range-space solution from Eq. (23).

2.2.3. Complete solution

The complete solution for the forced system may be constructed to represent the displacement and velocity using a linear combination of the $2N$ fundamental-time-modes of the homogeneous (null-space) solution and the $N(n-2)$ fundamental-time-modes of the non-homogeneous (range-space) solution $\mathbf{q}^R(\tau)$ [31], as shown

$$\begin{Bmatrix} \mathbf{q}(\tau) \\ \mathbf{q}'(\tau) \end{Bmatrix} = [\boldsymbol{\Psi}(\tau)]\{([\mathbf{E}]_N \boldsymbol{\beta}_N + \mathbf{A}_R)\} = [\boldsymbol{\Psi}(\tau)][\mathbf{E}]_N \boldsymbol{\beta}_N + \begin{Bmatrix} \mathbf{q}^R(\tau) \\ \mathbf{q}^R(\tau) \end{Bmatrix} = \begin{Bmatrix} \backslash \\ \mathbf{q}^*(\tau) \\ \backslash \\ \mathbf{q}^*(\tau) \\ \backslash \\ \end{Bmatrix}_N \boldsymbol{\beta}_N + \begin{Bmatrix} \backslash \\ \mathbf{q}^*(\tau) \\ \backslash \\ \mathbf{q}^{*'}(\tau) \\ \backslash \\ \end{Bmatrix}_R \boldsymbol{\beta}_R \tag{26}$$

Rearranging Eq. (26), results in

$$\boldsymbol{\beta}_N = ([\boldsymbol{\Psi}(0)][\mathbf{E}]_N)^{-1} \begin{Bmatrix} \mathbf{q}(0) - \mathbf{q}^R(0) \\ \mathbf{q}'(0) - \mathbf{q}^R(0) \end{Bmatrix}, \tag{27}$$

where the modal coordinates $\boldsymbol{\beta}_N$ may be determined using the initial conditions $\mathbf{q}_i(0)$ and $\mathbf{q}'_i(0)$ and the initial states of the range-space solution $\mathbf{q}_i^R(0)$ and $\mathbf{q}'_i^R(0)$. The complete response of the N -degree-of-freedom system may then be constructed from Eq. (26) using $\boldsymbol{\beta}_N$ and the range-space response $\mathbf{q}^R(\tau)$ and $\mathbf{q}^R(\tau)$.

The expansion coefficients for the complete solution are composed of both the $2N$ null-space and $N(n-2)$ range-space basis vectors and their modal coordinates. Therefore, the iteration method for the complete solution is implemented in a slightly different fashion than for the system exhibiting free-motion, in that the null- and range-space basis vectors and their modal coordinates are simultaneously calculated as part of the iteration process for the complete solution. In contrast, the process for linear systems [25] calculates the null-space modal coordinates after the basis vectors are generated. The expansion coefficients of the complete solution are calculated using the following

recursive relationship

$$\mathbf{A}_{h+1} = \left\{ \begin{array}{c} \mathbf{A}^1 \\ \mathbf{A}^2 \\ \vdots \\ \mathbf{A}^N \end{array} \right\}_{h+1} = \{[\mathbf{E}]_N \boldsymbol{\beta}_N + [\mathbf{E}]_R \boldsymbol{\beta}_R\}_h = \{[\mathbf{E}]_N \boldsymbol{\beta}_N + \mathbf{A}_R\}_h, \quad (28)$$

where the null- and range-space modal coordinates are determined using Eqs. (27) and (25), respectively. The expansion coefficients for the h th iteration of the current transition interval, may be compared to the $(h-1)$ iterate to determine convergence. When the coefficients have converged and there are $2N$ zero eigenvalues, the complete response may be generated using a linear combination of the $2N$ fundamental-time-modes of the null-space solution and the $N(n-2)$ fundamental-time-modes of the range-space solution \mathbf{q}^R .

The system response may be marched in time, by updating the algebraic equations of motion, Eqs. (7) or (8), at the beginning of each subsequent transition interval, and by taking the initial conditions of the current transition interval from the final conditions of the previous transition interval. Once the solution is generated, the response may be evaluated at any time within the transition interval since the response for each transition interval is represented by continuous functions of time via the temporal-basis-function expansion.

2.2.4. Utilizing the singular-value decomposition

Up to this point, the universal procedure has been presented using an eigenvalue analysis. However, the singular value decomposition also provides the null- and range-space basis vectors. The singular value decomposition produces two orthonormal matrices $[\mathbf{U}]$, $[\mathbf{V}]$ and a diagonal matrix $[\mathbf{S}]$ of singular values $\boldsymbol{\sigma}$, which are related to $[\mathbf{P}]$ as follows [32,33]

$$[\mathbf{P}] = [\mathbf{U}][\mathbf{S}][\mathbf{V}]^T. \quad (29)$$

When implementing the singular value decomposition, $2N$ null singular values are sought after, the corresponding columns of $[\mathbf{V}]$ providing the null-space basis vectors $\{\mathbf{E}_N = [\mathbf{V}_i] : \sigma_{ii} = 0, i = 1, 2N, \dots, 2N\}$. The columns of $[\mathbf{U}]$ corresponding to the non-zero diagonal elements of $[\mathbf{S}]$ are an orthonormal basis for the range-space $\{\mathbf{E}_R = [\mathbf{U}_i] : \sigma_{ii} \neq 0, i = 2N+1, \dots, nN\}$.

The range-space expansion coefficients \mathbf{A}_R may be computed directly [32,33]

$$\mathbf{A}_R = [\mathbf{P}]^+ \mathbf{b} = [\mathbf{V}][\mathbf{S}]^{-1}[\mathbf{U}]^T \mathbf{b}, \quad (30)$$

where the singular value decomposition inverse of $[\mathbf{P}]$ denoted as $[\mathbf{P}]^+$ has been used, since $[\mathbf{P}]$ is singular and therefore cannot be inverted to solve for \mathbf{A}_R . The inverse of $[\mathbf{S}]$ in Eq. (30) is a diagonal matrix containing the reciprocals of the singular values, i.e., σ_j^{-1} , where σ_j^{-1} is replaced by 0 if $\sigma_j = 0$. Thus the singular value decomposition of $[\mathbf{P}]$ may be used exclusively to calculate the null- and range-space response solutions. The complete response may be obtained by solely using either the eigenvalue analysis or singular value decomposition or a combination of both. The singular value decomposition provides orthonormal null- and range-space basis vectors that are often times advantageous in computational settings. When using the singular value decomposition to calculate the response, the degree of nullity of the $2N$ singular values is an indicator of satisfactory temporal-basis-functions. Ultimately, the accuracy of the approximate response is evaluated as outlined in Section 2.2.5.

2.2.5. Accuracy

In many of the previous papers on Hamilton's Law of Varying Action by other authors, the accuracy of the approximate solution was determined by substituting the calculated displacement and its derivatives into the differential equations of the system (obtainable by integrating Hamilton's Law of Varying Action by parts with respect to time, and then recovering the differential equations from the integrand), and observing how well the differential equations were satisfied. Although this is a legitimate approach for checking accuracy, it seems rather inconsistent to generate a "direct solution" using Hamilton's Law of Varying Action, only to resort to an "indirect method" using differential equations to check the accuracy. The point here is not to disparage the use of differential equations, but merely to offer a consistent approach. Using the following procedure results in a consistent method whereby the solution and its accuracy are ascertained using Hamilton's Law of Varying Action solely.

Once the solution of the algebraic equations of motion is obtained, and the expansion coefficients are re-attached to the temporal-basis-functions, the dependent variables are now known functions of time. As described in Ref. [24], the Law of Evolutionary Energy allows the (evolutional) operator δ to act both on the A-parameters and the time-parameter 't' along the actual path. Therefore, in Eq. (1), δ is a total parameter change operation along the actual path. Since both the A-parameter changes and the time t-parameter changes are independent, Eq. (1) must also be satisfied for the time-parameter change operation. In this regard, the evolution with respect to the time-parameter 't' will be denoted by the symbol δ_t through which an infinitesimal real time-parameter change (or increment) $\delta t = t^*$ will appear in the process along with the running time differential dt for time-integrations. Consequently, since the A's will already be available through the process of A-parameter changes δA , one can proceed to carry out the t-parameter change process δt in Eq. (1)

by employing the chain rule with respect to time in the definition of the δ operator, denoted as δ_t

$$\delta_t(\dots) = \frac{\partial(\dots)}{\partial(\sim)_i} \frac{\partial(\sim)_i}{\partial t} \delta t. \tag{31}$$

Einstein summation notation has been used, where (\sim) represents any quantity. Since, the solution of the dynamic system is already known, because the A 's are known, satisfaction of Eq. (1) through the time operator δ_t automatically becomes a step for verification (of closed-form solutions) or accuracy check (of computational solutions). Hence, using the operator as defined in Eq. (31), Eq. (1) may be expressed as

$$\int_{t_i}^{t_f} \delta_t(T+W) dt - \sum_r \frac{\partial T}{\partial \dot{q}_r} \delta_t(q_r) \Big|_{t_i}^{t_f} = 0, \tag{32}$$

and will be denoted from here on as the *accuracy integral*. The accuracy integral can be recognized as the evaluation of the time-integral of the energy–work interactions along the energy conservation path of the motion, and therefore serves to show how well the solution satisfies the underlying energy conservation equation. The error in the approximate solution may be determined by substituting the approximate solution into the accuracy integral, and noting its degree of nullity.

2.2.6. Universal procedure

Having presented the theory involved in obtaining the unique solutions for free and forced nonlinear systems, it is useful at this point to present a concise sequence of steps, a “universal procedure”, to be used to generate the response solutions for nonlinear systems.

1. Representing the dependent variables with trial temporal-basis-functions, choose initial iteration values for the trial expansion coefficients \mathbf{A} . Initial values of $\{\mathbf{A}\} = \{0\}$ and $\{\mathbf{A}\} = \{1\}$ have been used successfully. Also, an initial estimate of \mathbf{A} may be obtained from Eq. (21) where \mathbf{A} is equal to the singular value decomposition inverse of $\Psi(0)$ multiplied by the initial conditions.
2. Perform an eigenvalue analysis or singular value decomposition of $[\mathbf{P}(\mathbf{A})]$.
3. Choose as \mathbf{E}_N the $2N$ eigenvectors corresponding to the $2N$ “zero” eigenvalues or $2N$ basis vectors from $[\mathbf{V}]$, corresponding to $2N$ “zero” singular values. Choose as \mathbf{E}_R the remaining $N(n-2)$ basis vectors or the $N(n-2)$ column vectors of $[\mathbf{U}]$ corresponding to the non-zero singular values.
4. Obtain \mathbf{A}_R from Eq. (30) using a singular value decomposition of $[\mathbf{P}]$, or from Eq. (22) using \mathbf{E}_R from step 3 and β_R from Eq. (25).
5. Generate the range-space solution using Eq. (23) and \mathbf{A}_R , or \mathbf{E}_R and β_R .
6. Using the known initial conditions and initial states of the range-space solution, solve for the null-space modal coordinates β_N , using Eq. (27).
7. Using \mathbf{E}_N from step 3, β_N from step 6, and \mathbf{A}_R from step 4, calculate new expansion coefficients \mathbf{A} , using Eq. (28).
8. Determine the difference between the old and new values of \mathbf{A} . If the difference is greater than a specified tolerance, go to step 2 using the new values of \mathbf{A} .
9. Once the values of \mathbf{A} have converged, check for the existence of $2N$ zero eigenvalues/singular values. If the $2N$ eigenvalues/singular values are not within a specified tolerance of zero, alter the quantity and/or character of the trial temporal-basis-functions and their associated parameters and/or the length of the transition interval (t_k, t_{k+1}) , and go to step 1. The $[\mathbf{P}]$ matrix representing Hamilton’s Law of Varying Action will be obtained, when \mathbf{A} have converged to within a specified tolerance, and when $2N$ eigenvalues/singular values of $[\mathbf{P}]$ are as close to zero as deemed necessary for the particular application. At this point, $[\mathbf{P}]$ provides \mathbf{E}_N , \mathbf{E}_R and consequently the fundamental-time-modes. \mathbf{A}_R , β_N and β_R have also been determined as a matter of course.
10. Generate the response of the system within the transition interval (t_k, t_{k+1}) utilizing \mathbf{E}_N , β_N and $\mathbf{A}_R(\mathbf{E}_R, \beta_R)$ in Eq. (26) by sweeping τ from 0 to 1.
11. Check the accuracy of the response using Eq. (32). If the accuracy is not within a specified tolerance, the nullity of the $2N$ eigenvalues/singular values may not have been sufficient. In this case, alter the quantity and/or character of the trial temporal-basis-functions and their associated parameters and/or the length of the transition interval (t_k, t_{k+1}) , and go to step 1.
12. Set the final values of displacement, velocity and forcing function for the current transition interval equal to the initial values of the following transition interval. Go to step 2.

This procedure results in the complete solution, but is also applicable solely to the null-space solution where \mathbf{A}_R , β_R , $\mathbf{q}^R(\tau)$ and $\mathbf{q}^R(\tau)$ are zero. This procedure may also be used to generate the response solution for linear systems, in which case step eight is trivial, i.e., no iteration is needed.

The above procedure may be applied directly to holonomic systems, but may be modified for non-holonomic systems, where the constraints may be integrated in time via the temporal-basis-function expansions via proper procedures of the evolutionary energy perspective.

3. Fundamental-time-modes

Each fundamental-time-mode consists of a vector or N -tuple of N component functions $q_{ri}^*(t)$, for an N -degree-of-freedom system corresponding to a transition interval (t_k, t_{k+1}) . By factoring out one of the component functions, the fundamental-time-mode may be represented by a product of vector and scalar-valued parts as shown

$$\mathbf{q}_i^*(t) = \left\{ \begin{array}{c} q_{1i}^*(t)/q_{ri}^*(t) \\ \vdots \\ 1 \\ \vdots \\ q_{Ni}^*(t)/q_{ri}^*(t) \end{array} \right\} q_{ri}^*(t), \tag{33}$$

where $q_{ri}^*(t)$ is the r th component function of the i th fundamental-time-mode. The vector-valued portion may have temporal dependencies or consist solely of scalar constants, but nonetheless provides the relative displacement information of each degree-of-freedom. As such, the vector-valued portion will be denoted as the *fundamental-time-mode-shape*. The factored-out component function is temporal and is common to each degree-of-freedom.

Although not used herein, the fundamental-time-modes may be put in a form compatible with phase space applications by including the derivatives of the component functions. However, for the work presented herein, the standard configuration space form of the fundamental-time-mode, as shown in Eq. (33), will be used.

When the component functions in a fundamental-time-mode are proportional to each other, the fundamental-time-mode shape consists solely of scalar proportionality constants, and in this case, where a single component function common to each degree-of-freedom may be factored out, the spatial dependence of the fundamental-time-mode is separable from the temporal dependence. Hence, the fundamental-time-mode will be denoted as a *space-time-separable-fundamental-time-mode*. In this situation, all degrees-of-freedom will share the same temporal characteristics, resulting in synchronous motion. When the component functions are not (all) proportional to each other, the above space-time separation cannot be accomplished, and therefore the fundamental-time-mode shape consists of temporal functions. In this case, the fundamental-time-mode will be denoted as a *space-time-nonseparable fundamental-time-mode*.

The fundamental-time-mode shape may be viewed as a modal line (curved or straight) in the N -dimensional configuration space by plotting one component function versus the others (for example: $q_{ri}^*(\tau)$ vs. $q_{si}^*(\tau)$, $r \neq s$). These modal lines will be referred to as *fundamental-time-modal-lines*. Space-time-nonseparable-fundamental-time-modes exhibit curved fundamental-time-modal-lines. Space-time-separable fundamental-time-modes exhibit straight fundamental-time-modal-lines. It is convenient to generate $(N - 1)$ fundamental-time-modal-line plots for systems with more than three degrees-of-freedom.

For the same dynamic system, the fundamental-time-modes may exhibit different characteristics, depending upon the number and type of temporal-basis-functions chosen, and the size of the transition interval (t_k, t_{k+1}) . This concise sketch of the characteristics of fundamental-time-modes will be further enhanced by illustrative examples in the following sections.

4. Computational examples

This section illustrates by way of two degrees-of-freedom examples, the linear algebraic and vector-space concepts involved in generating a response solution for the free-motion of nonlinear systems. A forced nonlinear system is considered in Section 5. The examples considered herein, provide a novel view of the composition of the nonlinear normal mode response of nonlinear systems. Since nonlinear normal modes are not widely familiar, a brief overview of their characteristics will be presented prior to the computational examples.

4.1. Brief overview of nonlinear normal modes

Normal modes associated with linear systems have their nonlinear counterpart denoted as nonlinear normal modes, which characterize a synchronous mode of response for nonlinear systems. The concept of normal modes for nonlinear systems is not new. However, their existence is not widely known, in spite of their introduction in 1962 [34]. Interest in nonlinear normal modes has been renewed in recent years as demonstrated in Refs. [35–38].

Ref. [34] described the normal mode vibrations of nonlinear systems as exhibiting the following characteristics: All masses execute periodic motions of the same period, passing through their equilibrium position at the same time with the position of any one mass uniquely determining the position of all other masses. Ref. [39] characterizes the m th normal mode vibration of an N -degree-of-freedom linear or nonlinear system as movement along a modal line in space defined by $(N - 1)$ single valued functions

$$q_{im} = q_{im}(q_{1m}), \quad i = 2, 3, \dots, N, \tag{34}$$

in an N -dimensional configuration space (q_1, q_2, \dots, q_N) . Ref. [39] further describes nonlinear normal mode vibrations as “vibrations-in-unison” of nonlinear systems. These normal mode vibrations are denoted as similar nonlinear normal mode

vibrations if Eq. (34) is linear resulting in the ratio of any two coordinates at any time equaling a constant as indicated

$$q_i(t)/q_j(t) = c_{ij} = \text{constant}, \quad i = 1, \dots, N. \tag{35}$$

The qualifier “similar” indicates that the nonlinear normal mode exhibits the same characteristics as linear normal modes. Vibrations-in-unison in which Eq. (34) is nonlinear are characterized as non-similar nonlinear normal mode vibrations. Similar and non-similar nonlinear normal modes are characterized by straight and curved modal lines, respectively, in N -dimensional configuration space.

Refs. [35] and [37] provide further characterizations of nonlinear normal modes. This overview has briefly described the characteristics of nonlinear normal modes and associated definitions, providing sufficient familiarity with nonlinear normal modes for the computational examples that follow.

4.2. Formulation of the algebraic equations of motion

Consider the two degree-of-freedom system shown in Fig. 2. Upon applying the δ operator to the kinetic energy and work function [40] for this system, the resulting real variation of the kinetic energy is

$$\delta T = m_i \dot{q}_i(t) \delta \dot{q}_i(t), \quad i = 1, 2, \tag{36}$$

and the real variational work expression is

$$\delta W = \{-k_{l_i}(q_i - q_{i-1}) + k_{l_{i+1}}(q_{i+1} - q_i) - k_{nl_i}(q_i - q_{i-1})^3 + k_{nl_{i+1}}(q_{i+1} - q_i)^3 - c_i(\dot{q}_i - \dot{q}_{i-1}) + c_{i+1}(\dot{q}_{i+1} - \dot{q}_i) + f_i(t)\} \delta q_i(t) \tag{37}$$

$i = 1, 2, \quad q_0(t) = q_3(t) = 0.$

Upon substituting δT and δW from Eqs. (36) and (37) into Hamilton's Law of Varying Action (Eq. (1)) and non-dimensionalizing the time with the transition interval, the following expression is obtained

$$\int_0^1 \left\{ \frac{m_1}{\Delta t^2} q'_1 \delta q'_1 + \frac{m_2}{\Delta t^2} q'_2 \delta q'_2 - k_{l_1} q_1 \delta q_1 - k_{nl_1} q_1^3 \delta q_1 - k_{l_2} (q_2 - q_1) \delta q_2 + k_{l_2} (q_2 - q_1) \delta q_1 - k_{nl_2} (q_2 - q_1)^3 \delta q_2 + k_{nl_2} (q_2 - q_1)^3 \delta q_1 - k_{l_3} q_2 \delta q_2 - k_{nl_3} q_2^3 \delta q_2 - \frac{c_1}{\Delta t} q'_1 \delta q_1 - \frac{c_2}{\Delta t} (q'_2 - q'_1) \delta q_2 + \frac{c_2}{\Delta t} (q'_2 - q'_1) \delta q_1 - \frac{c_3}{\Delta t} q'_2 \delta q_2 + f_1(\tau) \delta q_1 + f_2(\tau) \delta q_2 \right\} d\tau - \frac{m_1}{\Delta t^2} q'_1 \delta q_1 \Big|_0^1 - \frac{m_2}{\Delta t^2} q'_2 \delta q_2 \Big|_0^1 = 0. \tag{38}$$

Representing the dependent variables in terms of unconstrained temporal-basis-function expansions

$$q_i(\tau) = \Psi(\tau) \mathbf{A}^i, \quad q'_i(\tau) = \Psi'(\tau) \mathbf{A}^i$$

$$\delta q_i(\tau) = \Psi(\tau) \delta \mathbf{A}^i, \quad \delta q'_i(\tau) = \Psi'(\tau) \delta \mathbf{A}^i, \quad i = 1, 2, \tag{39}$$

and substituting into Eq. (38) results in the following nonlinear algebraic equations of motion

$$\begin{bmatrix} \mathbf{M}_{11} - \mathbf{KL}_{11} - \mathbf{KNL}_{11}(\mathbf{A}^1, \mathbf{A}^2) - \mathbf{C}_{11} & \mathbf{KL}_{12} + \mathbf{KNL}_{12}(\mathbf{A}^1, \mathbf{A}^2) \\ \mathbf{KL}_{21} + \mathbf{KNL}_{21}(\mathbf{A}^1, \mathbf{A}^2) & \mathbf{M}_{22} - \mathbf{KL}_{22} - \mathbf{KNL}_{22}(\mathbf{A}^1, \mathbf{A}^2) - \mathbf{C}_{22} \end{bmatrix} \begin{Bmatrix} \mathbf{A}^1 \\ \mathbf{A}^2 \end{Bmatrix} = \begin{Bmatrix} -\mathbf{F}_1 \\ -\mathbf{F}_2 \end{Bmatrix}, \tag{40}$$

where the matrix elements are defined in general form in Appendix B, and in terms of power series and Gaussian temporal-basis-functions in Appendices C and D, respectively.

Using the approach outlined in Section 2.2.5, the accuracy integral for the system yields

$$\int_{t_k}^{t_{k+1}} \{ (m_1 \dot{q}_1 - k_{l_1} q_1 - k_{nl_1} q_1^3 + k_{l_2} (q_2 - q_1) + k_{nl_2} (q_2 - q_1)^3 - c_1 \dot{q}_1 + c_2 (\dot{q}_2 - \dot{q}_1) + f_1) \dot{q}_1 + (m_2 \dot{q}_2 - k_{l_2} (q_2 - q_1) - k_{nl_2} (q_2 - q_1)^3 - k_{l_3} q_2 - k_{nl_3} q_2^3 - c_2 (\dot{q}_2 - \dot{q}_1) - c_3 \dot{q}_2 + f_2) \dot{q}_2 \} dt - m_1 \dot{q}_1^2 \Big|_{t_k}^{t_{k+1}} - m_2 \dot{q}_2^2 \Big|_{t_k}^{t_{k+1}} = 0. \tag{41}$$

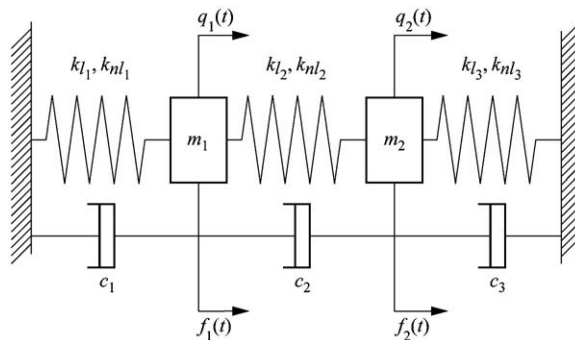


Fig. 2. Two degree-of-freedom discrete dynamic system.

The accuracy of the response may now be determined by the degree to which the calculated displacement and its derivatives satisfy Eq. (41).

In the following examples, it is desired to generate the nonlinear response using global fundamental-time-modes, because they approximate the genuine fundamental-time-modes and the response over a characteristic time. In generating the global fundamental-time-modes, the temporal-basis-functions will be fully exploited and as a result, will approximate the displacement response more accurately than that of the velocity and the velocity response more accurately than that of the acceleration. In this case, it makes it difficult to check the accuracy of the displacement response using differential equations or Eq. (41) which requires the velocity and acceleration responses as well. Therefore, the accuracy of the displacement response generated using global fundamental-time-modes will be compared against the computationally “exact” response generated using local fundamental-time-modes. The accuracy of the “exact” response will be assured by satisfying the integral Eq. (41). Although not necessary, the accuracy of the response will also be checked using differential equations for those readers more comfortable with that approach.

4.3. Similar nonlinear normal mode example

A nonlinear 2 degrees-of-freedom system, as shown in Fig. 2, exhibiting a similar nonlinear normal mode is one in which both masses are the same and all potential energy functions are equivalent. The following parameters in consistent units, considered for such a system are

$$m_1 = m_2 = 1, \quad k_i = 100, \quad k_{nl_i} = 100, \quad c_i = 0, \quad i = 1, 2, 3. \tag{42}$$

The similar nonlinear normal mode shapes for this system are known to be $[q_1(\tau) \ q_2(\tau)]^T = [1 \ 1]^T$ and $[q_1(\tau) \ q_2(\tau)]^T = [-1 \ 1]^T$ and are characterized by straight modal lines. The following initial conditions

$$q_1(0) = 0.15, \quad q_2(0) = 0.15, \quad \dot{q}_1(0) = \dot{q}_2(0) = 0, \tag{43}$$

initiate vibration in the first similar nonlinear normal mode. Substituting the parameters, Eqs. (42) and (43), into Eq. (38) result in the algebraic equations of motion, Eq. (40). The first similar nonlinear normal mode response of this system over approximately 1 period, or an elapsed time of 0.625 s, was generated by solving Eq. (40) without time marching, using 9 Gaussian temporal-basis-functions. Thus, global fundamental-time-modes were generated. The global fundamental-time-modes may be characterized as follows,

$$\mathbf{q}_1^*(\tau) = \begin{Bmatrix} 1 \\ 1 \end{Bmatrix} q_{21}^*(\tau), \quad \mathbf{q}_2^*(\tau) = \begin{Bmatrix} -1 \\ 1 \end{Bmatrix} q_{22}^*(\tau), \quad \mathbf{q}_3^*(\tau) = \begin{Bmatrix} -1 \\ 1 \end{Bmatrix} q_{23}^*(\tau), \quad \mathbf{q}_4^*(\tau) = \begin{Bmatrix} 1 \\ 1 \end{Bmatrix} q_{24}^*(\tau), \tag{44}$$

Table 1

Component functions of the fundamental-time-modes comprising the first similar nonlinear normal mode response of the system: $\ddot{q}_1 + 200q_1 - 100q_2 - 100(q_2 - q_1)^3 + 100q_1^3 = 0$, $\ddot{q}_2 + 200q_2 - 100q_1 + 100(q_2 - q_1)^3 + 100q_2^3 = 0$, $q_i(0) = 0.15, \dot{q}_i(0) = 0, i = 1, 2. \Delta t = 0.625$ s.

<i>i</i>	τ_i	E(i,1)	E(i,2)	E(i,3)	E(i,4)
$q_{1j}^*(\tau) = \sum_{i=1}^9 \mathbf{E}(i,j)e^{-5.0(\tau-\tau_i)^2}$					
1	-0.1500	-4.880354606 × 10 ⁻²	6.226576197 × 10 ⁻²	-4.763787598 × 10 ⁻²	2.756313807 × 10 ⁻²
2	0.0125	1.469695560 × 10 ⁻¹	-1.149994098 × 10 ⁻¹	1.968821830 × 10 ⁻¹	2.242127451 × 10 ⁻²
3	0.1750	-2.409971991 × 10 ⁻¹	-2.523191652 × 10 ⁻²	-3.489107159 × 10 ⁻¹	-4.047628894 × 10 ⁻²
4	0.3375	3.208278097 × 10 ⁻¹	3.297280487 × 10 ⁻¹	2.959404448 × 10 ⁻¹	1.908132943 × 10 ⁻²
5	0.5000	3.596004361 × 10 ⁻¹	-4.956735987 × 10 ⁻¹	-2.116542759 × 10 ⁻³	7.459936291 × 10 ⁻²
6	0.6625	3.211930967 × 10 ⁻¹	3.322365942 × 10 ⁻¹	-2.933163100 × 10 ⁻¹	-1.920450452 × 10 ⁻²
7	0.8250	-2.417283012 × 10 ⁻¹	-2.819307909 × 10 ⁻²	3.491908291 × 10 ⁻¹	4.032210246 × 10 ⁻²
8	0.9875	1.473759261 × 10 ⁻¹	-1.133357038 × 10 ⁻¹	-1.983368187 × 10 ⁻¹	-2.199128721 × 10 ⁻²
9	1.1500	-4.876749929 × 10 ⁻²	6.186775415 × 10 ⁻²	4.835224132 × 10 ⁻²	-2.992466195 × 10 ⁻²
$q_{2j}^*(\tau) = \sum_{i=1}^9 \mathbf{E}(i,j)e^{-5.0(\tau-\tau_i)^2}$					
1	-0.1500	-4.880354730 × 10 ⁻²	-6.226576843 × 10 ⁻²	4.763786666 × 10 ⁻²	2.756313697 × 10 ⁻²
2	0.0125	1.469695793 × 10 ⁻¹	1.149994270 × 10 ⁻¹	-1.968821543 × 10 ⁻¹	2.242127478 × 10 ⁻¹
3	0.1750	-2.409972696 × 10 ⁻¹	2.523188868 × 10 ⁻²	3.489106686 × 10 ⁻¹	-4.047628914 × 10 ⁻¹
4	0.3375	3.208279089 × 10 ⁻¹	-3.297280090 × 10 ⁻¹	-2.959403826 × 10 ⁻¹	1.908132930 × 10 ⁻¹
5	0.5000	-3.596004999 × 10 ⁻¹	4.956735527 × 10 ⁻¹	2.116473539 × 10 ⁻³	7.459973666 × 10 ⁻⁴
6	0.6625	3.211930828 × 10 ⁻¹	-3.322365518 × 10 ⁻¹	2.933163714 × 10 ⁻¹	-1.920450478 × 10 ⁻¹
7	0.8250	-2.417282378 × 10 ⁻¹	2.819304518 × 10 ⁻²	-3.491908747 × 10 ⁻¹	4.032210242 × 10 ⁻¹
8	0.9875	1.473758735 × 10 ⁻¹	1.133357243 × 10 ⁻¹	1.983368465 × 10 ⁻¹	-2.199128704 × 10 ⁻¹
9	1.1500	-4.876748212 × 10 ⁻²	-6.186776018 × 10 ⁻²	-4.835225076 × 10 ⁻²	-2.992466282 × 10 ⁻²

where the component functions $q_{1i}^*(\tau)$ and $q_{2i}^*(\tau)$ are presented in Table 1, along with the Gaussian temporal-basis-function parameters. The spatial (vector) portions of these space-time-separable fundamental-time-modes are approximated by plotting one component function versus the other and calculating the linearity and slope of the fundamental-time-modal-lines shown in Fig. 3. This can also be determined by inspection of Table 1. The fundamental-time-mode composition of the response is shown in Fig. 4. Summing the products of the fundamental-time-modes and their modal coordinates as shown in Figs. 4(a–d) produces the similar nonlinear normal mode response shown in Fig. 4(e). It may be seen from Fig. 4, that the first similar nonlinear normal mode, is primarily composed of two fundamental-time-modes; $\mathbf{q}_1^*(\tau)$ and $\mathbf{q}_4^*(\tau)$, the influence of $\mathbf{q}_2^*(\tau)$ and $\mathbf{q}_3^*(\tau)$ being insignificant.

The numerically “exact” response for vibration in the first similar nonlinear normal mode was generated in a time marching fashion over 0.625 s using 100 transition intervals of 0.00625 s each. Local fundamental-time-modes were generated. Nine power series temporal-basis-functions were used, resulting in peak errors in the accuracy integral and differential equations of magnitude 2.9×10^{-11} and 7.3×10^{-9} , respectively. The maximum absolute difference between the responses generated using the global fundamental-time-modes (Gaussian temporal-basis-functions) and the local fundamental-time-modes (power series temporal-basis-functions) was 5.04×10^{-5} for both the first and second degree-of-freedom.

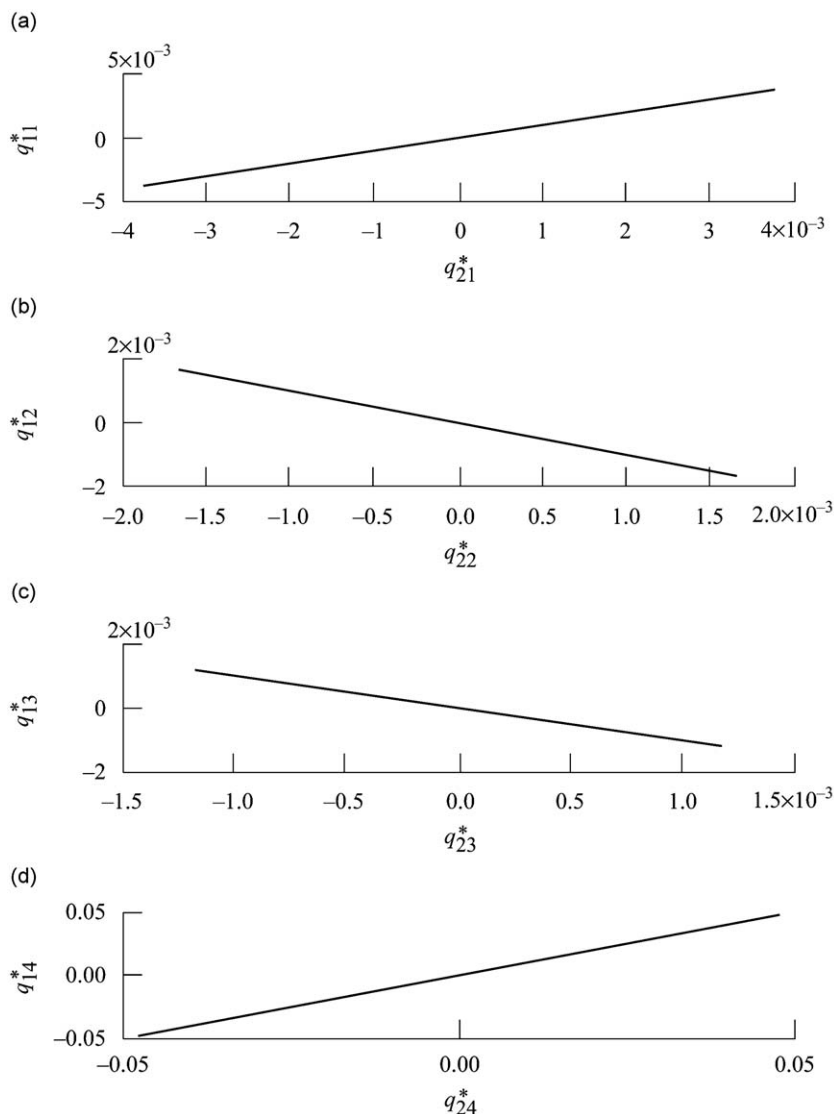


Fig. 3. Fundamental-time-modal-lines for the first similar nonlinear normal mode of the system: $\ddot{q}_1 + 200q_1 - 100q_2 - 100(q_2 - q_1)^3 + 100q_1^3 = 0$, $\ddot{q}_2 + 200q_2 - 100q_1 + 100(q_2 - q_1)^3 + 100q_2^3 = 0$, using nine Gaussian temporal-basis-functions. (a) q_{11}^* vs. q_{21}^* , (b) q_{12}^* vs. q_{22}^* , (c) q_{13}^* vs. q_{23}^* , (d) q_{14}^* vs. q_{24}^* . $q_i(0) = 0.15$, $\dot{q}_i(0) = 0$, $i = 1, 2$. $\Delta t = 0.625$ s.

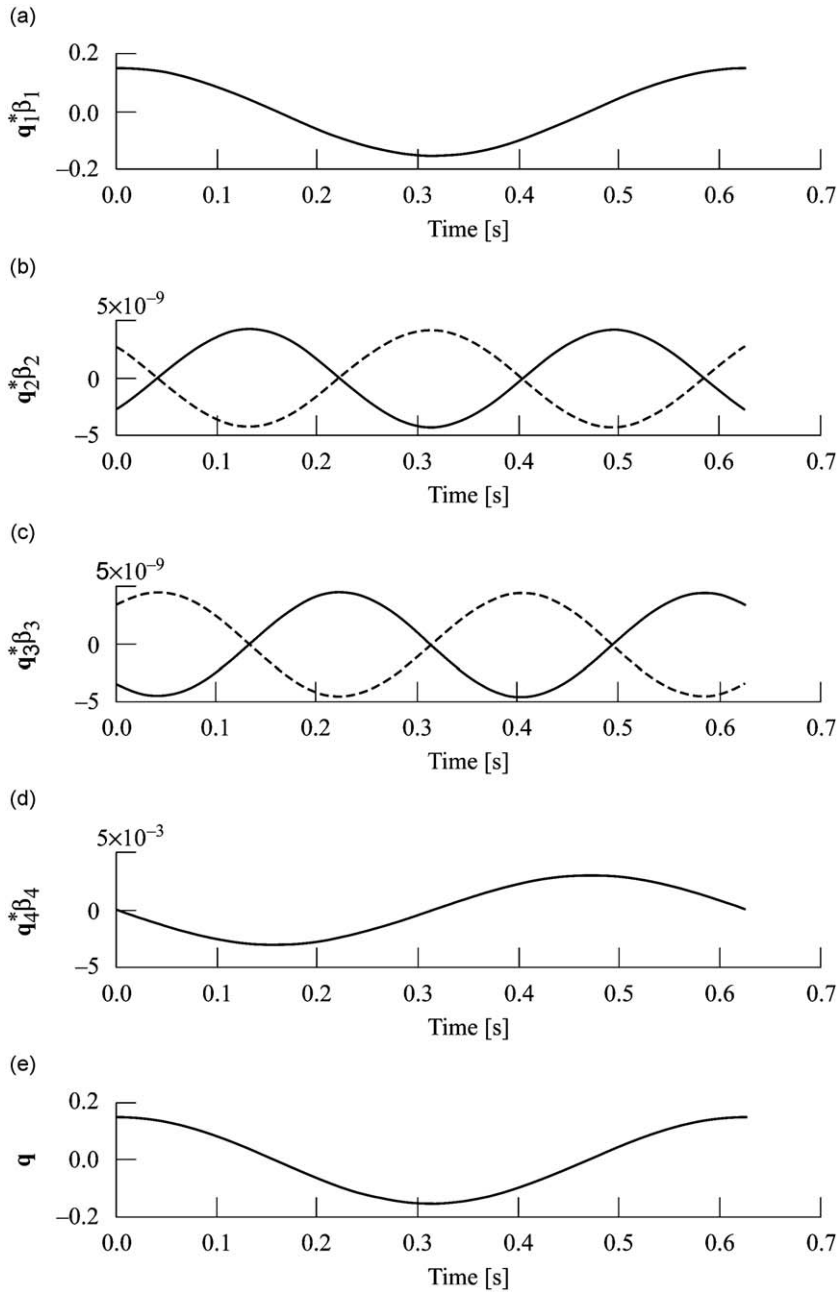


Fig. 4. Fundamental-time-modal composition of first similar nonlinear normal mode response for the system: $\ddot{q}_1 + 200q_1 - 100q_2 - 100(q_2 - q_1)^3 + 100q_1^3 = 0$, $\ddot{q}_2 + 200q_2 - 100q_1 + 100(q_2 - q_1)^3 + 100q_2^3 = 0$, using nine Gaussian temporal-basis-functions. (a) $\mathbf{q}_1^* \beta_1$; $-q_{11}^*$, $-q_{21}^*$, (b) $\mathbf{q}_2^* \beta_2$; $-q_{12}^*$, $-q_{22}^*$, (c) $\mathbf{q}_3^* \beta_3$; $-q_{13}^*$, $-q_{23}^*$, (d) $\mathbf{q}_4^* \beta_4$; $-q_{14}^*$, $-q_{24}^*$, (e) \mathbf{q} ; $-q_1$, $-q_2$. $q_i(0) = 0.15$, $\dot{q}_i(0) = 0$, $i = 1, 2$. $\Delta t = 0.625$ s.

In addition, each fundamental-time-mode composing the first similar nonlinear normal mode was substituted into the accuracy integral to determine if it was an eigenfunction. Satisfaction of the accuracy integral by a fundamental-time-mode indicates that the fundamental-time-mode is an eigenfunction of Hamilton’s Law of Varying Action corresponding to the null eigenvalue. The first through fourth fundamental-time-modes satisfied the accuracy integral, to within magnitudes of 2.0×10^{-6} , 2.7×10^{-8} , 5.9×10^{-8} and 2.3×10^{-4} , respectively and therefore are a reasonable global approximation to the genuine eigenfunctions and genuine fundamental-time-modes.

Vibration in the second similar nonlinear normal mode is simulated using the following initial conditions

$$q_1(0) = -0.15, \quad q_2(0) = 0.15, \quad \dot{q}_1(0) = \dot{q}_2(0) = 0. \tag{45}$$

Table 2

Component functions of the fundamental–time-modes composing the second similar nonlinear normal mode response of the system: $\ddot{q}_1 + 200q_1 - 100q_2 - 100(q_2 - q_1)^3 + 100q_1^3 = 0$, $\ddot{q}_2 + 200q_2 - 100q_1 + 100(q_2 - q_1)^3 + 100q_2^3 = 0$, $q_i(0) = -0.15$, $q_2(0) = 0.15$, $\dot{q}_i(0) = 0, i = 1, 2$. $\Delta t = 0.355$ s.

i	τ_i	$E(i,1)$	$E(i,2)$	$E(i,3)$	$E(i,4)$
$q_{1i}^*(\tau) = \sum_{i=1}^{10} E(i,j)e^{-7.0(\tau-\tau_i)^2}$					
1	-0.1000	$2.281666851 \times 10^{-2}$	$6.174840568 \times 10^{-3}$	$-7.673367476 \times 10^{-2}$	$1.066318339 \times 10^{-1}$
2	0.0333	$-1.028286395 \times 10^{-1}$	$-6.217340780 \times 10^{-2}$	$2.288895528 \times 10^{-1}$	$-2.369096017 \times 10^{-1}$
3	0.1667	$1.395681767 \times 10^{-1}$	$1.697014227 \times 10^{-1}$	$-3.142280316 \times 10^{-1}$	$3.124891080 \times 10^{-1}$
4	0.3000	$-2.912873279 \times 10^{-1}$	$-2.844735189 \times 10^{-1}$	$2.831193805 \times 10^{-1}$	$-2.747460336 \times 10^{-1}$
5	0.4333	$3.415166076 \times 10^{-1}$	$3.676359415 \times 10^{-1}$	$-1.217028614 \times 10^{-1}$	$9.769689114 \times 10^{-2}$
6	0.5667	$-3.414615321 \times 10^{-1}$	$3.684066909 \times 10^{-1}$	$-1.204777177 \times 10^{-1}$	$9.809745969 \times 10^{-2}$
7	0.7000	$2.912044387 \times 10^{-1}$	$2.862965506 \times 10^{-1}$	$2.810555936 \times 10^{-1}$	$-2.747219566 \times 10^{-1}$
8	0.8333	$-1.935277610 \times 10^{-1}$	$-1.716374524 \times 10^{-1}$	$-3.122269822 \times 10^{-1}$	$3.121909079 \times 10^{-1}$
9	0.9667	$1.028716291 \times 10^{-1}$	$6.344195780 \times 10^{-2}$	$2.266344759 \times 10^{-1}$	$-2.364662722 \times 10^{-1}$
10	1.1000	$-2.287669465 \times 10^{-2}$	$-6.566115815 \times 10^{-3}$	$-7.522028671 \times 10^{-2}$	$1.065328855 \times 10^{-1}$
$q_{2i}^*(\tau) = \sum_{i=1}^{10} E(i,j)e^{-7.0(\tau-\tau_i)^2}$					
1	-0.1000	$2.281667031 \times 10^{-2}$	$-6.174833566 \times 10^{-3}$	$7.673367443 \times 10^{-2}$	$1.066318342 \times 10^{-1}$
2	0.0333	$-1.028286640 \times 10^{-1}$	$6.217336942 \times 10^{-2}$	$-2.288895527 \times 10^{-1}$	$-2.369096013 \times 10^{-1}$
3	0.1667	$1.935682473 \times 10^{-1}$	$1.697013465 \times 10^{-1}$	$3.142280323 \times 10^{-1}$	$3.124891051 \times 10^{-1}$
4	0.3000	$-2.912874493 \times 10^{-1}$	$2.844733987 \times 10^{-1}$	$-2.831193827 \times 10^{-1}$	$-2.747460273 \times 10^{-1}$
5	0.4333	$3.415167675 \times 10^{-1}$	$-3.676357942 \times 10^{-1}$	$1.217028652 \times 10^{-1}$	$9.769688150 \times 10^{-2}$
6	0.5667	$-3.414616955 \times 10^{-1}$	$3.684065380 \times 10^{-1}$	$1.204777127 \times 10^{-1}$	$9.809747077 \times 10^{-2}$
7	0.7000	$2.912045681 \times 10^{-1}$	$-2.862964150 \times 10^{-1}$	$-2.810555882 \times 10^{-1}$	$-2.747219663 \times 10^{-1}$
8	0.8333	$-1.935278405 \times 10^{-1}$	$1.716373587 \times 10^{-1}$	$3.122269779 \times 10^{-1}$	$3.121909145 \times 10^{-1}$
9	0.9667	$1.028716600 \times 10^{-1}$	$-6.344190609 \times 10^{-2}$	$-2.266344732 \times 10^{-1}$	$-2.364662752 \times 10^{-1}$
10	1.1000	$-2.287669857 \times 10^{-2}$	$6.566102792 \times 10^{-3}$	$7.522028579 \times 10^{-2}$	$1.065328861 \times 10^{-1}$

The second similar nonlinear normal mode response of this system over an elapsed time of approximately 1 period, or 0.355 s, was generated by solving Eq. (40) without time marching, using the initial conditions from Eq. (45) and 10 Gaussian temporal-basis-functions. The global fundamental-time-modes may be characterized as follows

$$\mathbf{q}_1^*(\tau) = \begin{Bmatrix} 1 \\ 1 \end{Bmatrix} q_{21}^*(\tau), \quad \mathbf{q}_2^*(\tau) = \begin{Bmatrix} -1 \\ 1 \end{Bmatrix} q_{22}^*(\tau), \quad \mathbf{q}_3^*(\tau) = \begin{Bmatrix} -1 \\ 1 \end{Bmatrix} q_{23}^*(\tau), \quad \mathbf{q}_4^*(\tau) = \begin{Bmatrix} 1 \\ 1 \end{Bmatrix} q_{24}^*(\tau), \quad (46)$$

where the component functions $q_{1i}^*(\tau)$ and $q_{2i}^*(\tau)$ are presented in Table 2 along with the Gaussian temporal-basis-function parameters. The spatial (vector) portions of these space-time-separable fundamental-time-modes are approximated as was done for the first similar nonlinear normal mode. This may also be determined by inspecting Table 2. The spatial part of the fundamental-time-modes is the same for the first and second nonlinear normal modes, as indicated by Eqs. (44) and (46). The fundamental-time-mode composition of the response is shown in Fig. 5. Summing the products of the fundamental-time-modes and their modal coordinates, as shown in Figs. 5(a–d), produces the similar nonlinear normal mode response shown in Fig. 5(e). It may be seen from Fig. 5 that the second similar nonlinear normal mode is primarily composed of two fundamental-time-modes, $\mathbf{q}_2^*(\tau)$ and $\mathbf{q}_3^*(\tau)$, the influence of $\mathbf{q}_1^*(\tau)$ and $\mathbf{q}_4^*(\tau)$ being insignificant.

The numerically “exact” response for vibration in the second similar nonlinear normal mode was generated in a time marching fashion over 0.355 s using 100 transition intervals of 0.00355 s each. Eight power series temporal-basis-functions were used, resulting in peak errors in the accuracy integral and differential equations of magnitude 8.8×10^{-11} and 4.0×10^{-9} , respectively. The maximum absolute difference between the responses as generated using the global fundamental-time-modes (Gaussian temporal-basis-functions) and local fundamental-time-modes (power series temporal-basis-functions) was 8.3×10^{-5} and 6.9×10^{-5} for the first and second degree-of-freedom, respectively.

Each fundamental-time-mode composing the second similar nonlinear normal mode was substituted into the accuracy integral to determine if it was an eigenfunction of Hamilton’s Law of Varying Action. The first through fourth fundamental-time-modes satisfied the accuracy equation, to within magnitudes of 1.3×10^{-6} , 3.4×10^{-6} , 1.5×10^{-4} and 2.3×10^{-6} , respectively and therefore are a reasonable global approximation to the genuine eigenfunctions and genuine fundamental-time-modes.

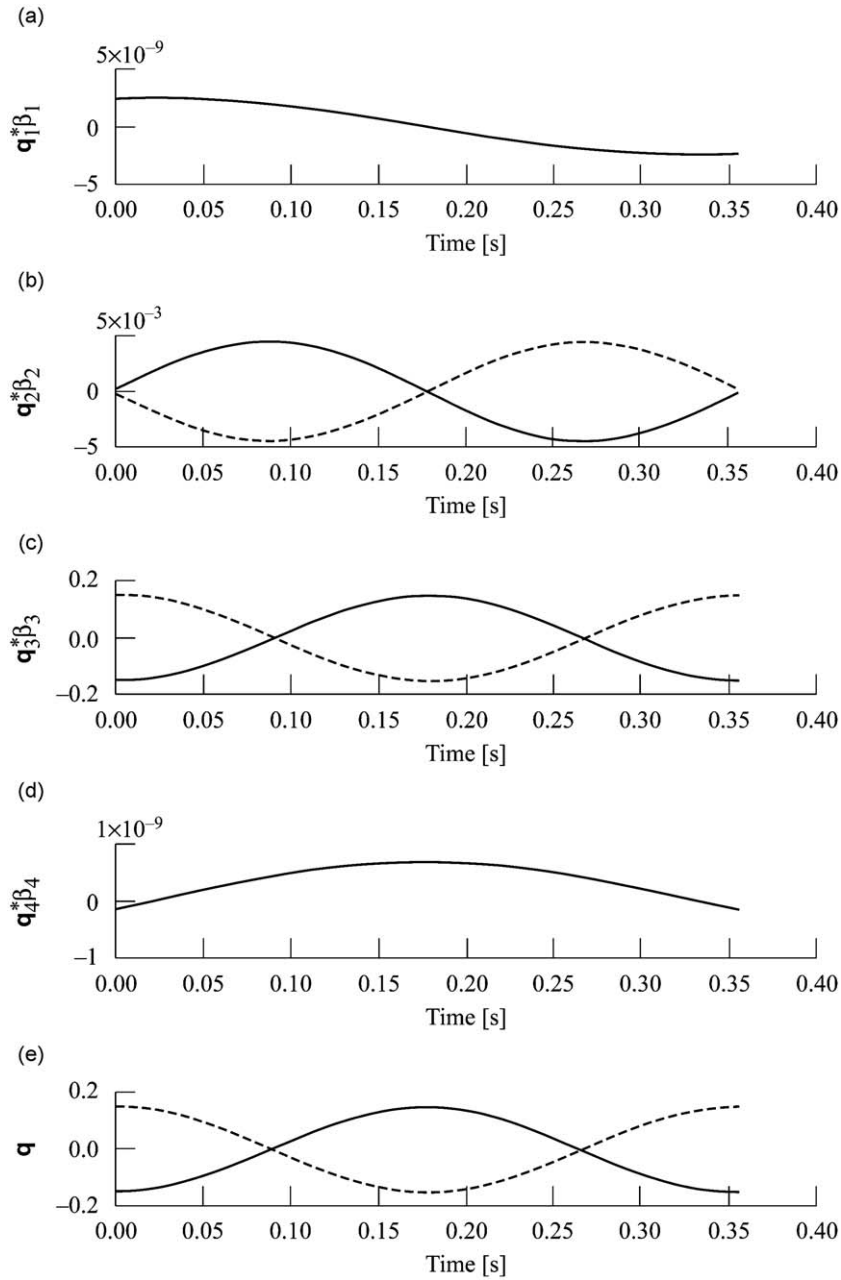


Fig. 5. Fundamental-time-modal composition of second similar nonlinear normal mode response for the system: $\ddot{q}_1 + 200q_1 - 100q_2 - 100(q_2 - q_1)^3 + 100q_1^3 = 0$, $\ddot{q}_2 + 200q_2 - 100q_1 + 100(q_2 - q_1)^3 + 100q_2^3 = 0$, using nine Gaussian temporal-basis-functions. (a) $q_1^* \beta_1; -q_{11}^*, -q_{21}^*$, (b) $q_2^* \beta_2; -q_{12}^*, -q_{22}^*$, (c) $q_3^* \beta_3; -q_{13}^*, -q_{23}^*$, (d) $q_4^* \beta_4; -q_{14}^*, -q_{24}^*$, (e) $q; -q_1, -q_2$. $q_1(0) = -0.15$, $q_2(0) = 0.15$, $\dot{q}_i(0) = 0$, $i = 1, 2$. $\Delta t = 0.355$ s.

4.4. Non-similar nonlinear normal mode example

A nonlinear two degree-of-freedom system, as shown in Fig. 2, with the following system parameters in consistent units

$$m_1 = m_2 = 1, \quad k_i = 1, \quad c_i = 0, \quad i = 1, 2, 3$$

$$k_{nl_1} = 0.5, \quad k_{nl_2} = k_{nl_3} = 0, \tag{47}$$

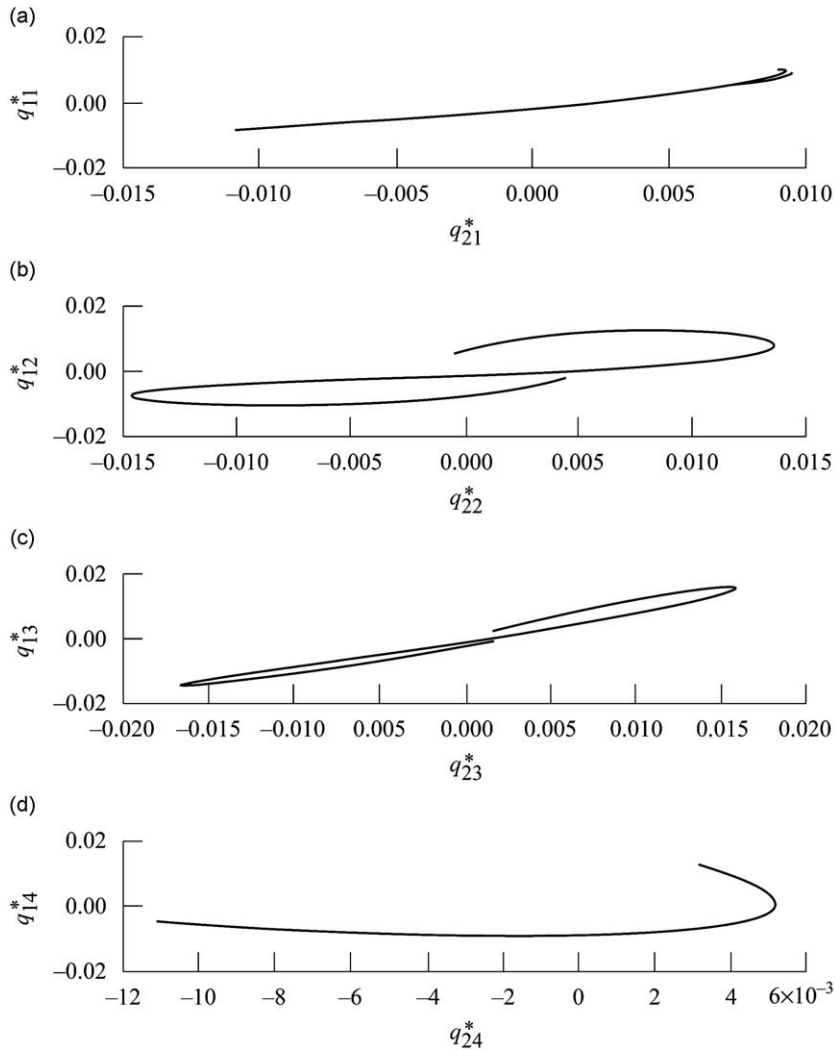


Fig. 6. Fundamental-time-modal-lines for the first non-similar nonlinear normal mode of the system: $\dot{q}_1 + 2q_1 - q_2 + 0.5q_1^3 = 0$, $\ddot{q}_2 + 2q_2 - q_1 = 0$, using eleven Gaussian temporal-basis-functions. (a) q_{11}^* vs. q_{21}^* , (b) q_{12}^* vs. q_{22}^* , (c) q_{13}^* vs. q_{23}^* , (d) q_{14}^* vs. q_{24}^* . $q_1(0) = 0.5$, $q_2(0) = 25/48$, $\dot{q}_i(0) = 0, i = 1, 2$. $\Delta t = 6.145$ s.

exhibit non-similar nonlinear normal modes. This system has been studied in Refs. [36–38]. Vibration in the first non-similar nonlinear normal mode may be initiated using the following initial conditions [36,38]

$$q_1(0) = 0.5, \quad q_2(0) = 25/48, \quad \dot{q}_1(0) = \dot{q}_2(0) = 0. \quad (48)$$

Substituting the parameters, Eqs. (47) and (48) into Eq. (38) result in Eq. (40). The first non-similar nonlinear normal mode response of this system over approximately one period, or an elapsed time of 6.145 s, was generated by solving Eq. (40) without time marching, using 11 Gaussian temporal-basis-functions. The global space-time-nonseparable fundamental-time-modes exhibit curved fundamental-time-modal-lines as shown in Fig. 6. The component functions of each fundamental-time-mode are presented in Table 3 along with the Gaussian temporal-basis-function parameters. The fundamental-time-mode composition of the response is shown in Fig. 7. A larger detail of the response is presented in Fig. 8. Summing the products of the fundamental-time-modes and their modal coordinates, shown in Figs. 7(a–d), produces the non-similar nonlinear normal mode response presented in Figs. 7(e) or 8. It can be seen from Fig. 7 that all fundamental-time-modes significantly contribute to the vibration in the first nonlinear normal mode.

The numerically “exact” response for the first nonlinear normal mode was generated in a time marching fashion over 6.145 s using 100 transition intervals of 0.06145 s each. Local fundamental-time-modes were generated. Eight power series

Table 3

Component functions of the fundamental-time-modes composing the first non-similar nonlinear normal mode response for the system: $\ddot{q}_1 + 2q_1 - q_2 + 0.5q_1^3 = 0, \ddot{q}_2 + 2q_2 - q_1 = 0, q_1(0) = 0.5, q_2(0) = 25/48, \dot{q}_i(0) = 0, i = 1, 2, \Delta t = 6.145 \text{ s}$.

i	τ_i	$E(i,1)$	$E(i,2)$	$E(i,3)$	$E(i,4)$
$q_{1j}^*(\tau) = \sum_{i=1}^{11} E(i,j)e^{-K_i(\tau-\tau_i)^2}, K_i = 5.9 \ i \neq 6, K_6 = 3.9$					
1	-0.800	$5.46236738610 \times 10^{-1}$	$9.704633839 \times 10^{-2}$	$6.813603814 \times 10^{-1}$	$6.006790057 \times 10^{-3}$
2	-0.540	$-2.954439504 \times 10^{-1}$	$-2.052547780 \times 10^{-1}$	$-2.530429417 \times 10^{-1}$	$1.634037505 \times 10^{-2}$
3	-0.280	$1.091244501 \times 10^{-1}$	$2.081812215 \times 10^{-1}$	$4.576129645 \times 10^{-2}$	$-6.072921835 \times 10^{-2}$
4	0.000	$-2.445713998 \times 10^{-2}$	$-1.372640315 \times 10^{-1}$	$-2.111849292 \times 10^{-2}$	$1.043163204 \times 10^{-1}$
5	0.244	$3.451258956 \times 10^{-2}$	$6.978011788 \times 10^{-2}$	$5.592454053 \times 10^{-2}$	$-2.734092146 \times 10^{-1}$
6	0.505	$-5.225440249 \times 10^{-2}$	$-2.854281512 \times 10^{-2}$	$-4.126422343 \times 10^{-2}$	$3.450693341 \times 10^{-1}$
7	0.766	$4.504402454 \times 10^{-2}$	$-2.391397537 \times 10^{-2}$	$1.079818423 \times 10^{-2}$	$-2.874613778 \times 10^{-1}$
8	1.027	$-5.307102917 \times 10^{-2}$	$1.134620009 \times 10^{-1}$	$-1.083494541 \times 10^{-2}$	$1.312644101 \times 10^{-1}$
9	1.288	$1.562808518 \times 10^{-1}$	$-1.690631149 \times 10^{-1}$	$-7.311809523 \times 10^{-3}$	$-1.048169757 \times 10^{-1}$
10	1.549	$-3.542093124 \times 10^{-1}$	$1.243945828 \times 10^{-1}$	$2.012005775 \times 10^{-1}$	$9.416541299 \times 10^{-2}$
11	1.810	$6.107475554 \times 10^{-1}$	$5.673782401 \times 10^{-2}$	$-6.300560341 \times 10^{-1}$	$-1.243852228 \times 10^{-1}$
$q_{2j}^*(\tau) = \sum_{i=1}^{11} E(i,j)e^{-K_i(\tau-\tau_i)^2}, K_i = 5.9 \ i \neq 6, K_6 = 3.9$					
1	-0.800	$-9.078534769 \times 10^{-2}$	$-4.512552331 \times 10^{-1}$	$1.038512472 \times 10^{-1}$	$-4.704610778 \times 10^{-1}$
2	-0.540	$2.351178982 \times 10^{-2}$	$3.221960081 \times 10^{-1}$	$-6.881682249 \times 10^{-2}$	$2.492504666 \times 10^{-1}$
3	-0.280	$-6.086327640 \times 10^{-3}$	$2.083713012 \times 10^{-1}$	$2.059080302 \times 10^{-2}$	$-4.643052487 \times 10^{-2}$
4	0.000	$2.712224997 \times 10^{-4}$	$1.568492348 \times 10^{-1}$	$-2.678502835 \times 10^{-2}$	$-7.399802529 \times 10^{-2}$
5	0.244	$4.963357784 \times 10^{-2}$	$-1.042800672 \times 10^{-1}$	$2.936784569 \times 10^{-2}$	$1.930820274 \times 10^{-1}$
6	0.505	$6.919825713 \times 10^{-2}$	$8.738592833 \times 10^{-3}$	$1.720324296 \times 10^{-2}$	$-2.270139808 \times 10^{-1}$
7	0.766	$3.031530762 \times 10^{-2}$	$8.506904336 \times 10^{-2}$	$-6.304089044 \times 10^{-2}$	$2.030906320 \times 10^{-1}$
8	1.027	$3.109541911 \times 10^{-2}$	$-1.424141534 \times 10^{-1}$	$4.709942201 \times 10^{-2}$	$-9.589198574 \times 10^{-2}$
9	1.288	$5.008294615 \times 10^{-2}$	$2.079911200 \times 10^{-1}$	$-1.956464016 \times 10^{-2}$	$-1.267313113 \times 10^{-2}$
10	1.549	$9.686571935 \times 10^{-2}$	$-3.452456133 \times 10^{-1}$	$3.228282203 \times 10^{-2}$	$2.063249379 \times 10^{-1}$
11	1.810	$-2.007569153 \times 10^{-1}$	$4.934376915 \times 10^{-1}$	$-3.419126434 \times 10^{-2}$	$-4.278237171 \times 10^{-1}$

temporal-basis-functions were used resulting in peak errors in the accuracy integral and differential equations of magnitudes 3.4×10^{-12} and 3.2×10^{-11} , respectively. The maximum absolute difference between the responses as generated using global fundamental-time-modes (Gaussian temporal-basis-functions) and local fundamental-time-modes (power series temporal-basis-functions) was 9.6×10^{-4} and 3.2×10^{-4} for the first and second degree-of-freedom respectively.

Each fundamental-time-mode composing the first nonsimilar nonlinear normal mode was substituted into the accuracy integral to determine if it was an eigenfunction of Hamilton’s Law of Varying Action. The first through fourth fundamental-time-modes satisfied the accuracy integral to within magnitudes of 1.5×10^{-6} , 2.5×10^{-6} , 4.2×10^{-6} and 1.4×10^{-7} , respectively and are therefore a reasonable global approximation to the genuine eigenfunctions and genuine fundamental-time-modes.

Vibration in the second non-similar nonlinear normal mode of the same system, was initiated using the following initial conditions [35,37]

$$q_1(0) = 0.5, \quad q_2(0) = -99/208, \quad \dot{q}_1(0) = \dot{q}_2(0) = 0. \tag{49}$$

The second non-similar nonlinear normal mode response of this system over approximately 1 period, or an elapsed time of 3.6s, was generated by solving the algebraic equations of motion Eq. (40) without time marching using the initial conditions from Eq. (49) and 11 Gaussian temporal-basis-functions. The component functions of each fundamental-time-mode are presented in Table 4 along with the Gaussian temporal-basis-function parameters. The fundamental-time-mode composition of the response is shown in Fig. 9. Summing the products of the fundamental-time-modes and their modal coordinates, shown in Figs. 9(a–d), produced the non-similar nonlinear normal mode response shown in Fig. 9(e). It can also be seen from Fig. 9 that all of the fundamental-time-modes significantly contribute to the vibration in the second non-similar nonlinear normal mode.

The numerically “exact” response for the second nonlinear normal mode over 3.6s was generated in a time marching fashion using 100 transition intervals of 0.036s each. Local fundamental-time-modes were generated. Eight

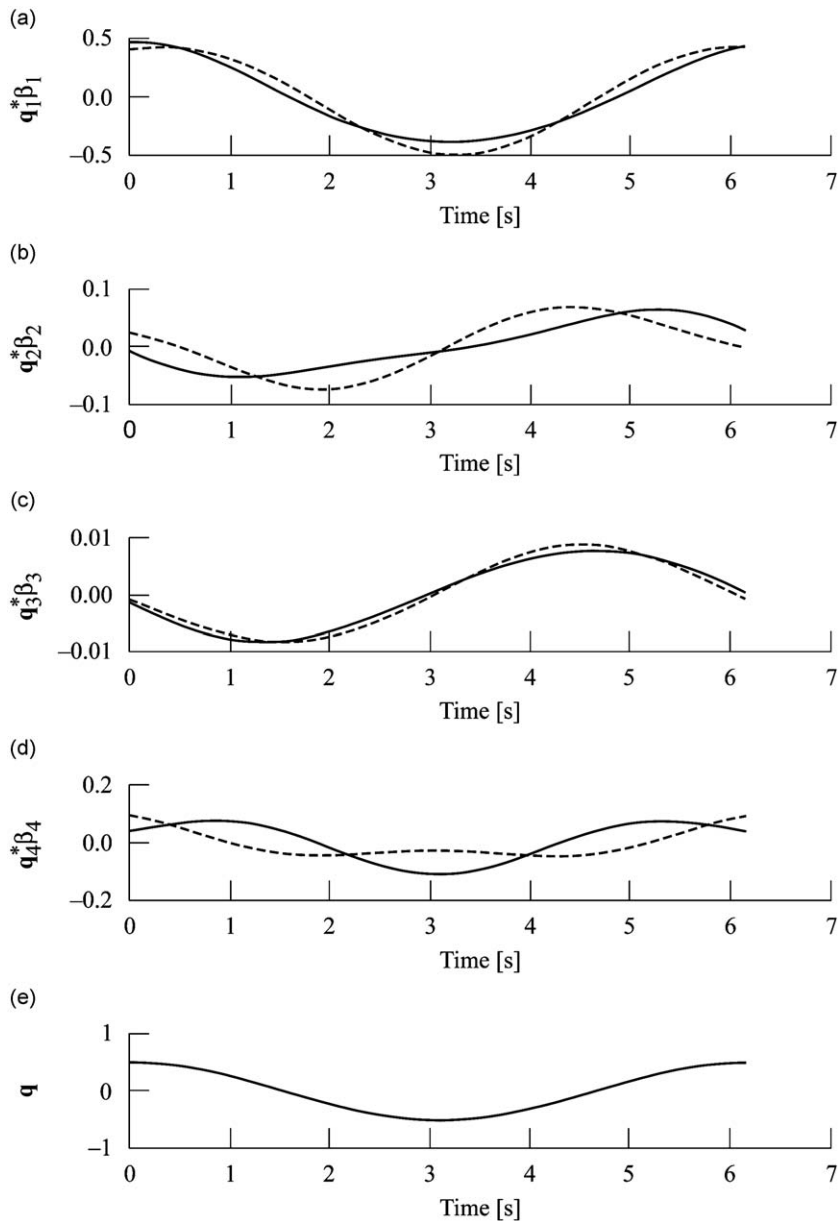


Fig. 7. Fundamental-time-modal composition of the first non-similar nonlinear normal mode response of the system: $\ddot{q}_1 + 2q_1 - q_2 + 0.5q_1^3 = 0, \ddot{q}_2 + 2q_2 - q_1 = 0$, using eleven Gaussian temporal-basis-functions. (a) $\mathbf{q}_1^* \beta_1; -q_{11}^*, -q_{21}^*$, (b) $\mathbf{q}_2^* \beta_2; -q_{12}^*, -q_{22}^*$, (c) $\mathbf{q}_3^* \beta_3; -q_{13}^*, -q_{23}^*$, (d) $\mathbf{q}_4^* \beta_4; -q_{14}^*, -q_{24}^*$, (e) $\mathbf{q}; -q_1, -q_2, q_1(0) = 0.5, q_2(0) = 25/48, \dot{q}_i(0) = 0, i = 1, 2, \Delta t = 6.145 \text{ s}$.

power series temporal-basis-functions were used resulting in peak errors in the accuracy integral and differential equations of magnitudes 9.1×10^{-12} and 1.1×10^{-10} , respectively. The maximum absolute difference between the displacement responses as generated using global fundamental-time-modes (Gaussian temporal-basis-functions) and local fundamental-time-modes (power series temporal-basis-functions) was 2.3×10^{-4} and 2.3×10^{-5} for the first and second degree-of-freedom respectively.

Each fundamental-time-mode composing the second nonsimilar nonlinear normal mode was substituted into the accuracy integral to determine if it was an eigenfunction. The first through fourth fundamental-time-modes satisfied the accuracy integral, to within magnitudes of 3.4×10^{-7} , 3.9×10^{-6} , 3.7×10^{-5} and 2.8×10^{-5} , respectively and are therefore a reasonable global approximation to the genuine eigenfunctions and genuine fundamental-time-modes.

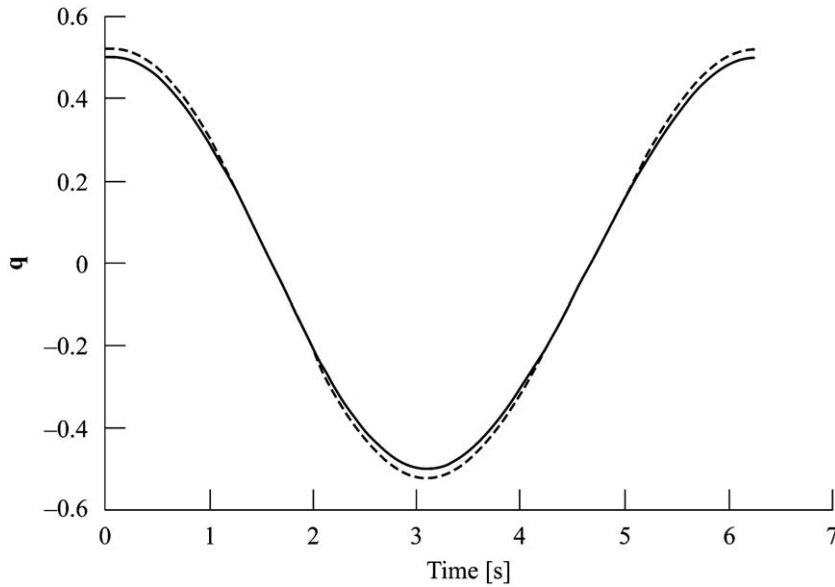


Fig. 8. First non-similar nonlinear normal mode response for the system: $\ddot{q}_1 + 2q_1 - q_2 + 0.5q_1^3 = 0$, $\ddot{q}_2 + 2q_2 - q_1 = 0$, using eleven Gaussian temporal-basis-functions. $q_1(0) = 0.5$, $q_2(0) = 25/48$, $\dot{q}_i(0) = 0, i = 1, 2$. $\Delta t = 6.145$ s.

Table 4

Component functions of the fundamental-time-modes composing the second non-similar nonlinear normal mode response for the system: $\ddot{q}_1 + 2q_1 - q_2 + 0.5q_1^3 = 0$, $\ddot{q}_2 + 2q_2 - q_1 = 0$. $q_1(0) = 0.5$, $q_2(0) = -99/208$, $\dot{q}_i(0) = 0, i = 1, 2$. $\Delta t = 3.6$ s.

i	τ_i	$\mathbf{E}(i,1)$	$\mathbf{E}(i,2)$	$\mathbf{E}(i,3)$	$\mathbf{E}(i,4)$
$q_{1j}^*(\tau) = \sum_{i=1}^{11} \mathbf{E}(i,j) e^{-K_i(\tau-\tau_i)^2}, \quad K_i = 5.9 \quad i \neq 6, \quad K_6 = 3.9$					
1	-0.800	$-4.100779561 \times 10^{-1}$	$4.690150863 \times 10^{-1}$	$-3.473987090 \times 10^{-1}$	$4.703770926 \times 10^{-1}$
2	-0.540	$3.904966908 \times 10^{-1}$	$-3.885240430 \times 10^{-1}$	$1.018618446 \times 10^{-1}$	$1.127587956 \times 10^{-1}$
3	-0.280	$-2.688571173 \times 10^{-1}$	$-7.186569784 \times 10^{-2}$	$-3.750478249 \times 10^{-1}$	$-2.752798491 \times 10^{-1}$
4	0.000	$-4.415316443 \times 10^{-2}$	$1.512577559 \times 10^{-1}$	$2.353464687 \times 10^{-1}$	$-1.200088291 \times 10^{-1}$
5	0.244	$2.458352972 \times 10^{-2}$	$5.479100833 \times 10^{-2}$	$-1.154054864 \times 10^{-1}$	$1.555191436 \times 10^{-1}$
6	0.505	$-2.443055801 \times 10^{-3}$	$-7.538115996 \times 10^{-2}$	$2.198303450 \times 10^{-1}$	$-4.834185777 \times 10^{-3}$
7	0.766	$-2.273621380 \times 10^{-2}$	$6.134310656 \times 10^{-2}$	$-1.103582469 \times 10^{-1}$	$-1.509367423 \times 10^{-1}$
8	1.027	$6.202534845 \times 10^{-2}$	$1.462404267 \times 10^{-1}$	$2.485988471 \times 10^{-1}$	$1.271434600 \times 10^{-1}$
9	1.288	$2.583955903 \times 10^{-1}$	$-1.204118448 \times 10^{-1}$	$-3.760531830 \times 10^{-1}$	$2.730614428 \times 10^{-1}$
10	1.549	$-4.329925472 \times 10^{-1}$	$-3.247636154 \times 10^{-1}$	$9.258439344 \times 10^{-2}$	$-1.261595705 \times 10^{-1}$
11	1.810	$4.93233212 \times 10^{-1}$	$4.232378892 \times 10^{-1}$	$-3.330491297 \times 10^{-1}$	$-4.652378375 \times 10^{-1}$
$q_{2j}^*(\tau) = \sum_{i=1}^{11} \mathbf{E}(i,j) e^{-K_i(\tau-\tau_i)^2}, \quad K_i = 5.9 \quad i \neq 6, \quad K_6 = 3.9$					
1	-0.800	$5.142151173 \times 10^{-2}$	$-2.811133111 \times 10^{-2}$	$3.259743759 \times 10^{-2}$	$-6.768626094 \times 10^{-2}$
2	-0.540	$1.058141194 \times 10^{-2}$	$6.613775570 \times 10^{-2}$	$-1.501346980 \times 10^{-2}$	$-2.172872476 \times 10^{-3}$
3	-0.280	$8.651291178 \times 10^{-2}$	$-5.805243224 \times 10^{-2}$	$-9.400606214 \times 10^{-2}$	$2.019403034 \times 10^{-1}$
4	0.000	$-8.529945513 \times 10^{-2}$	$-1.973589101 \times 10^{-1}$	$-1.987509359 \times 10^{-1}$	$-7.592573797 \times 10^{-2}$
5	0.244	$-1.884858604 \times 10^{-2}$	$-5.092060405 \times 10^{-2}$	$-4.210251323 \times 10^{-2}$	$-3.224485300 \times 10^{-1}$
6	0.505	$1.919029068 \times 10^{-2}$	$4.025189136 \times 10^{-1}$	$4.221198864 \times 10^{-1}$	$8.651072105 \times 10^{-3}$
7	0.766	$1.814650892 \times 10^{-2}$	$-8.274629456 \times 10^{-2}$	$-3.364289343 \times 10^{-2}$	$3.177578623 \times 10^{-1}$
8	1.027	$6.605257158 \times 10^{-2}$	$-2.088219764 \times 10^{-1}$	$-1.906325785 \times 10^{-1}$	$6.780069189 \times 10^{-2}$
9	1.288	$-9.106989466 \times 10^{-2}$	$-3.852504612 \times 10^{-2}$	$-8.972011227 \times 10^{-2}$	$-2.041064944 \times 10^{-1}$
10	1.549	$-1.424685932 \times 10^{-2}$	$6.176603761 \times 10^{-2}$	$-2.347792800 \times 10^{-2}$	$1.153113958 \times 10^{-2}$
11	1.810	$-6.008697196 \times 10^{-2}$	$-1.561217928 \times 10^{-2}$	$2.640676673 \times 10^{-2}$	$5.683037473 \times 10^{-2}$

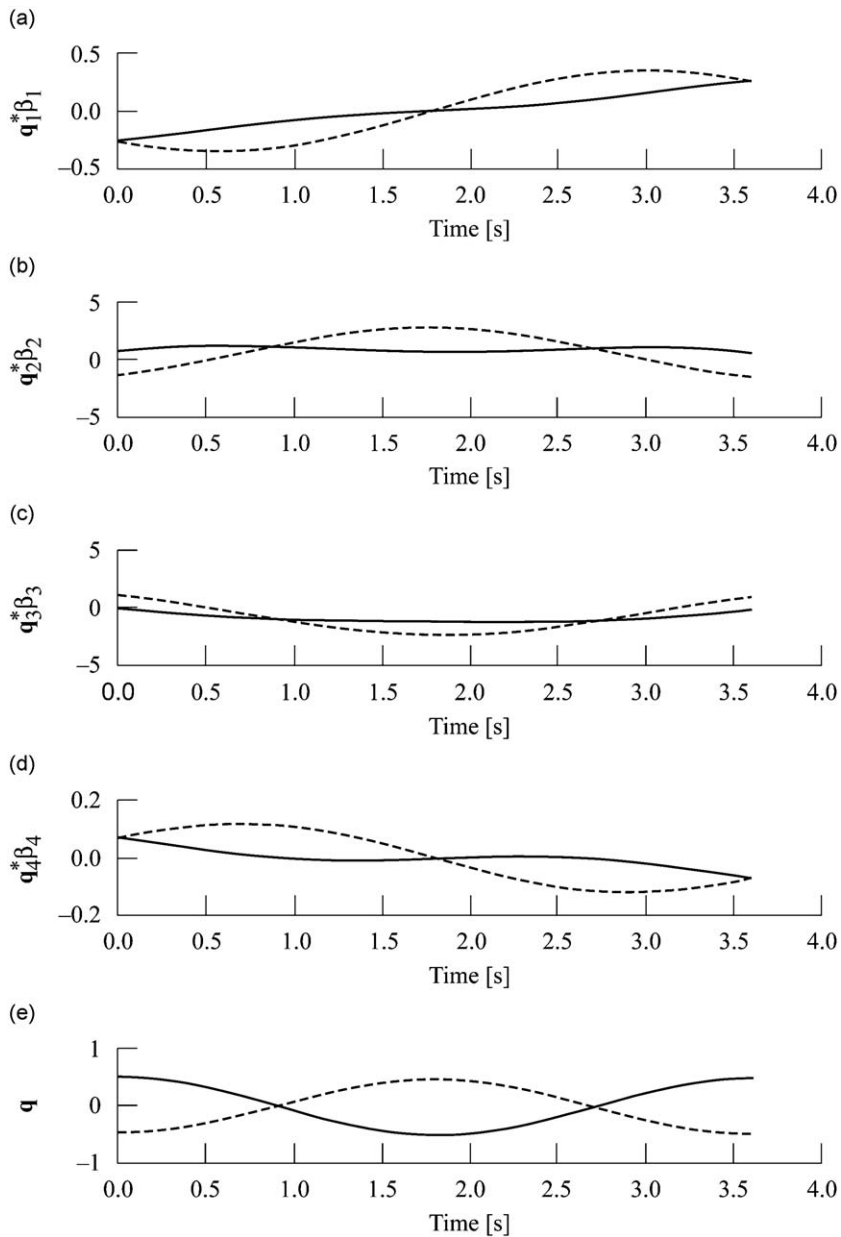


Fig. 9. Fundamental-time-modal composition of the second non-similar nonlinear normal mode response of the system: $\ddot{q}_1 + 2q_1 - q_2 + 0.5q_1^3 = 0$, $\ddot{q}_2 + 2q_2 - q_1 = 0$, using eleven Gaussian temporal-basis-functions. (a) $\mathbf{q}_1^* \beta_1$; $-q_{11}^*$, $-q_{21}^*$, (b) $\mathbf{q}_2^* \beta_2$; $-q_{12}^*$, $-q_{22}^*$, (c) $\mathbf{q}_3^* \beta_3$; $-q_{13}^*$, $-q_{23}^*$, (d) $\mathbf{q}_4^* \beta_4$; $-q_{14}^*$, $-q_{24}^*$, (e) \mathbf{q} ; $-q_1$, $-q_2$. $q_1(0) = 0.5$, $q_2(0) = -99/208$, $\dot{q}_i(0) = 0, i = 1, 2$. $\Delta t = 3.6$ s.

5. Model reduction

The process of omitting modes from a solution process in the spatial domain is known as model reduction, modal truncation [41] or mode summation [42]. The classical model reduction concepts are herein applied to the coordinate vector-space \mathbf{F}^n , and consequently extended to the vector-space of functions \mathcal{F}^{HLVA} in the time domain. Model reduction can be implemented in the null-space for both free and forced systems, and in the range-space for forced systems. The model reduction method presented herein is applicable to both linear and nonlinear systems, and may be implemented where it is desirable or necessary to simulate the response of a dynamic system, while omitting the basis vectors and consequently the fundamental-time-modes that do not play an active role in characterizing the response. In this manner, smaller modal matrices are involved in the solution process thereby providing some gain in

computational efficiency, particularly for linear systems. For nonlinear systems, the effects of the reduced modal matrices on convergence of the expansion coefficients **A**, must be considered when contemplating model reduction. The concept of model reduction implies that knowledge of the dominant fundamental-time-modes has been acquired by some means, usually through prior generation of the response. The dominant basis vectors and thus the dominant fundamental-time-modes may be tracked by observing their modal coordinates, which indicate the degree of fundamental-time-mode participation.

The initial conditions may be expressed in terms of the null-space modal matrix and modal coordinates as shown in Eq. (26) with $\tau = 0$. Left multiplying Eq. (26) by $\tilde{\mathbf{E}}_N^T \Psi^T(0)$, and rearranging, the modal coordinates $\tilde{\mathbf{\beta}}_N$ are shown in terms of the reduced null-space modal matrix $\tilde{\mathbf{E}}_N$

$$\tilde{\mathbf{\beta}}_N = (\tilde{\mathbf{E}}_N^T \Psi^T(0) \Psi(0) \tilde{\mathbf{E}}_N)^{-1} \tilde{\mathbf{E}}_N^T \Psi^T(0) \left\{ \begin{matrix} \mathbf{q}(0) - \mathbf{q}^R(0) \\ \dot{\mathbf{q}}(0) - \dot{\mathbf{q}}^R(0) \end{matrix} \right\}. \tag{50}$$

Here $\tilde{\mathbf{E}}_N$ indicates that the modal matrix has been reduced by omitting the non-dominant null-space basis vectors. Model reduction may be implemented by utilizing Eq. (50) in place of Eq. (27) in the universal procedure.

Eq. (50) provides model reduction for both free and forced systems by considering only the null-space modal matrix. For forced systems, it is also possible to include the reduced range-space modal matrix $\tilde{\mathbf{E}}_R$ in the modal reduction effort as well. Eq. (25) expresses the range-space modal coordinates $\tilde{\mathbf{\beta}}_R$, in terms of the range-space modal matrix \mathbf{E}_R and the forcing functions **b**, and is shown here in terms of the reduced range-space modal matrix $\tilde{\mathbf{E}}_R$

$$\tilde{\mathbf{\beta}}_R = \left[\begin{matrix} \backslash \\ \lambda^{-1} \\ \backslash \end{matrix} \right]_R (\tilde{\mathbf{E}}_R^T \tilde{\mathbf{E}}_R)^{-1} \tilde{\mathbf{E}}_R^T \mathbf{b}. \tag{51}$$

By employing a range-space modal matrix reduced by omitting non-dominant range-space basis vectors, the reduced range-space modal coordinates may be determined.

The displacement and velocity response of the reduced model may therefore be expressed in terms of the reduced modal matrices and modal coordinates as

$$\left\{ \begin{matrix} \tilde{\mathbf{q}}(\tau) \\ \dot{\tilde{\mathbf{q}}}(\tau) \end{matrix} \right\} = [\Psi(\tau)] \{ (\tilde{\mathbf{E}}_N \tilde{\mathbf{\beta}}_N + [\tilde{\mathbf{E}}]_R \tilde{\mathbf{\beta}}_R) \}. \tag{52}$$

For nonlinear systems, the $[\mathbf{P}(\mathbf{A})]$ matrix will in general change with each transition interval. As a result, the null- and range-space modal matrices will generally change from one transition interval to the next throughout the response trajectory. An exception to this would occur when the nonlinear system is synchronous, with the transition interval exactly spanning the period. However, in general the modal matrix will be variant with respect to transition interval. Therefore, in order to implement model reduction for nonlinear systems, it may be necessary to omit different basis vectors at different transition intervals along the response trajectory. Although the modal matrices will likely be variant with respect to

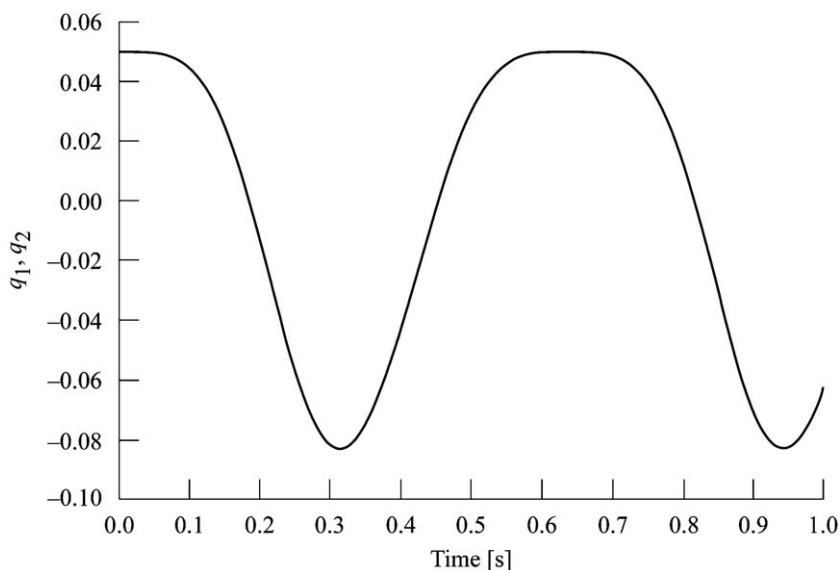


Fig. 10. Response of the full and reduced models for the system: $\ddot{q}_1 + 0.02\dot{q}_1 - 0.01q_2 + 200q_1 - 100q_2 - 20(q_2 - q_1)^3 + 20q_1^3 = 5.0\cos(20t)$, $\ddot{q}_2 + 0.02\dot{q}_2 - 0.01\dot{q}_1 + 200q_2 - 100q_1 + 20(q_2 - q_1)^3 + 20q_2^3 = 5.0\cos(20t)$, using six power series temporal-basis-functions. $q_i(0) = 0.05$, $\dot{q}_i(0) = 0$, $i = 1, 2$. $\Delta t = 0.004$ s.

transition interval, the mode index associated with the dominant basis vectors may remain the same. Under these circumstances, tracking the dominant basis vectors and consequently the dominant fundamental-time-modes is trivial, as the following example demonstrates.

Consider the nonlinear system of Fig. 2 characterized by the following system parameters in consistent units,

$$\begin{aligned}
 m_i &= 1, & f_i &= 5.0 \cos(20t), & i &= 1, 2 \\
 k_{li} &= 100, & k_{nl_i} &= 20, & c_i &= 0.01, & i &= 1, 2, 3 \\
 q_i(0) &= 0.05, & \dot{q}_i(0) &= 0.0, & i &= 1, 2
 \end{aligned}
 \tag{53}$$

Six power series temporal-basis-functions were used, making $[\mathbf{P}(\mathbf{A})]$ of dimension 12×12 for this 2 degree-of-freedom system. From the rank and nullity theorem, the range-space modal matrix will consist of eight basis vectors. The algebraic equations of motion, Eq. (40), were solved for each of the 250 transition intervals of 0.004 s each, resulting in peak errors in the accuracy integral and differential equations of magnitudes 3.4×10^{-12} and 2.7×10^{-7} respectively. By inspecting the products of the fundamental-time-modes and their modal coordinates, it was determined that the 4th null-space basis vector and the 2nd, 4th, 6th and 8th range-space basis vectors were non-dominant fundamental-time-modes since they exhibited amplitudes less than 1.0×10^{-5} over the entire response history. Therefore, model reduction was implemented by omitting these basis vectors.

The reduced model response was generated over an elapsed time of 1 s in a time-marching fashion, using the Universal Procedure, with the reduced null- and range-space modal matrices, $[\tilde{\mathbf{E}}]_N = [\mathbf{E}_1 \mathbf{E}_2 \mathbf{E}_3]_N$ and $[\tilde{\mathbf{E}}]_R = [\mathbf{E}_1 \mathbf{E}_3 \mathbf{E}_5 \mathbf{E}_7]_R$ respectively, replacing the full modal matrices, and Eqs. (27) and (25) replaced by Eqs. (50) and (51) respectively. Eq. (40) was solved for each of 250 transition intervals of 0.004 s each. The eigenvalue analysis was used exclusively, along with 6 power series temporal-basis-functions, resulting in peak errors in the accuracy integral and differential equations of magnitudes 7.5×10^{-12} and 3.8×10^{-7} respectively. The response of the full and reduced models is shown in Fig. 10, where it can be observed that there is no noticeable loss in the accuracy of the response using the reduced model. The peak difference between the responses for the full and reduced models was of magnitude 2.4×10^{-6} for both degrees-of-freedom.

The reduced model required an increased number of iterations to reach convergence of the expansion coefficients \mathbf{A} as compared to the full model. Even though computational savings were not realized in this example, it cannot be concluded that computational savings are not possible for all nonlinear systems.

6. Superposition

It has been shown that the response of linear [25] and nonlinear systems are composed of fundamental-time-modes. Up to this point, the assemblage of fundamental-time-modes has been referred to as a linear combination, or as an expansion, and has not been specifically characterized as a superposition. The intent here is to demonstrate that superposition of trajectories coincident with fundamental-time-modes characterizing the free-motion of nonlinear systems is possible.

To begin, the definitions of superposition with regard to this work need to be defined. A superposition of fundamental-time-modes implies that each individual fundamental-time-mode can be excited individually, and is, in and of itself, a

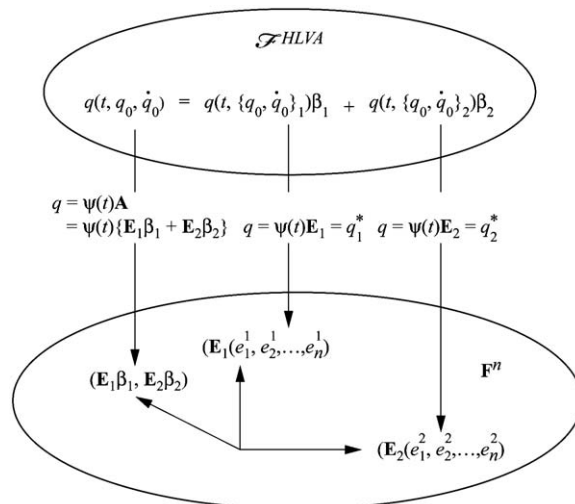


Fig. 11. Superposition principle for one degree-of-freedom system.

Table 5
Fundamental initial conditions generating individual fundamental-time-mode responses for nonlinear system.

$$\ddot{q}_1 + 200q_1 - 100q_2 - 100(q_2 - q_1)^3 + 100q_1^3 = 0, \ddot{q}_2 + 200q_2 - 100q_1 + 100(q_2 - q_1)^3 + 100q_2^3 = 0$$

<i>i</i>	1	2	3	4	Superposed
$q_{1i}(0)$	4.7775371979000e-03	-1.071590371680e-03	-9.0707391991432e-04	-6.3121877401517e-04	2.16765524808e-03
$q_{2i}(0)$	4.7775371410700e-03	1.071590439990e-03	9.0707393070520e-04	-6.3121878474566e-04	6.12498424585e-03
$\dot{q}_{1i}(0)$	-7.9147415607932e-04	2.204716414427e-02	-1.3280322533850e-02	-4.4146891626453e-01	-4.33493550000e-01
$\dot{q}_{2i}(0)$	-7.9147232697552e-04	-2.204717246662e-02	1.3280330021490e-02	-4.4146891628019e-01	-4.51027230000e-01

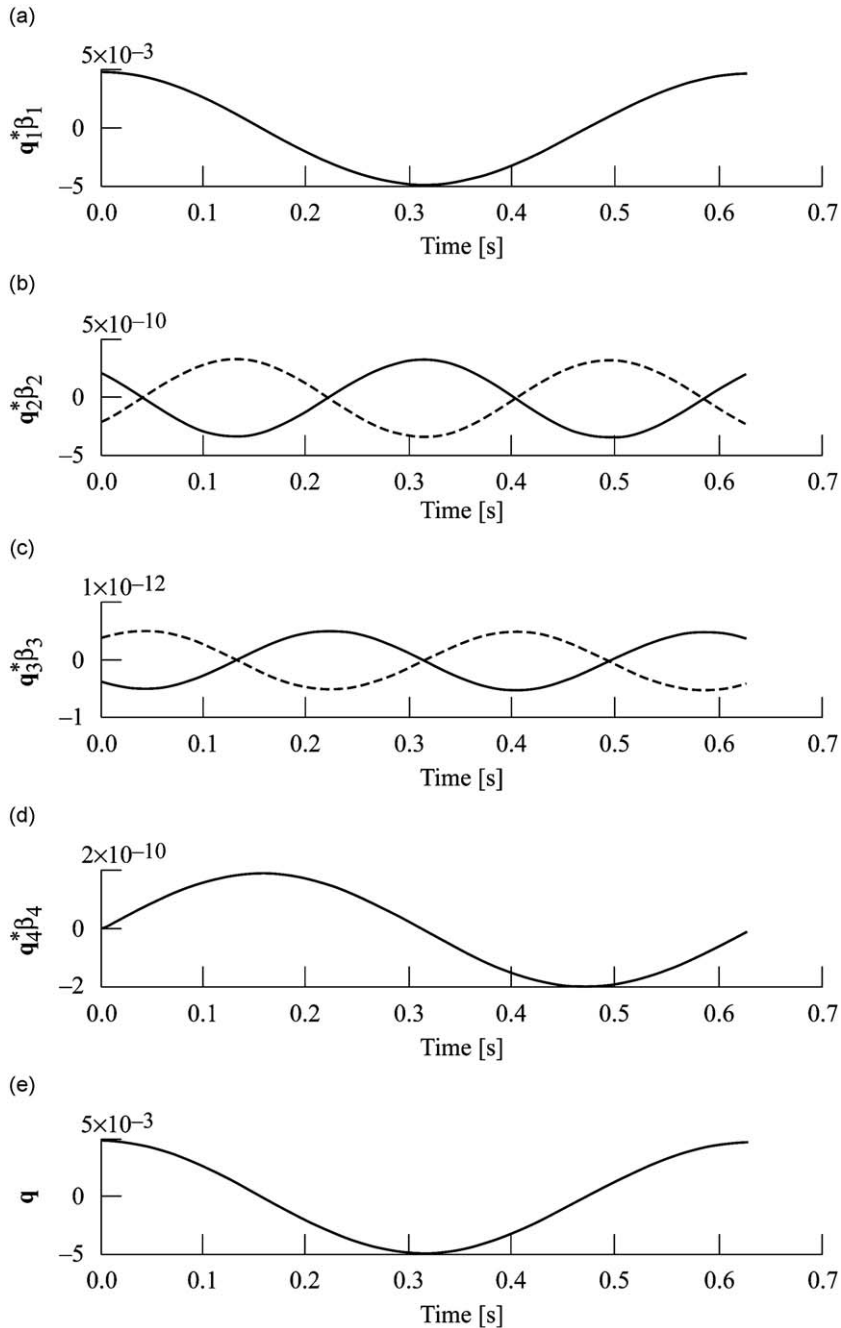


Fig. 12. First global fundamental-time-mode response for the system: $\ddot{q}_1 + 200q_1 - 100q_2 - 100(q_2 - q_1)^3 + 100q_1^3 = 0, \ddot{q}_2 + 200q_2 - 100q_1 + 100(q_2 - q_1)^3 + 100q_2^3 = 0$ using nine Gaussian temporal-basis-functions. (a) $\mathbf{q}_1^* \beta_1; -q_{11}^*, -q_{21}^*$, (b) $\mathbf{q}_2^* \beta_2; -q_{12}^*, -q_{22}^*$, (c) $\mathbf{q}_3^* \beta_3; -q_{13}^*, -q_{23}^*$, (d) $\mathbf{q}_4^* \beta_4; -q_{14}^*, -q_{24}^*$, (e) $\mathbf{q}; -q_1, -q_2$.

response trajectory satisfying Hamilton’s Law of Varying Action, where the direct sum of the individual fundamental-time-mode trajectories composes a superposed trajectory that is yet another response trajectory satisfying Hamilton’s Law of Varying Action. Moreover, this superposed trajectory can be excited by using the sum of the initial conditions that excite each individual fundamental-time-mode trajectory. Along with superposition, the concept of scalability is considered.

The fundamental-time-modes $\mathbf{q}_i^*(t)$, are represented in coordinate space \mathbf{F}^n , by their respective basis vectors \mathbf{E}_i . These basis vectors may be viewed as coordinate vectors in \mathbf{F}^n , according to their geometric interpretation. The endpoint of each coordinate vector is given by the nN coordinates, or scalars, composing each coordinate vector \mathbf{E}_i .

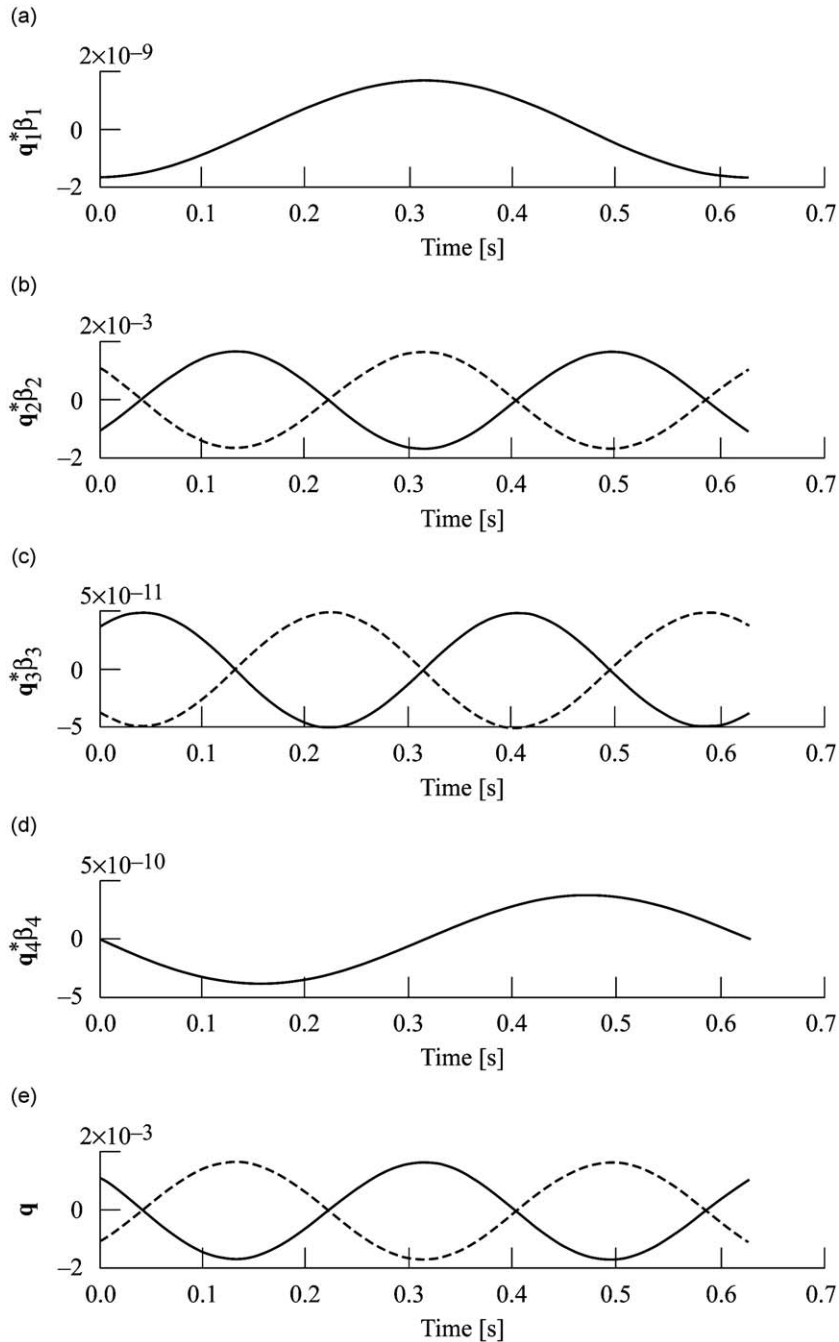


Fig. 13. Second global fundamental-time-mode response for the system: $\ddot{q}_1 + 200q_1 - 100q_2 - 100(q_2 - q_1)^3 + 100q_1^3 = 0$, $\ddot{q}_2 + 200q_2 - 100q_1 + 100(q_2 - q_1)^3 + 100q_2^3 = 0$ using nine Gaussian temporal-basis-functions. (a) $\mathbf{q}_1^* \beta_1; -q_{11}^*, -q_{21}^*$, (b) $\mathbf{q}_2^* \beta_2; -q_{12}^*, -q_{22}^*$, (c) $\mathbf{q}_3^* \beta_3; -q_{13}^*, -q_{23}^*$, (d) $\mathbf{q}_4^* \beta_4; -q_{14}^*, -q_{24}^*$, (e) $\mathbf{q}; -q_1, -q_2$.

For linear time-invariant systems, the $[P]$ matrix does not change from one transition interval to another, when equi-spaced transition intervals are used. In such situations, the coordinate vectors E_i are fixed in F^n for all transition intervals. Moreover, these $2N$ coordinate vectors remain fixed in F^n regardless of the initial conditions imposed on the system in \mathcal{F}^{HLVA} [34]. Therefore, it is possible to choose initial conditions

$$\left\{ \begin{matrix} \mathbf{q}(0) \\ \Delta t \dot{\mathbf{q}}(0) \end{matrix} \right\}_i = \left\{ \begin{matrix} \mathbf{q}^*(0) \\ \Delta t \dot{\mathbf{q}}^*(0) \end{matrix} \right\}_i = \Psi(0) \mathbf{E}_i \quad i = 1, 2, \dots, 2N \tag{54}$$

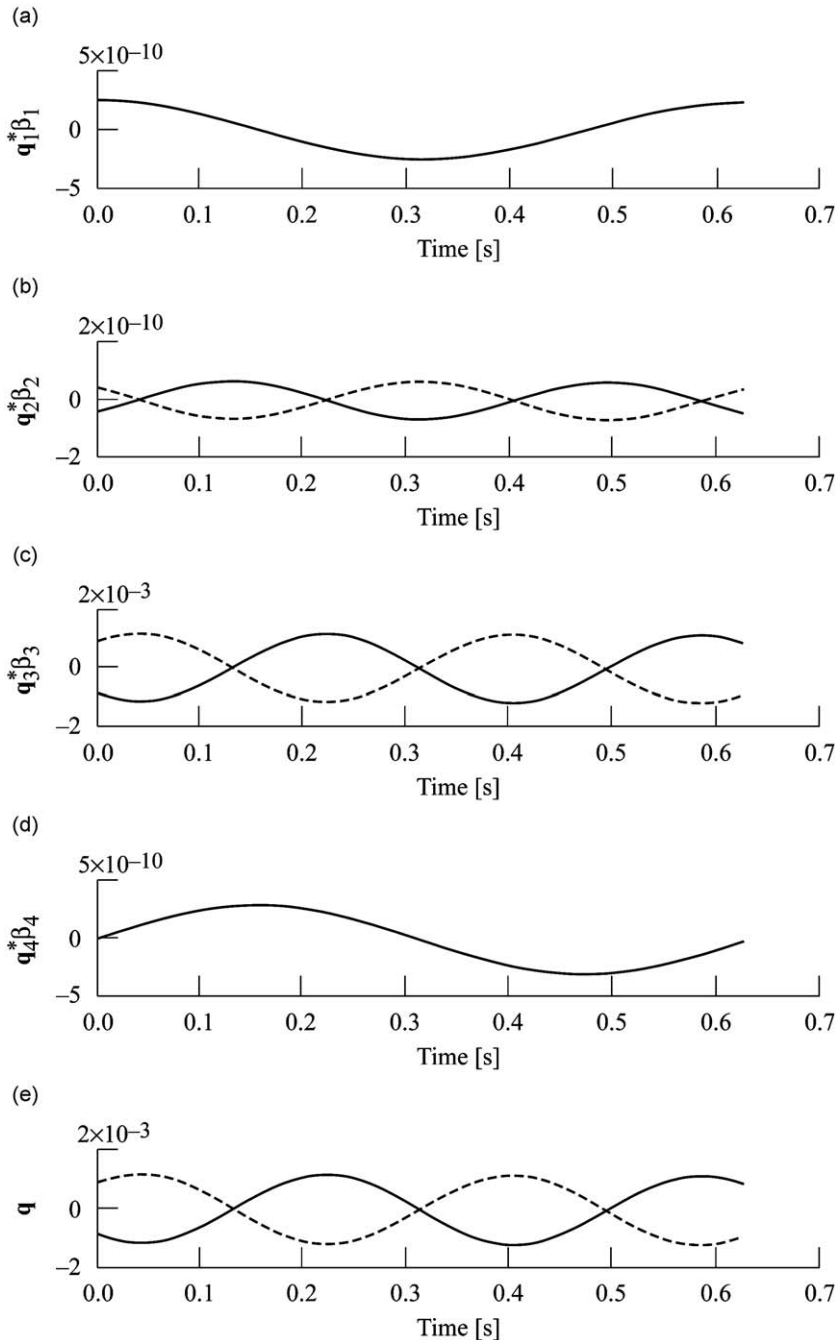


Fig. 14. Third global fundamental-time-mode response for the system: $\ddot{q}_1 + 200q_1 - 100q_2 - 100(q_2 - q_1)^3 + 100q_1^3 = 0$, $\ddot{q}_2 + 200q_2 - 100q_1 + 100(q_2 - q_1)^3 + 100q_2^3 = 0$ using nine Gaussian temporal-basis-functions. (a) $q_1^* \beta_1$; $-q_1^*$, $-q_{21}^*$, (b) $q_2^* \beta_2$; $-q_2^*$, $-q_{22}^*$, (c) $q_3^* \beta_3$; $-q_{13}^*$, $-q_{23}^*$, (d) $q_4^* \beta_4$; $-q_{14}^*$, $-q_{24}^*$, (e) q ; $-q_1$, $-q_2$.

such that the response is a function of only one coordinate vector \mathbf{E}_i , where $\Psi(\tau)$ is described in Eq. (15) and where \mathbf{E}_i and Δt are known

$$\mathbf{q}_i(t) = \mathbf{q}_i^*(t) = \begin{bmatrix} \backslash \\ \Psi(\tau) \\ \backslash \end{bmatrix} \mathbf{A} = \begin{bmatrix} \backslash \\ \Psi(\tau) \\ \backslash \end{bmatrix} \mathbf{E}_i. \tag{55}$$

The initial conditions described by Eq. (54) will be denoted as *fundamental initial conditions*. Eq. (54) involves the evaluation of the fundamental-time-modes at $t=0$. Thus, the response along each of $2N$ individual coordinate vectors \mathbf{E}_i , can be generated independently as shown in Eq. (55) using their corresponding $2N$ fundamental initial conditions. This is shown schematically for a 1 degree-of-freedom system in Fig. 11. For the linear system, all of the responses may then be scaled and superposed in \mathcal{F}^{HLVA} , to generate the response for any specific initial conditions. An iterative form of this procedure is illustrated herein for a nonlinear system.

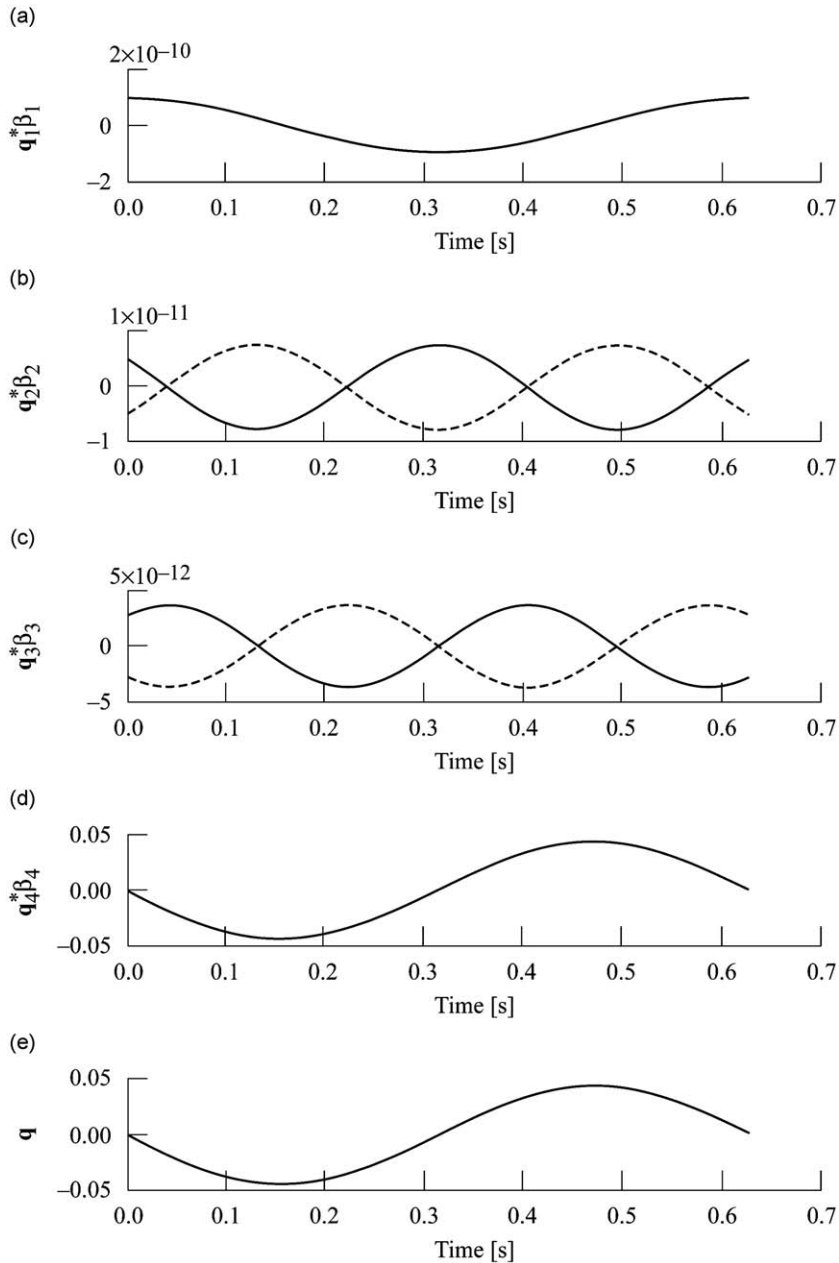


Fig. 15. Fourth global fundamental-time-mode response for the system: $\ddot{q}_1 + 200q_1 - 100q_2 - 100(q_2 - q_1)^3 + 100q_1^3 = 0$, $\ddot{q}_2 + 200q_2 - 100q_1 + 100(q_2 - q_1)^3 + 100q_2^3 = 0$ using nine Gaussian temporal-basis-functions. (a) $\mathbf{q}_1^* \beta_1; -q_{11}^*, -q_{21}^*$, (b) $\mathbf{q}_2^* \beta_2; -q_{12}^*, -q_{22}^*$, (c) $\mathbf{q}_3^* \beta_3; -q_{13}^*, -q_{23}^*$, (d) $\mathbf{q}_4^* \beta_4; -q_{14}^*, -q_{24}^*$, (e) $\mathbf{q}; -q_1, -q_2$.

The algebraic equations of motion and thus $[P]$ will likely change from one transition interval to the next for nonlinear systems, as well as for time-variant linear systems and linear systems where non-equispaced transition intervals are used. Regardless of the type of system, and in particular nonlinear systems, the vector-space approach provides a basis of fundamental-time-modes spanning the solution space over the transition interval in question. This transition interval may span a fraction of a second to a complete period or to infinite-time, depending on the temporal-basis-functions chosen.

In F^n , these individual fundamental-time-mode responses may be described by their respective coordinate vectors E_i as shown in Eq. (55). Eq. (55) represents a fundamental-time-mode response characterized by a single coordinate direction E_i , or eigen-direction in F^n . Since these basis vectors are linearly independent, a fundamental-time-mode response obtained solely as a function of a single basis vector will not be a function of the other responses. Individual responses that are generated solely as functions of their respective linearly independent vectors provide a set of linearly independent response trajectories for a nonlinear system for the current transition interval. To search for fundamental initial conditions that would result in a set of superposable linearly independent response trajectories, $2N$ individual response solutions $q_i(t)$ are sought by setting $A = E_i$ in the universal procedure, while at the same time requiring $\{\lambda_i = 0, i = 1, 2, \dots, 2N\}$, providing a basis $\{E_1, E_2, \dots, E_i, \dots, E_{2N}\}$. This procedure is denoted as *single eigen-direction iteration*. This process results in $2N$ sets of fundamental initial conditions, via Eq. (54) that produces $2N$ individual admissible fundamental-time-mode responses satisfying Hamilton’s Law of Varying Action. If $2N$ independent fundamental-time-mode response solutions can be obtained, as shown in Eq. (55), their superposition is possible since they form a basis for the null-space for the current transition interval.

Eigen-direction iteration will be illustrated by considering the previous nonlinear system characterized by Eq. (42). The initial conditions are not explicitly specified a priori, although unpremeditated initial conditions are implicitly specified through the arbitrary choice of the initial starting value of E_i . The fundamental initial conditions are only known via Eq. (54), once the solution has converged.

Using single eigen-direction iteration, four individual response solutions over an elapsed time of 0.625 s were generated without time marching, by solving the algebraic equations of motion as represented by Eq. (40). Nine Gaussian temporal-basis-functions were used with spreads $k_i = 5.0, i = 1, 2, \dots, 9$, and centers $\{-0.15, 0.0125, 0.175, \dots, 1.15\}$. In each case, A was set equal to E_i during iteration. Once the solution had converged, the fundamental initial conditions necessary to generate each fundamental-time-mode response were obtained using Eq. (54). These four sets of fundamental initial conditions are presented in Table 5.

Four separate fundamental-time-mode response solutions corresponding to these four fundamental initial conditions were generated using the universal procedure for nonlinear systems. Implementing the universal procedure with the fundamental initial conditions corresponding to the first fundamental-time-mode produced the results shown in Fig. 12. This process was repeated three more times for the other three fundamental-time-modes, with the corresponding results shown in Figs. 13–15. In each case, it can be seen that a single fundamental-time-mode (eigen-direction) response was achieved. Superposing each individual fundamental-time-mode response, i.e., part (e) of Figs. 12–15, produces the response shown in Fig. 16. The initial conditions corresponding to the superposed response are also presented in Table 5, and were determined using Eq. (54) where all of the basis vectors $[E_1\beta_1 + E_2\beta_2 + E_3\beta_3 + E_4\beta_4]$ were used instead of only E_i , and where $(\beta_1 = \beta_2 = \beta_3 = \beta_4 = 1)$. Furthermore, it may be verified that the superposed initial conditions are also the direct sum of the fundamental initial conditions for each of the four fundamental-time-modes shown in Table 5.

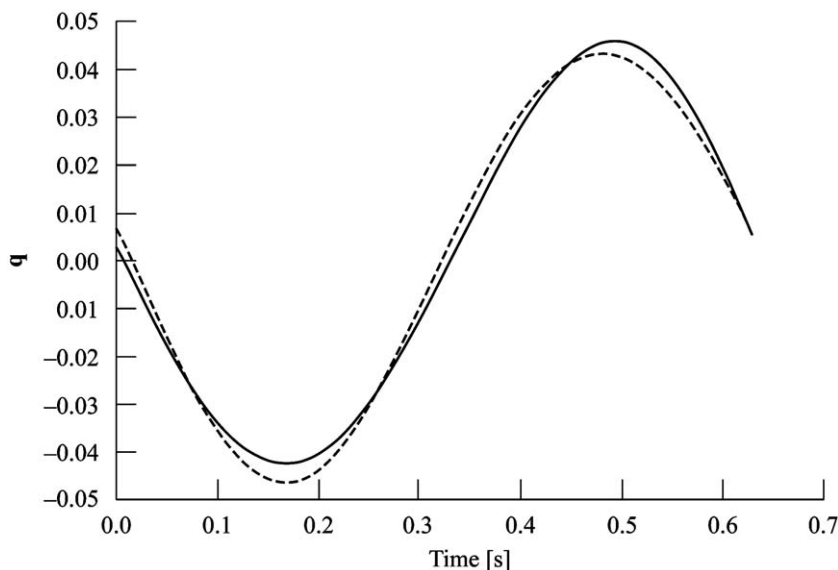


Fig. 16. Superposed response for the system: $\ddot{q}_1 + 200q_1 - 100q_2 - 100(q_2 - q_1)^2 + 100q_1^3 = 0, \ddot{q}_2 + 200q_2 - 100q_1 + 100(q_2 - q_1)^2 + 100q_2^3 = 0$ using nine Gaussian temporal basis-functions. $-q_1, -q_2$.

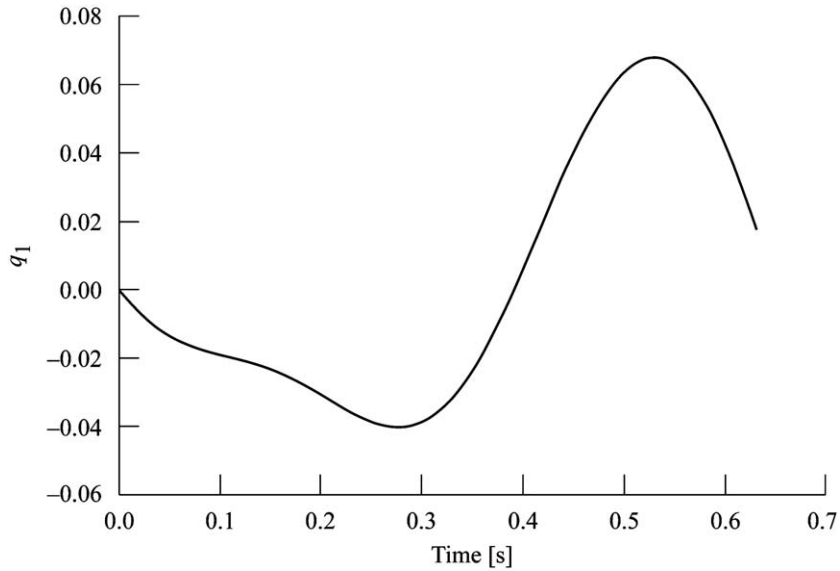


Fig. 17. Superposed, combined, and exact response for the first degree-of-freedom for the system: $\ddot{q}_1 + 200q_1 - 100q_2 - 100(q_2 - q_1)^3 + 100q_1^3 = 0$, $\ddot{q}_2 + 200q_2 - 100q_1 + 100(q_2 - q_1)^3 + 100q_2^3 = 0$. Scaled (weighted) fundamental-time-modes used for superposed response. – Superposed, ⋯ Combined, - - Exact.

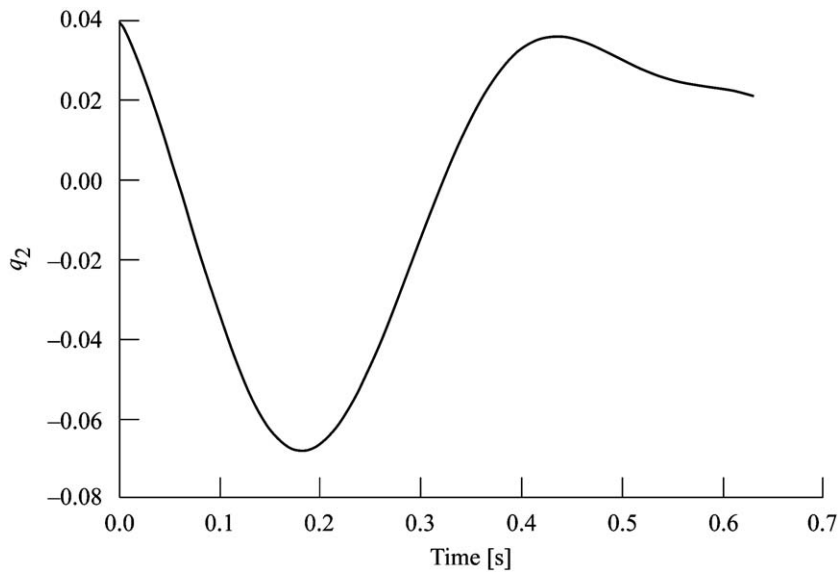


Fig. 18. Superposed, combined, and exact response for the second degree-of-freedom for the system: $\ddot{q}_1 + 200q_1 - 100q_2 - 100(q_2 - q_1)^3 + 100q_1^3 = 0$, $\ddot{q}_2 + 200q_2 - 100q_1 + 100(q_2 - q_1)^3 + 100q_2^3 = 0$. Scaled (weighted) fundamental-time-modes used for superposed response. – Superposed, ⋯ Combined, - - Exact.

The computationally “exact” solution using 8 power series temporal-basis-functions and the initial conditions for the superposed case, resulted in peak integral and differential equation errors of magnitude 2.5×10^{-12} and 3.8×10^{-10} , respectively. The superposed response was then compared to the exact response resulting in a peak difference in magnitude of 3.3×10^{-5} and 1.2×10^{-5} for the first and second degree-of-freedom respectively. Therefore, superposition without scaling for a nonlinear system has been demonstrated successfully.

Consider the fundamental initial conditions presented in Table 5. To illustrate scalability, each set of fundamental initial conditions are scaled as shown

$$4 \begin{Bmatrix} \mathbf{q}_1^*(0) \\ \dot{\mathbf{q}}_1^*(0) \end{Bmatrix}, \quad 10 \begin{Bmatrix} \mathbf{q}_2^*(0) \\ \dot{\mathbf{q}}_2^*(0) \end{Bmatrix}, \quad 10 \begin{Bmatrix} \mathbf{q}_3^*(0) \\ \dot{\mathbf{q}}_3^*(0) \end{Bmatrix}, \quad \begin{Bmatrix} \mathbf{q}_4^*(0) \\ \dot{\mathbf{q}}_4^*(0) \end{Bmatrix}, \quad (56)$$

i.e., $\beta_1 = 4$, $\beta_2 = 10$, $\beta_3 = 10$, $\beta_4 = 1$, where the combined initial conditions are a sum of the scaled fundamental initial conditions

$$\begin{aligned} q_1(0) &= -0.0013077132 \\ q_2(0) &= 0.038265573 \\ \dot{q}_1(0) &= -0.35696641 \\ \dot{q}_2(0) &= -0.53230323. \end{aligned} \quad (57)$$

Using the universal procedure, four individual fundamental-time-mode response solutions over an elapsed time of 0.625 s were generated without time-marching, by solving the algebraic equations of motion as represented by Eq. (40) using the scaled fundamental initial conditions as shown in Eq. (56). The same Gaussian temporal-basis-functions were used as before. Superimposing the individual fundamental-time-mode responses produced the superposed response q_{1s} and q_{2s} for the first and second degree-of-freedom respectively, as shown in Figs. 17 and 18 respectively. A combined response q_{1c} and q_{2c} , for the first and second degree-of-freedom respectively, was generated using the combined initial conditions, as shown in Eq. (57), and are also represented in Figs. 17 and 18 respectively. The combined response exhibited a peak difference in magnitude of 2.1×10^{-4} and 1.4×10^{-4} with the superposed response, for the first and second degree-of-freedom respectively.

The numerically “exact” response was also generated using the combined initial conditions, shown in Eq. (57), over an elapsed time of 0.625 s by solving the algebraic equations of motion for each of 100 transition intervals, using 8 power series temporal-basis-functions. This resulted in peak integral and differential equation errors of magnitude 5.6×10^{-12} and 6.2×10^{-10} , respectively. The exact response trajectories q_{1e} and q_{2e} , for the first and second degree-of-freedom respectively, are also shown in Figs. 17 and 18 respectively, along with the superposed and combined responses. The peak difference in magnitude between the “exact” and combined responses was 1.4×10^{-4} and 1.0×10^{-4} respectively for the first and second degree-of-freedom respectively. Thus, scalable superposition has been successfully demonstrated for this particular nonlinear system.

As initial conditions are imposed further away from the fundamental initial conditions, the original coordinate vectors corresponding to the fundamental initial conditions will no longer scale to adequately span the null-space of the new $[\mathbf{P}]$ associated with the new initial conditions. Correspondingly then, the fundamental-time-modes will no longer scale to span the solution space in \mathcal{F}^{HLVA} . This means that the amount of scaling is limited to a finite domain. For nonlinear systems, however, this is expected/not surprising since different domains of attraction with different characteristics will/may exist in which case characteristics of no single domain will apply to the global domain.

In the previous examples, the single eigen-direction iteration was implemented using transition intervals of a full period or characteristic length. However, the single eigen-direction iteration works for transition intervals with non-characteristic lengths as well.

7. Conclusion

The vector-space perspective of Hamilton’s Law of Varying Action, having been previously developed by the authors for linear systems has been extended to nonlinear systems herein. The advantages of the vector-space perspective result from the generation of linearly independent coordinate (basis) vectors spanning the null- and range-space of Hamilton’s Law of Varying Action in \mathbf{F}^n , and correspondingly a set of linearly independent fundamental-time-modes spanning the solution space of Hamilton’s Law of Varying Action in \mathcal{F}^{HLVA} using the methods presented herein. The generation of these basis vectors and fundamental-time-modes provide several capabilities for nonlinear systems that have been demonstrated, and include the ability to perform model reduction, superposition of trajectories with moderate scalability, and the use of unconstrained temporal-basis-functions without the need for Lagrange multipliers.

The scalable superposition of response trajectories for nonlinear systems as demonstrated herein is remarkable. This was made possible not only by the vector-space perspective in general, but more specifically by the novel concepts introduced herein, namely fundamental-time-modes and eigen-direction iteration. Since each fundamental-time-mode is characterized by a single linearly independent coordinate vector or eigen-direction in \mathbf{F}^n , a response solely along each eigen-direction, i.e., a fundamental-time-mode response, can be superposed to generate yet another admissible response. The initial conditions necessary to initiate a response in each eigen-direction in \mathbf{F}^n are denoted as fundamental initial conditions, and are determined using the aforementioned eigen-direction iteration technique.

The concepts presented herein were verified using nonlinear systems exhibiting similar and non-similar nonlinear normal modes wherein their response was shown to be composed of fundamental-time-modes, or equivalently in this case, vector-valued eigenfunctions of Hamilton’s Law of Varying Action. The novel concepts of genuine, global and local fundamental-time-modes were introduced.

The equation referred to as Hamilton’s Law of Varying Action as used in this article from a real evolutionary perspective is a manifestation for mechanical systems of the Law of Evolutionary Energy which is an ultimate statement of energy

conservation in the form of the time-integral of all energy–work interactions for real physical processes of a dynamic system, and inherently encompasses the First Law of Thermodynamics.

Appendix A. The Law of Evolutionary Energy [23,24], Hamilton’s Law of Varying Action and the Principle of Virtual Work

This appendix describes in more detail the basis for Eq. (1) of this paper, referred to from a real evolutionary perspective as Hamilton’s Law of Varying Action, so that the reader does not misinterpret it as having been derived from or equivalent to the Principle of Virtual Work.

It is shown in Ref. [24] that Hamilton’s Law of Varying Action for mechanical systems is a consequence of the Law of Evolutionary Energy recently proposed in Refs. [23,24] for all energetic systems inherently encompassing the First Law of Thermodynamics which is the ultimate and most direct known statement of energy conservation to date. According to the Law of Evolutionary Energy, all dynamic systems undergo a process of change while satisfying energy conservation via the time-integral of all interacting energy–work expenditures occurring in the dynamics. These changes denoted here as evolutions and by the symbol \mathcal{D} in Ref. [24] are thus confined to physically realizable paths representing real changes/evolutions along the actual dynamic paths. In general, evolving energy is defined as the time-integral of an energy–work expression. In particular, the Law of Evolutionary Energy states that the evolving energy of a dynamic system is the time-integral of all of the running energy expenditures occurring in the process. The Law of Evolutionary Energy is presented in Ref. [24] as:

$$\mathcal{D}\mathcal{E} = 0 \tag{A.1a}$$

$$\mathcal{E} = \int_{t_0}^{t_f} \int_{t_0}^t dE dt = 0, \quad dE = 0 \tag{A.1b,c}$$

in which (A.1c) results as the First Law of Thermodynamics, where dE is the totality of the energy–work increments occurring in the system during the incremental time dt , (A.1b) being the total evolving energy expenditure. Accordingly, (A.1b) also stands for a time-integral statement of the First Law of Thermodynamics, i.e., the total evolving energy expenditure is always zero. Consequently (A.1a,b) together enunciated as the Law of Evolutionary Energy, indicates that any directional changes in the evolving energy must occur so as not to violate energy conservation, in other words they must be energy–conservation-compliant changes. Therefore, these evolutions (directional changes) are real changes associated with the actual dynamic paths. Such qualified evolutionary processes are characterized by a new symbol \mathcal{D} in Ref. [24] and a class of them is initiated by infinitesimally altering the initial states of a dynamic system, or effectively altering the initial state energy of the system as described in Ref. [24].

Changes described by the evolutionary \mathcal{D} symbol (or \mathcal{D} operation) are diametrically opposite to the concept of virtual variations (almost universally denoted by the (variational) symbol δ) accompanying the virtual work principles, where any contemplated (virtual) changes in the mathematical energy–work expressions or functions are required to satisfy only the geometric boundary conditions of the generalized coordinates with vanishing variations at the endpoints in time. This mathematical construct well known as coterminus conditions in time was introduced by Lagrange. Because the virtual variations of coordinates presented in classical dynamics are not required to satisfy any constraining natural law(s) such as the energy conservation law, but only the geometric boundary constraints, they are admitted as being only virtual changes that do not correspond to any realizable/real dynamic path and are merely mathematical.

However, in this article and in all of our previous work in the literature under the framework of Hamilton’s Law of Varying Action, the variational changes that were also denoted by the symbol δ do not represent virtual variations of classical dynamics. Instead, these variations are real changes in the sense of the evolutionary operator \mathcal{D} advanced within the framework of the Law of Evolutionary Energy and described above. The fact that our use of the symbol δ for real changes did not correspond to its common use as a virtual variation symbol, has and does create misunderstandings. Henceforth beyond this article, the physical and mathematical character of the new evolutionary symbol \mathcal{D} will be used in our efforts, leaving the symbol δ exclusively for virtual applications. For the last time, to preserve uniformity with our previous publications and the main body of this article, our use of the symbol δ is both physically and mathematically equated to the evolutionary operator \mathcal{D} , and must not be misconstrued as the virtual variational operator of classical dynamics. The following constitutes an original exposition behind what has been presented in Refs. [23,24]. Ref. [24] includes a more general description of the evolutionary operator that can also operate on time, which is not discussed below.

It is shown in Ref. [24] that for mechanical systems, the Law of Evolutionary Energy takes on the form (where now for consistency with this and previous papers $\delta = \mathcal{D}$)

$$\delta\mathcal{E} = \delta \int_{t_0}^{t_f} \int_{t_0}^t dE dt = \delta \int_{t_0}^{t_f} \int_{t_0}^t (dT - dW) dt = 0 \tag{A.2}$$

$$dE = dT - dW = 0 \tag{A.3}$$

from which Eq. (A.3) is recognized as the statement of the First Law of Thermodynamics for Newtonian dynamic systems, where dT is the internal (kinetic) energy change and dW is the mechanical work done through the internal boundaries of

infinitesimal internal volume elements and the external boundaries of the domain, where the negative sign indicates that positive work done on the system is thermodynamically negative. Consider the evolutionary operator given in Ref. [24] for the particular definition of traditional energy–work increments where generalized loads are held constant through incremental real displacements. Observing the consistent operational short-cut rule that evolutionary operations are similarly to apply to the generalized coordinates and not to the generalized loads, one obtains as per the Law of Evolutionary Energy

$$\delta\mathcal{E} = \int_{t_0}^{t_f} (\delta T - \delta W - \delta E_0) dt = 0, \quad \delta E_0 = \delta T_0 - \delta W_0 \quad (\text{A.4})$$

in which δE_0 represents the evolutionary change in the initial energy–work quantities. For clarity, consider a single degree-of-freedom system. Next, in the integrand of Eq. (A.4), add and subtract the term $(\delta T - \dot{z}_\delta)$ where

$$\dot{z}_\delta = \frac{d}{dt} \left(\left\{ \frac{\partial T}{\partial \dot{q}} \right\} \delta q \right).$$

Eq. (A.4) yields:

$$\mathcal{D}\mathcal{E} = \int_{t_0}^{t_f} (2\delta T - \dot{z}_\delta - \delta E_0) dt + \int_{t_0}^{t_f} (\dot{z}_\delta - \delta T - \delta W) dt = 0 \quad (\text{A.5a})$$

Thus, the Law of Evolutionary Energy leads to the equation:

$$\int_{t_0}^{t_f} (2\delta T - \dot{z}_\delta - \delta E_0) dt = - \int_{t_0}^{t_f} (\dot{z}_\delta - \delta T - \delta W) dt \quad (\text{A.5b})$$

Now consider the left-hand-side of Eq. (A.5b) and evaluate it by recognizing from the Law of Evolutionary Energy, (A.4), $\delta E_0 = \delta T - \delta W$ and using the apparently mathematical identity $\delta T - \dot{z}_\delta = -m\ddot{q} + Q$ one has

$$\int_{t_0}^{t_f} (2\delta T - \dot{z}_\delta - \delta E_0) dt = \int_{t_0}^{t_f} (\delta T - \dot{z}_\delta + \delta W) dt = \int_{t_0}^{t_f} (-m\ddot{q} + Q) \delta q dt = 0 \quad (\text{A.5c})$$

In Eq. (A.5c) one can either propose that the left-most expression with the initial energy change is “0” or recognize the appearance of Newton’s 2nd Law under the right-most integrand resulting from it on basis of the Law of Evolutionary Energy which has been invoked in getting it, to conclude that it is “0”. Thus, it follows from Eqs. (A.5c) and (A.5b) that

$$\int_{t_0}^{t_f} (2\delta T - \dot{z}_\delta - \delta E_0) dt = - \int_{t_0}^{t_f} (\dot{z}_\delta - \delta T - \delta W) dt = 0 \quad (\text{A.5d})$$

The left-most integral expression equated to “0” is exactly in the form of the authentic non-virtual variational law stated by Hamilton [26] as the Law of Varying Action; the 2nd integral expression with negative sign equated to “0” is the alternate derived and equivalent form of Hamilton’s Law of Varying Action. This latter form was never presented explicitly by Hamilton, but it is the form we have used in our previous publications and is Eq. (1) of this article alternately and equivalently referred to as Hamilton’s Law of Varying Action. Based on Eq. (A.5d) the right-hand integral form of Eq. (A.5d) has δE_0 implicitly in it. Therefore, Eq. (1) must and can be used without rendering the initial state changes equal to “0”. Finally, we note that both integral expressions appear or are imbedded in the alternate form of the Law of Evolutionary Energy in Eq. (A.5a). In Eq. (A.5d), one can transition from one integral to the other by invoking the Law of Evolutionary Energy in Eq. (A.4). The third integral expression on the right equated to “0” in Eq. (A.5c) resulted from the Law of Evolutionary Energy or is another form of the Law of Evolutionary Energy for mechanical systems. It was an end product. It is not the principle of virtual work since the exposed δq ’s emanating from the evolutionary kinetic energy and work expressions are evolutionary not virtual, and all assumptions of the principle of virtual work were defied in obtaining it. It was not the starting expression for any of the equations presented in our previous work and in this article. In contrast, the original starting point of the Principle of Virtual Work is an expression that symbolically appears like the third integral on the right-hand side of Eq. (A.5c) known as the D’Alembert’s Principle multiplied by virtual variational coordinates. Whereas, no concept of virtuality is needed to evaluate dynamics from the perspective of the Law of Evolutionary Energy.

Next, by invoking the temporal-basis-function expansion (6) of the generalized coordinates in Eq. (A.1a) one can write in general

$$\delta\mathcal{E}(\mathbf{A}) = \delta\mathbf{A}^T \frac{\delta\mathcal{E}}{\delta\mathbf{A}} = 0, \quad \frac{\delta\mathcal{E}(\mathbf{A})}{\delta\mathbf{A}} = 0 \quad (\text{A.6a, b})$$

where Eq. (A.6b) follows directly from the Law of Evolutionary Energy. Eq. (A.6b) does not necessarily imply a partial derivative operation nor the explicit existence of a function $\mathcal{E}(\mathbf{A})$. However, the indicated operation on the left-hand-side of Eq. (A.6b) is always well-defined as the ratio of two infinitesimal evolutionary quantities, and identified in the limit as the gradient of the evolving energy \mathcal{E} hypersurface, which is normal to it. Eq. (A.6a) then indicates that the $\delta\mathbf{A}$ ’s must be normal to this gradient, hence in the hypertangent plane of the surface $\mathcal{E}(\mathbf{A})$, which constitutes the evolution space.

Specifically from Eq. (A.6a) in the resulting expression for a mechanical system one obtains

$$\delta \mathbf{A}^\top (\mathbf{P}\mathbf{A} - \mathbf{b}) = 0, \quad \frac{\delta \mathcal{E}}{\delta \mathbf{A}} = \mathbf{P}\mathbf{A} - \mathbf{b} = 0 \tag{A.7a,b}$$

Eq. (A.7b) corresponds to Eqs. (7) and (8). In Eq. (A.6) the changes $\delta \mathbf{A}$ (which are now recognized as \mathbf{A} -parameter alterations on the temporal-basis-functions) are not arbitrary but must satisfy the energy conservation law just as the coordinates, \mathbf{A} , in Eq. (A.7) are required to do the same. Indeed, assuming a linear system for simplicity, taking the directional change or evolution of Eq. (A.7b) one more time, one will obtain the equations that the energy-conservation-compliant $\delta \mathbf{A}$'s must satisfy:

$$\delta \left(\frac{\delta \mathcal{E}}{\delta \mathbf{A}} \right) = \delta (\mathbf{P}\mathbf{A} - \mathbf{b}) = \mathbf{P}\delta \mathbf{A} - \delta \mathbf{b} = \mathbf{P}\delta \mathbf{A} = 0 \tag{A.8}$$

where $\delta \mathbf{b} = 0$ as per the operational rule that the evolution operator is not to operate on forces. However, in general, force alterations $\delta \mathbf{b}$ are allowable under the Law of Evolutionary Energy, a topic beyond the scope of this appendix. It follows that $\delta \mathbf{A}$'s are not arbitrary but in the null-space of \mathbf{P} (and in the null- and range-space of \mathbf{P} if $\delta \mathbf{b} \neq 0$) which describes the dynamics of the energy-conservation path. Therefore, the $\delta \mathbf{A}$'s now are energy-compliant following the same dynamic features of the actual \mathbf{A} 's.

The nature of the changes in \mathbf{A} are in a particular non-arbitrary direction (evolutional) which is in the evolution space. If no force alterations $\delta \mathbf{b}$ are considered, then the $\delta \mathbf{A}$'s ensue due to infinitesimal alterations in the initial states of the system by virtue of the time-basis function expansion of the generalized states. Because the $\delta \mathbf{A}$'s are energy-conservation-compliant per Eqs. (A.6)–(A.8), they are associated with the real dynamic path. To satisfy Eqs. (A.7b) and (A.8) without making any a priori judgment about the values of the $\delta \mathbf{A}$'s, and upon substituting Eqs. (16) and (25) into Eq. (28) the algebraic coordinates \mathbf{A} due to Eq. (A.7b) become,

$$\mathbf{A} = [\mathbf{E}]_N [\Psi(0)] [\mathbf{E}]_N^{-1} \begin{Bmatrix} q(0) \\ \dot{q}(0) \end{Bmatrix} + [\mathbf{E}]_R \begin{bmatrix} \lambda^{-1} \\ \end{bmatrix}_R ([\mathbf{E}]_R^\top [\mathbf{E}]_R)^{-1} [\mathbf{E}]_R^\top \mathbf{b} \tag{A.9a}$$

And due to Eq. (A.8), but allowing for force alteration for generality

$$\delta \mathbf{A} = [\mathbf{E}]_N [\Psi(0)] [\mathbf{E}]_N^{-1} \begin{Bmatrix} \delta q(0) \\ \delta \dot{q}(0) \end{Bmatrix} + [\mathbf{E}]_R \begin{bmatrix} \lambda^{-1} \\ \end{bmatrix}_R ([\mathbf{E}]_R^\top [\mathbf{E}]_R)^{-1} [\mathbf{E}]_R^\top \delta \mathbf{b} \tag{A.9b}$$

which also follows consistently from Eq. (A.9a). Attaching the $\delta \mathbf{A}$'s to the temporal-basis-functions, we obtain the evolutional real path alterations

$$\begin{Bmatrix} \delta q(t) \\ \delta \dot{q}(t) \end{Bmatrix} = \begin{bmatrix} \Psi(t) \\ \dot{\Psi}(t) \end{bmatrix} \delta \mathbf{A} = \begin{bmatrix} \Psi(t) \\ \dot{\Psi}(t) \end{bmatrix} \left\{ [\mathbf{E}]_N [\Psi(0)] [\mathbf{E}]_N^{-1} \begin{Bmatrix} \delta q(0) \\ \delta \dot{q}(0) \end{Bmatrix} + [\mathbf{E}]_R \begin{bmatrix} \lambda^{-1} \\ \end{bmatrix}_R ([\mathbf{E}]_R^\top [\mathbf{E}]_R)^{-1} [\mathbf{E}]_R^\top \delta \mathbf{b} \right\} \tag{A.9c}$$

It can be observed from Eq. (A.9b), (A.9c) that if no force alterations are envisioned $\delta \mathbf{b} = 0$, then the $\delta \mathbf{A}$'s and hence the $\delta \mathbf{q}(t)$, and $\delta \dot{\mathbf{q}}(t)$ will result from alterations of initial states only. The initial energy levels of the system are arbitrary only to the extent of arbitrariness in these initial state alterations. In this case, if as practiced or required for virtual variations one takes $\delta \mathbf{q}(0) = \delta \dot{\mathbf{q}}(0) = 0$ because the initial conditions are specified a priori, these would lead to $\delta \mathbf{A} = 0$, and consequently no $\delta \mathbf{q}(t)$ and $\delta \dot{\mathbf{q}}(t)$ would result. Therefore, the Law of Evolutionary Energy and the Principle of Virtual Work have no physical foundational commonality. Comparing Eq. (A.9a), (A.9b) we also conclude that $\delta \mathbf{A}$ satisfies the same natural law and the same transition dynamics features since they share the same null-space characterization that \mathbf{A} 's uniquely describe albeit with initial conditions $\delta \mathbf{q}(0)$ and $\delta \dot{\mathbf{q}}(0)$ instead of $\mathbf{q}(0)$ and $\dot{\mathbf{q}}(0)$. These features exist regardless of whether any force alterations exist or not. In Eq. (A.9b), any force alteration can be considered without changing this feature. As a special application of the above results, for real evolutional paths attached to the dynamics of \mathbf{A} 's, take $\delta \mathbf{q}(0) = \dot{\mathbf{q}}(0)t^*$ and $\delta \dot{\mathbf{q}}(0) = \ddot{\mathbf{q}}(0)t^*$ where t^* is an infinitesimally small time-increment. As $t^* \rightarrow 0$, $\delta \mathbf{q}(0)$ and $\delta \dot{\mathbf{q}}(0)$ would be the initial mathematical path variations of the real dynamic path characterized by \mathbf{A} 's, and Eq. (A.9b), (A.9c) in addition allow nonzero $\delta \mathbf{b}$ due to variation of the underlying physical forces f in the form $\delta f = \dot{f}t^*$. Eq. (A.9a) also includes the altered range-space solution for $\delta \mathbf{A}$ in Eq. (A.9b) exactly as it would follow from Eqs. (A.8) and (A.9a) by letting $\mathbf{b} \rightarrow \delta \mathbf{b}$. The $\delta \mathbf{A}$'s and therefore $\delta \mathbf{q}(t)$ and $\delta \dot{\mathbf{q}}(t)$, would be the evolution along the real dynamic path $\mathbf{q}(t)$ parameterized by the \mathbf{A} 's given by Eq. (A.9a). Alternately, if it is assumed that $\delta \mathbf{b} = 0$ in Eq. (A.9c), the same mathematical path variations $\delta \mathbf{q}(t) = \dot{\mathbf{q}}(t)t^*$ and $\delta \dot{\mathbf{q}}(t) = \ddot{\mathbf{q}}(t)t^*$ along the forced dynamic path of $\mathbf{q}(t)$, $\dot{\mathbf{q}}(t)$, when substituted on the left-hand-side of Eq. (A.9c), would be realized as having resulted from another set of uniquely different alterations in the initial states $\delta \mathbf{q}(0)$, $\delta \dot{\mathbf{q}}(0)$ that would not be the same as the initial path variations of the forced system. This follows from the invertibility of the null-space transition matrix evident in Eq. (A.9c) to be able to find the generating initial states $\delta \mathbf{q}(0)$, $\delta \dot{\mathbf{q}}(0)$ in Eq. (A.9c) for any given $\delta \mathbf{q}(t)$, $\delta \dot{\mathbf{q}}(t)$ (those of the actual path) even with $\delta \mathbf{b} \neq 0$. Whatever the perspective, Eq. (A.9c) describes real changes along the real dynamic path.

The Law of Evolutionary Energy and its associated procedures referred to as the “Evolutionary Energy Method” in Öz [23,24] constitute a novel and unique approach to dynamics which is different than the concepts and practices of virtual work principles which require and render the initial (and other boundary) variations to be zero. However, no such a priori requirements on the initial states alterations are made in the Universal Procedure presented in this article. Initial states are to be imposed after the spectral solution is obtained. The spectral characterization of the null-space is essential for discovering the transition dynamics of the system, which must and can only be formed without requiring zero initial state alterations per the procedure of this article. Equivalently, initial states are to be specified on the system of equations that carry the null-space information, that is on the system of equations that are required to have $2N$ zero eigenvalues. Any assignment of \mathbf{A} 's on these equations for whatever reason (such as in the iterative nonlinear solution procedure) is equivalent to specifying the initial states at the correct phase of the solution process and implies nothing about the initial state alterations. They are still unassigned, available, and are left genuinely free in the spectral solution process.

The objective of this exposition was to show that virtual work principles were not used in this manuscript or in earlier works by the authors. As a matter of course, the Mechanical Law of Evolutionary Energy was shown to encompass Hamilton's Law of Varying Action from a real evolutionary perspective.

Appendix B. Integral form of matrix elements for two degrees-of-freedom system

$$\mathbf{M}_{ii} = \int_0^1 \left(\frac{m_i}{\Delta t^2} \Psi^T \Psi' \right) d\tau - \frac{m_i}{\Delta t^2} \Psi^T \Psi' \Big|_0^1 \quad i = 1, 2 \quad (\text{B.1})$$

$$\mathbf{KL}_{ii} = \int_0^1 (k_i + k_{i+1}) \Psi^T \Psi d\tau \quad i = 1, 2 \quad (\text{B.2})$$

$$\mathbf{KL}_{12} = \mathbf{KL}_{21} = \int_0^1 k_{l_2} \Psi^T \Psi + \frac{c_2}{\Delta t} \Psi^T \Psi' d\tau \quad (\text{B.3})$$

$$\mathbf{C}_{ii} = \int_0^1 \frac{c_i + c_{i+1}}{\Delta t} \Psi^T \Psi' d\tau \quad i = 1, 2 \quad (\text{B.4})$$

$$\mathbf{KNL}_{11} = \int_0^1 \left\{ k_{nl_1} \Psi^T \Psi \mathbf{A}^1 \mathbf{A}^{1T} \Psi^T \Psi + k_{nl_2} \Psi^T \Psi (\mathbf{A}^2 - \mathbf{A}^1) (\mathbf{A}^{2T} - \mathbf{A}^{1T}) \Psi^T \Psi \right\} d\tau \quad (\text{B.5})$$

$$\mathbf{KNL}_{22} = \int_0^1 \left\{ k_{nl_2} \Psi^T \Psi (\mathbf{A}^2 - \mathbf{A}^1) (\mathbf{A}^{2T} - \mathbf{A}^{1T}) \Psi^T \Psi + k_{nl_3} \Psi^T \Psi \mathbf{A}^2 \mathbf{A}^{2T} \Psi^T \Psi \right\} d\tau \quad (\text{B.6})$$

$$\mathbf{KNL}_{12} = \mathbf{KNL}_{21} = \int_0^1 k_{nl_2} \Psi^T \Psi (\mathbf{A}^2 - \mathbf{A}^1) (\mathbf{A}^{2T} - \mathbf{A}^{1T}) \Psi^T \Psi d\tau \quad (\text{B.7})$$

$$\mathbf{F}_i = \int_0^1 \Psi^T f_i^T(\tau) d\tau \quad i = 1, 2 \quad (\text{B.8})$$

Appendix C. Matrix elements using power series temporal-basis-functions

Upon substituting power series temporal-basis-functions

$$\Psi(\tau) = [1, \tau, \tau^2, \dots, \tau^{n-1}] \quad (\text{C.1})$$

into Eqs. (B.1)–(B.8) and integrating, the following matrix elements are obtained.

$$\mathbf{M}_{11}(J, I) = \frac{m_1(1-i)i}{\Delta t^2(i+j-1)}, \quad \mathbf{M}_{22}(J, I) = \frac{m_2(1-i)i}{\Delta t^2(i+j-1)} \quad (\text{C.2, C.3})$$

$$\mathbf{KL}_{11}(J, I) = \frac{k_{l_1} + k_{l_2}}{(i+j+1)}, \quad \mathbf{KL}_{22}(J, I) = \frac{k_{l_2} + k_{l_3}}{(i+j+1)} \quad (\text{C.4, C.5})$$

$$\mathbf{KL}_{12}(J, I) = \mathbf{KL}_{21}(J, I) = \frac{k_{l_2}}{(i+j+1)} + \frac{c_2 i}{\Delta t(i+j)} \quad (\text{C.6, C.7})$$

$$\mathbf{C}_{11}(J, I) = \frac{(c_1 + c_2)i}{\Delta t(i+j)}, \quad \mathbf{C}_{22}(J, I) = \frac{(c_2 + c_3)i}{\Delta t(i+j)} \quad (\text{C.8, C.9})$$

$$i, j = 0, 1, 2, \dots, n-1 \quad \begin{array}{l} J = j+1 \text{ (row indices)} \\ I = i+1 \text{ (column indices)} \end{array}$$

$$\mathbf{KNL}_{11}(K, L) = k_{nl_1} \frac{(\mathbf{A}^{1T} \mathbf{A}^1)}{(i+j+k+l+1)} + k_{nl_2} \frac{(\mathbf{A}^{2T} - \mathbf{A}^{1T})(\mathbf{A}^2 - \mathbf{A}^1)}{(i+j+k+l+1)} \quad (\text{C.10})$$

$$\mathbf{KNL}_{22}(K, L) = k_{nl_2} \frac{(\mathbf{A}^{2T} - \mathbf{A}^{1T})(\mathbf{A}^2 - \mathbf{A}^1)}{(i+j+k+l+1)} + k_{nl_3} \frac{(\mathbf{A}^{2T} \mathbf{A}^2)}{(i+j+k+l+1)} \quad (\text{C.11})$$

$$\mathbf{KNL}_{12}(K, L) = \mathbf{KNL}_{21}(K, L) = k_{nl_2} \frac{(\mathbf{A}^{2T} - \mathbf{A}^{1T})(\mathbf{A}^2 - \mathbf{A}^1)}{(i+j+k+l+1)} \quad (\text{C.12})$$

$$i, j, k, l = 0, 1, 2, \dots, n-1$$

$$I = i + 1 \text{ (row indices), } J = j + 1 \text{ (column indices)}$$

$$K = k + 1 \text{ (row indices), } L = l + 1 \text{ (column indices)}$$

For each k, l run the indices i, j to form the scalar

$$(\dots)_{1 \times N}^T \left[\frac{1}{i+j+k+l+1} \right]_{N \times N} (\dots)_{N \times 1}$$

which is located at K, L . For example, the first matrix element of Eq. (C.12) may be determined by running the indices $i, j = 0, 1, 2, \dots, n-1$, while $k = l = 0$

$$\mathbf{KNL}_{12}(1, 1) = k_{nl_2} (\mathbf{A}^{2T} - \mathbf{A}^{1T}) \left[\frac{1}{(i+j+0+0+1)} \right] (\mathbf{A}^2 - \mathbf{A}^1). \quad (\text{C.13})$$

Appendix D. Matrix elements using Gaussian temporal-basis-functions

Upon substituting Gaussian temporal-basis-functions

$$\Psi(\tau) = [e^{-K_i(\tau-\tau_i)^2}] \quad (\text{D.1})$$

into Eqs. (B.1)–(B.8)

$$\mathbf{M}_{11}(i, j) = \frac{m_1}{\Delta t^2} \int_0^1 4K_i K_j (\tau - \tau_i)(\tau - \tau_j) e^{\mu_1} d\tau - \frac{m_1}{\Delta t^2} [-2K_j(1 - \tau_j) e^{\mu_3} - 2K_j \tau_j e^{\mu_4}] \Big|_0^1 \quad (\text{D.2})$$

$$\mathbf{M}_{22}(i, j) = \frac{m_2}{\Delta t^2} \int_0^1 4K_i K_j (\tau - \tau_i)(\tau - \tau_j) e^{\mu_1} d\tau - \frac{m_2}{\Delta t^2} [-2K_j(1 - \tau_j) e^{\mu_3} - 2K_j \tau_j e^{\mu_4}] \Big|_0^1 \quad (\text{D.3})$$

$$\mathbf{KL}_{11}(i, j) = \int_0^1 (k_{l_1} + k_{l_2}) e^{\mu_1} d\tau, \quad \mathbf{KL}_{22}(i, j) = \int_0^1 (k_{l_2} + k_{l_3}) e^{\mu_1} d\tau \quad (\text{D.4, D.5})$$

$$\mathbf{KL}_{12}(i, j) = \mathbf{KL}_{21}(i, j) = \int_0^1 \left\{ k_{l_2} e^{\mu_1} - \frac{c_2}{\Delta t} [2K_j(\tau - \tau_j) e^{\mu_1}] \right\} d\tau \quad (\text{D.6})$$

$$\mathbf{C}_{11}(i, j) = \int_0^1 \frac{c_1 + c_2}{\Delta t} [-2K_j(\tau - \tau_j) e^{\mu_1}] d\tau, \quad \mathbf{C}_{22}(i, j) = \int_0^1 \frac{c_2 + c_3}{\Delta t} [-2K_j(\tau - \tau_j) e^{\mu_1}] d\tau \quad (\text{D.7, D.8})$$

$$\mathbf{KNL}_{11}(k, l) = \int_0^1 \left\{ k_{nl_1} \mathbf{A}^{1T} e^{\mu_1} \mathbf{A}^1 e^{\mu_2} + k_{nl_2} (\mathbf{A}^2 - \mathbf{A}^1)^T e^{\mu_1} (\mathbf{A}^2 - \mathbf{A}^1) e^{\mu_2} \right\} d\tau \quad (\text{D.9})$$

$$\mathbf{KNL}_{22}(k, l) = \int_0^1 \left\{ k_{nl_2} (\mathbf{A}^2 - \mathbf{A}^1)^T e^{\mu_1} (\mathbf{A}^2 - \mathbf{A}^1) e^{\mu_2} + k_{nl_3} \mathbf{A}^{2T} e^{\mu_1} \mathbf{A}^2 e^{\mu_2} \right\} d\tau \quad (\text{D.10})$$

$$\mathbf{KNL}_{12}(k, l) = \mathbf{KNL}_{21}(k, l) = \int_0^1 k_{nl_2} (\mathbf{A}^2 - \mathbf{A}^1)^T e^{\mu_1} (\mathbf{A}^2 - \mathbf{A}^1) e^{\mu_2} d\tau \quad (\text{D.11})$$

$$i, j, k, l = 1, 2, \dots, n-1 \quad \begin{array}{l} i, k = \text{(row indices)} \\ j, l = \text{(column indices)} \end{array}$$

$$\mu_1 = -K_i(\tau - \tau_i)^2 - K_j(\tau - \tau_j)^2, \quad \mu_2 = -K_k(\tau - \tau_k)^2 - K_l(\tau - \tau_l)^2 \quad (\text{D.12, D.13})$$

$$\mu_3 = -K_i(1 - \tau_i)^2 - K_j(1 - \tau_j)^2, \quad \mu_4 = -K_i \tau_i^2 - K_j \tau_j^2 \quad (\text{D.14, D.15})$$

Run the indices $i, j = 1, 2, \dots, n$ to form the scalar $(\dots)^T e^{\mu_1}(\dots)$, which is multiplied by e^{μ_2} at k, l . For example, the first matrix element of Eq. (D.11) may be determined by running the indices $i, j = 1, 2, \dots, n$, while $k = l = 1$

$$\mathbf{KNL}_{12}(k, l) = \int_0^1 k_{nl_2} (\mathbf{A}^2 - \mathbf{A}^1)^T e^{-K_1(\tau-\tau_1)^2 - K_2(\tau-\tau_j)^2} (\mathbf{A}^2 - \mathbf{A}^1) e^{-K_1(\tau-\tau_1)^2 - K_1(\tau-\tau_1)^2} d\tau \quad (\text{D.16})$$

References

- [1] C.D. Bailey, A new look at Hamilton's principle, *Foundation of Physics* (1975) 433–451.
- [2] C.D. Bailey, Application of Hamilton's law of varying action, *American Institute of Aeronautics and Astronautics Journal* 13 (9) (1975) 1154–1157.
- [3] C.D. Bailey, Hamilton, Ritz and Elastodynamics, *Transactions of the American Society of Mechanical Engineers. Journal of Applied Mechanics* 98 (4) (1976) 684–688.
- [4] C.D. Bailey, Direct analytical solutions to non-uniform beam problems, *Journal of Sound and Vibration* 56 (4) (1978) 501–507.
- [5] D.H. Hodges, Direct solutions for Sturm-Liouville systems with discontinuous coefficients, *American Institute of Aeronautics and Astronautics Journal* 17 (8) (1979) 924–926.
- [6] D.L. Hitzl, Implementing Hamilton's law of varying action with shifted Legendre polynomials, *Journal of Computational Physics* 38 (2) (1980) 185–211.
- [7] R. Riff, M. Baruch, Time finite element discretization of Hamilton's law of varying action, *American Institute of Aeronautics and Astronautics Journal* 22 (9) (1984) 1310–1318.
- [8] C.D. Bailey, R.D. Witchey, Harmonic motion of nonconservative, forced, damped systems subjected to nonpotential follower forces, *Computer Methods in Applied Mechanics and Engineering* 42 (1984) 71–88.
- [9] M. Baruch, R. Riff, Hamilton's Principle, Hamilton's Law, 6ⁿ correct formulations, *American Institute of Aeronautics and Astronautics Journal* 20 (5) (1984) 687–692.
- [10] H. Öz, E. Adigüzel, Hamilton's law of varying action, part I: assumed-time-modes method, *Journal of Sound and Vibration* 179 (4) (1995) 697–710.
- [11] M. Borri, G.L. Ghiringhelli, M. Lanz, P. Mantegazza, T. Merlini, Dynamic response of mechanical systems by a weak Hamiltonian formulation, *Computers and Structures* 20 (1–3) (1985) 495–508.
- [12] M. Borri, Helicopter rotor dynamics by finite element time approximation, *Computers & Mathematics with Applications* 12A (1) (1986) 149–160.
- [13] D.H. Hodges, L.J. Hou, Shape functions for mixed p-version finite elements in the time domain, *Journal of Sound and Vibration* 145 (2) (1991) 169–178.
- [14] D.A. Peters, A.P. Izadpanah, hp-version finite elements for space-time domain, *Computational Mechanics* 3 (1988) 73–88.
- [15] D.H. Hodges, R.R. Bless, Weak Hamiltonian finite element method for optimal control problems, *Journal of Guidance, Control and Dynamics* 14 (1) (1991) 148–156.
- [16] H. Öz, E. Adigüzel, Hamilton's Law of Varying Action, part II: direct optimal control of linear systems, *Journal of Sound and Vibration* 179 (4) (1995) 711–724.
- [17] H. Öz, E. Adigüzel, Direct optimal control of nonlinear systems via Hamilton's Law of Varying Action, *ASME Journal of Dynamic Systems, Measurement, and Control* 117 (1995) 262–268.
- [18] H. Öz, G. Yen, Direct optimal control: a hybrid approach, *International Journal of Control* 67 (2) (1997) 193–212.
- [19] H. Öz, J.K. Ramsey, Direct optimal control of the duffing dynamics, in: *Eleventh Symposium on Structural Dynamics and Control, Virginia Polytechnic Institute and State University, Blacksburg, Virginia, May 12–14, 1997* (Also NASA TM 2002-211582, September 2002).
- [20] M. Rajan, J.L. Junkins, Perturbation methods based upon varying action integrals, *International Journal of Non-Linear Mechanics* 18 (5) (1983) 335–351.
- [21] V.R. Sonti, O.P. Agrawal, Design sensitivity analysis of dynamic systems using Hamilton's Law of Varying Action, *International Journal Mechanical Science* 37 (6) (1995) 601–613.
- [22] O.P. Agrawal, V.R. Sonti, Modelling of stochastic dynamic systems using Hamilton's law of varying action, *Journal of Sound and Vibration* 192 (2) (1966) 399–412.
- [23] H. Öz, Algebraic evolutionary energy method for dynamics and control, in: *Computational Nonlinear Aeroelasticity for Multidisciplinary Analysis and Design*, DAGSI - Final Contract Report to AFRL, WPAFB, 2002, pp. 96–162.
- [24] H. Öz, Evolutionary Energy Method (EEM): An aerothermoservoelastical application, in: *Variational and Extremum Principles in Macroscopic Systems*, Elsevier, Amsterdam, 2005, pp. 641–670.
- [25] H. Öz, J.K. Ramsey, Time-modes and linear systems, *Journal of Sound and Vibration* 231 (5) (2000) 1189–1219.
- [26] W.R. Hamilton, On a general method in dynamics; by which the study of the motions of all free systems of attracting or repelling points is reduced to the search and differentiation of one central relation or characteristic function, *Philosophical Transactions of the Royal Society of London* (1834) 247–308.
- [27] W.R. Hamilton, Second essay on a general method in dynamics, *Philosophical Transactions of the Royal Society of London* (1835) 95–144.
- [28] O.P. Agrawal, S. Saigal, A Novel, computationally efficient, approach for Hamilton's law of varying action, *International Journal of Mechanical Sciences* 29 (4) (1987) 285–292.
- [29] C.P. Atkinson, B. Taskett, A Study of the nonlinearly related modal solutions of coupled nonlinear systems by superposition techniques, *Journal of Applied Mechanics* 1 (1965) 359–364.
- [30] A. Khare, U. Sukhatme, Linear superposition in nonlinear equations, *Physical Review Letters* 88 (24) (2002).
- [31] L.W. Johnson, R.D. Reiss, J.T. Arnold, *Introduction to Linear Algebra*, third ed., Addison-Wesley, Reading, MA, 1993.
- [32] W.H. Press, S.A. Teukolsky, W.T. Vetterling, B.P. Flannery, *Numerical Recipes in Fortran. The Art of Scientific Computing*, second ed., Cambridge University Press, Cambridge, MA, 1992.
- [33] J.T. Scheik, *Linear Algebra with Applications*, McGraw-Hill, New York, 1997.
- [34] R.M. Rosenberg, The normal modes of nonlinear n-degree-of-freedom systems, *Journal of Applied Mechanics* 29 (1962) 7–14.
- [35] S.W. Shaw, C. Pierre, Normal modes for non-linear vibratory systems, *Journal of Sound and Vibration* 164 (1) (1993) 85–124.
- [36] J.C. Slater, A numerical method for determining nonlinear normal modes, *Nonlinear Dynamics* 10 (1996) 19–30.
- [37] J.C. Slater, G. Agnes, Nonlinear modal control techniques and applications in structural dynamic systems, in: C.T. Leondes (Ed.), *Structural Dynamic Systems Computational Techniques and Optimization, Dynamic Analysis and Control Techniques, Gordon and Breach International Series in Engineering, Technology and Applied Science*, vol. 14, 1999, pp. 107–168.
- [38] A.F. Vakakis, L.I. Manevitch, Y.V. Mikhlin, V.N. Pilipchuk, A.A. Zevin, *Normal Modes and Localization in Nonlinear Systems*, Wiley, New York, 1996.
- [39] R.M. Rosenberg, *On Nonlinear Vibrations of Systems with Many Degrees-of-Freedom. Advances in Applied Mechanics*, vol. 9, Academic Press, New York, 1966, pp. 155–242.
- [40] J.K. Ramsey, Vector-Space Implementation of Hamilton's Law of Varying Action for Linear and Nonlinear Systems, *Ph.D. Dissertation*, The Ohio State University, 2000.
- [41] L. Meirovitch, *Computational Methods in Structural Dynamics*, Sijthoff & Noordhoff, Netherlands, 1980.
- [42] W.T. Thomson, *Theory of Vibration with Applications*, fourth ed, Prentice Hall, New Jersey, 1993.